mgr Laura Szafron

Charakterystyka wariantów genetycznych wybranych genów supresorowych i onkogenów oraz metylomu guzów granicznych jajnika oraz wysoko i nisko zróżnicowanych raków jajnika

**Rozprawa na stopień doktora nauk medycznych i nauk o zdrowiu
w dyscyplinie nauki medyczne**

Promotor: prof. dr hab. Jolanta Kupryjańczyk

Narodowy Instytut Onkologii, Państwowy Instytut Badawczy
im. Marii Skłodowskiej-Curie w Warszawie

Obrona rozprawy doktorskiej przed Radą Dyscypliny Nauk Medycznych
Warszawskiego Uniwersytetu Medycznego

Warszawa, 2025 r.

Słowa kluczowe: guzy jajnika, warianty genetyczne, metylacja, markery

Źródła finansowania

Wykaz publikacji wchodzących w skład rozprawy doktorskiej

- 1. **Szafron LA**.; Sobiczewski P.; Dansonka-Mieszkowska A.; Kupryjanczyk J.; Szafron LM. *„An Analysis of Genetic Polymorphisms in 76 Genes Related to the Development of Ovarian Tumors of Different Aggressiveness*". **International Journal of Molecular Sciences** (**2024),** doi.org/10.3390/ijms252010876

- 2. **Szafron LA**.; Iwanicka-Nowicka, R; Sobiczewski P.; Koblowska M.; Dansonka-Mieszkowska A.; Kupryjanczyk J.; Szafron LM *„The diversity of methylation patterns in serous borderline ovarian tumors and serous ovarian carcinomas"*. **Cancers (2024),** doi.org/10.3390/cancers16203524

- 3. **Szafron, LA**.; Kupryjanczyk, J.; Szafron, LM *"Special Issue "Biomarkers and Early Detection Strategies of Ovarian Tumors"* (editorial). **International Journal of Molecular Sciences** (**2025),** https://doi.org/10.3390/ijms26189071

Spis treści

Wykaz stosowanych skrótów

AUC – pole powierzchni pod krzywą ROC

BOT – guzy graniczne jajnika bez mutacji *BRAF* V600E

BOT.V600E – guzy graniczne jajnika z mutacją *BRAF* V600E

BOTS – guzy graniczne jajnika

BSA – albumina surowicy bydlęcej

CDS – sekwencja kodująca genu

DMP – nukleotyd o zróżnicowanej metylacji

DMR – region o zróżnicowanej metylacji

EMT – przejście epitelialno-mezenchymalne

FIGO – Międzynarodowa Federacja Ginekologii i Położnictwa

hgOvCa – nisko zróżnicowany rak jajnika

hot-spot – region w genomie o wysokiej częstości występowania wariantów genetycznych

HR – iloraz ryzyka

krzywa ROC -- krzywa charakterystyki operacyjnej odbiornika

lgOvCa – wysoko zróżnicowany rak jajnika

MHC – główny układ zgodności tkankowej

NGS – sekwencjonowanie następnej generacji

non-SNP – wariant genetyczny niebędący polimorfizmem pojedynczego nukleotydu

OvCa – rak jajnika

PETE – technika wzbogacania DNA, ang. „Primer Extension Target Enrichment"

Real-Time qPCR – ilościowa łańcuchowa reakcja polimerazy w czasie rzeczywistym

RT – choroba resztkowa

SNP – polimorfizm jednonukleotydowy

TAM – makrofagi związane z guzem nowotworowym

UTR – region genu nieulegający translacji

VEP – program „Variant Effect Predictor" do annotacji wariantów genetycznych

WB – technika „western blot"

Streszczenie

W przeciwieństwie do hgOvCa, które są dość dobrze poznaną jednostką chorobową, molekularne tło w BOTS i lgOvCa jest gorzej scharakteryzowane. W niniejszej pracy podjęto się analizy wariantów genetycznych w kluczowych supresorach i onkogenach oraz badania metylomu w BOTS z (BOT.V600E) i bez (BOT) mutacji *BRAF* V600E, lgOvCa i hgOvCa. Łącznie 225 guzów jajnika oceniono pod kątem zmian genetycznych w 76 genach związanych z nowotworzeniem, stosując sekwencjonowanie następnej generacji (NGS), a następnie walidację wybranych wariantów za pomocą sekwencjonowania Sangera. Na koniec przeprowadzono analizę Western blot, aby sprawdzić wpływ wytypowanych polimorfizmów na ekspresję odpowiadających im białek. Ponadto w podgrupie 128 guzów surowiczych wykonano profilowanie metylomu za pomocą mikromacierzy Infinium MethylationEPIC. Nasze badanie ujawniło rozbieżne profile polimorficzne w różnych nowotworach jajnika, wskazując na odrębne ścieżki sygnałowe zaangażowane w ich rozwój. Niektóre mutacje wydają się odgrywać ważną rolę w BOTS bez wariantu *BRAF* V600E (*KRAS*) i w lgOvCa (*KRAS* i *NRAS*), ale nie w hgOvCa. Co więcej, na podstawie wieloczynnikowej analizy regresji, zidentyfikowano potencjalne biomarkery w BOTS (*PARP1*) i hgOvCa (*FANCI, BRCA2, TSC2, FANCF*). Dla niektórych analizowanych genów, takich jak *FANCI, FANCD2* oraz *FANCI, FANCF, TSC2*, status odpowiednio BRCA1/2 i TP53 okazał się kluczowy. Jeśli chodzi o zmiany epigenetyczne, największą liczbę odmiennie zmetylowanych CpG i regionów (DMR) znaleziono między lgOvCa i hgOvCa. Co ciekawe, dziesięć najistotniejszych DMR, odróżniających BOT od lgOvCa, obejmowało region MHC na chromosomie 6. Zidentyfikowano również setki DMR, które mogą być potencjalnie użyte jako biomarkery predykcyjne lub prognostyczne w BOTS i hgOvCa. DMR z najlepszymi zdolnościami dyskryminacyjnymi obejmowały następujące geny: *BAIAP3, IL34, WNT10A, NEU1, SLC44A4* oraz *HMOX1, TCN2, PES1, RP1-56J10.8, ABR, NCAM1, RP11-629G13.1, AC006372.4, NPTXR* odpowiednio w BOTS i hgOvCa.

English title

The characterization of genetic variants in selected tumor suppressors and oncogenes as well as the methylomes of borderline ovarian tumors and low-grade and high-grade ovarian cancers

Summary

In contrast to the most frequent and well-described hgOvCa, the molecular background of BOTS and lgOvCa is less thoroughly characterized. Here, we aimed to analyze genetic variants in crucial tumor suppressors and oncogenes, as well as methylation changes in BOTS with (BOT.V600E) and without (BOT) the *BRAF* V600E mutation, lgOvCa, and hgOvCa. In total, 225 ovarian tumors were evaluated for genetic alterations in 76 cancer-related genes using next-generation sequencing, followed by validation of selected variants by Sanger sequencing. Finally, Western blot analyses were carried out to check the impact of the nominated polymorphisms on the expression of the corresponding proteins. Additionally, the subgroup of 128 serous tumors had their methylome profiled with Infinium MethylationEPIC microarrays. Our study unraveled divergent polymorphic patterns in different ovarian neoplasms pointing to distinct signaling pathways engaged in their development. Certain mutations seem to play an important role in BOTS without the *BRAF* V600E variant (*KRAS*) and in lgOvCa (*KRAS* and *NRAS*), but not in hgOvCa. Additionally, based on multivariable regression analyses, potential biomarkers in BOTS (*PARP1*) and hgOvCa (*FANCI*, *BRCA2*, *TSC2*, *FANCF*) were identified. Noteworthy, for some of the analyzed genes, such as *FANCI*, *FANCD2*, and *FANCI*, *FANCF*, *TSC2*, the status of BRCA1/2 and TP53, respectively, turned out to be crucial. As for epigenetic changes, the biggest number of differentially methylated CpGs and regions (DMRs) was found between lgOvCa and hgOvCa. Remarkably, the ten most significant DMRs, discriminating BOT from lgOvCa, encompassed the MHC region on chromosome 6. We also identified hundreds of DMRs, being of potential use as predictive or prognostic biomarkers in BOTS and hgOvCa. DMRs with the best discriminative capabilities overlapped the following genes: *BAIAP3*, *IL34*, *WNT10A*, *NEU1*, *SLC44A4*, and *HMOX1*, *TCN2*, *PES1*, *RP1-56J10.8*, *ABR*, *NCAM1*, *RP11-629G13.1*, *AC006372.4*, *NPTXR* in BOTS and hgOvCa, respectively.

Wstęp

Rak jajnika (OvCa) jest powszechnym nowotworem o złym rokowaniu i wysokiej śmiertelności na całym świecie (1). We wczesnym stadium zaawansowania szanse na wyleczenie są stosunkowo wysokie, jednakże często z powodu niespecyficznych i pozornie niegroźnych objawów (bóle brzucha, wzdęcia, etc.), rak jajnika wykrywany jest w późnym stadium, gdy śmiertelność jest już wysoka, a leczenie nie przynosi zadowalających efektów ze względu na nawroty choroby i oporność komórek nowotworowych na chemioterapię (2).

Istnieją dwa główne typy OvCa: nisko zróżnicowany rak jajnika (hgOvCa, ang. *high-grade*), oraz rzadziej występujący, wysoko zróżnicowany rak jajnika (lgOvCa, ang. *low-grade*). Pierwszy z nich jest najczęstszym typem (stanowi ok. 90% nowotworów tego narządu). Charakteryzuje się on wtórnie występującą chemioopornością i ekstremalną niestabilnością genomową, w tym rearanżacjami chromosomowymi i licznymi mutacjami w genach, zwłaszcza tych kodujących białka supresorowe, takie jak TP53, BRCA1 i BRCA2 (3). Z kolei, jak już wspomniano, lgOvCa jest rzadkim nowotworem jajnika charakteryzującym się młodszym wiekiem pacjentek w momencie rozpoznania, względną chemioopornością i dłuższym przeżyciem w porównaniu do swojego odpowiednika o wysokim stopniu złośliwości. Ponadto, w lgOvCa mutacje w genach *TP53* i *BRCA1/2* występują bardzo rzadko (4,5). lgOvCa (szczególnie typu surowiczego) posiadają podobną sygnaturę molekularną do guzów jajnika o granicznej złośliwości (BOTS, ang. *borderline ovarian tumors*) (6), które są również rzadką jednostką chorobową. W przeciwieństwie do OvCa BOTS występują głównie u kobiet w wieku rozrodczym, są zwykle diagnozowane w niższym stopniu zaawansowania klinicznego (wg FIGO), mają lepsze wskaźniki przeżywalności oraz nie są tak agresywne. Pomimo tych zalet, diagnostyka przedoperacyjna BOTS jest dość trudna. Metody obrazowania takie jak USG są przydatne, jednak nie dają 100% pewności w kwestii odróżnienia BOTS od raków. Co więcej, w przypadku BOTS brak jest specyficznych markerów molekularnych, a obecnie stosowane markery (np. CA125) mają niewystarczającą specyficzność (7–10). Operacja z całkowitą resekcją guza jest podstawą leczenia BOTS. Jednak u młodych kobiet rozważających prokreację, preferencyjnie stosuje się interwencję chirurgiczną oszczędzającą jajniki (8). Chemioterapia nie przynosi efektów w przypadku BOTS, m.in. ze względu na ich wolniejsze tempo podziałów (7). Co więcej, po całkowitym usunięciu guza nawet w 20% dochodzi do nawrotu. Większość BOTS nawraca jako guzy o granicznej złośliwości, jednak u około 30% pacjentek rozwija się OvCa (6,11,12) .

W przeciwieństwie do hgOvCa w BOTS mutacje w *TP53* i *BRCA1/2* nie występują często (13–15), podczas gdy najczęściej zmutowanymi genami są *BRAF* i *KRAS* (szczególnie w BOTS podtypu surowiczego). Mutacje w tych genach są czasem obecne również w lgOvCa, a ich występowanie w hgOvCa jest bardzo rzadkie (16,17). Na szczególną uwagę zasługuje gen *BRAF*, w którym najczęściej pojawiającym się patogennym wariantem aktywującym jest substytucja waliny w pozycji 600 (w egzonie 15) na kwas glutaminowy (Val600Glu, V600E). Zmiana ta jest klasyfikowana jako osobna grupa zmian w tym genie. Wykazano, że ze wszystkich polimorfizmów występujących w *BRAF*, wariant V600E wywołuje najsilniejszy efekt pronowotworowy (18). Nasz zespół wykazał dodatkowo, że obecność mutacji *BRAF* V600E jest negatywnym czynnikiem klinicznym, związanym z wcześniejszym wystąpieniem BOTS u pacjentek (19). Oprócz *KRAS*, *BRAF, BRCA1/2* i *TP53*, kilka zespołów naukowych zbadało również częstość mutacji w *PIK3CA, EGFR, CTNNB1, RAD51C, PALB2, CHEK2* i *PTEN* w BOTS (20,21). Niemniej wciąż niewiele wiadomo na temat statusu polimorficznego supresorów i onkogenów w guzach granicznych jajnika.

Również aspekt zmian metylacyjnych w guzach jajnika (szczególnie BOTS i lgOvCa) nie został dobrze zbadany. Zmiany we wzorach metylacji DNA są kluczowym mechanizmem nowotworzenia. Nieprawidłowa metylacja DNA w guzach może wystąpić wcześniej niż mutacje. Co więcej, w niektórych nowotworach ekspresja genów może być nawet częściej zmodyfikowana z powodu zmian metylacji niż poprzez mutacje (22,23). Biorąc pod uwagę zmiany metylomu, zaobserwowano, że surowicze hgOvCa tworzą oddzielny klaster w porównaniu z BOTS i lgOvCa (24). Jednak jak dotąd wzory metylacji BOTS i lgOvCa typu surowiczego oceniano wyłącznie za pomocą mikromacierzy o niskiej rozdzielczości. Ponadto liczba publikacji naukowych porównująca guzy jajnika o różnej agresywności jest wciąż niewielka (24,25).

Dlatego celem niniejszej pracy doktorskiej było przeanalizowanie 1) wariantów genetycznych w kluczowych genach supresorowych i onkogenach oraz 2) metylomu, w BOTS (w podgrupie guzów z mutacją *BRAF* V600E (BOT.V600E) lub bez niej (BOT)), lgOvCa i hgOvCa.

Status polimorficzny 76 genów został zbadany u 225 pacjentek z guzami jajnika przy użyciu dwóch paneli genowych oraz sekwencjonowania następnej generacji (NGS). Pierwszy z paneli obejmował onkogeny i geny supresorowe nowotworu zaangażowane w rozwój dziedzicznego raka jajnika (41 genów) oraz dodatkowo geny *CRNDE, IRX5* i *CEBPA*. Drugi panel zawierał „hot-spoty" w genach często zmutowanych w sporadycznych nowotworach ludzkich (37 genów), z których większość nie występowała w pierwszym panelu genowym. Poza dokładnym badaniem polimorfizmów genów i ich związku z różnymi parametrami kliniczno-patologicznymi przy użyciu modeli regresji jedno- i wieloczynnikowej, praca doktorska obejmowała potwierdzenie wybranych

wariantów genów za pomocą sekwencjonowania Sangera, a także weryfikację, czy istnieje korelacja między obecnością danego polimorfizmu a zmianami ekspresji odpowiadającego mu białka.

Analiza metylacyjna została przeprowadzona na mniejszej grupie 128 pierwotnych surowiczych guzów jajnika, przy użyciu mikromacierzy o wysokiej rozdzielczości. Nasz zespół, jako jeden z nielicznych, przeprowadził analizy metylacyjne DNA nie tylko całościowo, ale również z podziałem na nici (+) i (-). Uzyskane wyniki zweryfikowano za pomocą metylo-specyficznego PCR połączonego z sekwencjonowaniem Sangera. Ponadto przeprowadzona została szczegółowa analiza ontologiczna dla wszystkich porównań guzów. Wykorzystano również modele regresji jedno- i wieloczynnikowej w celu znalezienia najlepszych markerów (regionów o znamiennie zmienionej metylacji, DMR, ang. *differentially methylated regions*) oraz oceny ich przydatności klinicznej.

Cel pracy

Głównym celem pracy była charakterystyka porównawcza guzów jajnika: nisko zróżnicowanych (hgOvCa), wysoko zróżnicowanych (lgOvCa) oraz granicznych (BOTS) pod kątem parametrów molekularnych i poszukiwanie cech związanych z transformacją guzów granicznych w nowotwory złośliwe.

Celem szczegółowym omawianego projektu była identyfikacja wariantów polimorficznych oraz zmian wzoru metylacji w analizowanych genach jako potencjalnych biomarkerów, umożliwiających opracowanie nowych metod diagnostyki, monitorowania i leczenia nowotworów jajnika.

Materiały

W opisanych poniżej badaniach wykorzystano DNA/białko wyizolowane łącznie z retrospektywnej grupy 225 guzów jajnika, w większości typu surowiczego: 76 BOTS (w tym 53 BOT bez mutacji (BOT) i 23 BOT z mutacją *BRAF* V600E (BOT.V600E)), 10 lgOvCa i 139 hgOvCa. DNA izolowane było zarówno z materiału mrożonego (170 guzów), jak i z bloczków parafinowych (FFPE, 61 guzów), a białko wyłącznie z materiału mrożonego. Pojedyncze próbki DNA były izolowane zarówno z materiału mrożonego, jak i z ich odpowiednika parafinowego. Materiał zbierany był w latach 1995-2015 w Narodowym Instytucie Onkologii im. Marii Skłodowskiej-Curie w Warszawie. Każdy z guzów został szczegółowo scharakteryzowany pod kątem kliniczno-patologicznym z precyzyjną oceną odsetka utkania nowotworowego. W opisanych poniżej badaniach molekularnych wykorzystano jedynie te guzy, w których odsetek komórek nowotworowych wynosił co najmniej 50%. Zbiory guzów wykorzystane w badaniach opisanych w artykułach tworzących cykl oceniany w niniejszym postępowaniu doktorskim, różniły się pod względem jakościowym i ilościowym pomiędzy pracami. Dlatego też dokładna charakterystyka histopatologiczna grup guzów została przedstawiona w załączonych publikacjach.

Metody

- Izolacja DNA z materiału mrożonego (QIAmp DNA Mini Kit (Qiagen)) i parafinowego (MagCore Genomic DNA FFPE One-Step Kit (RBC Biosciences)) oraz ocena jego jakości metodą ilościowego PCR (Real-Time qPCR) z wykorzystaniem własnoręcznie zaprojektowanych primerów dla genu *GAPDH* (26).

- Tworzenie bibliotek do sekwencjonowania następnej generacji (NGS) i wzbogacanie DNA w sekwencje kodujące 41 genów (*ATM, ATR, ATRX, BAP1, BARD1, BCL2L1, BLM, BRCA1, BRCA2, BRIP1, CCNE1, CHEK1, CHEK2, EMSY, FANCA, FANCB, FANCC, FANCD2, FANCE, FANCF, FANCG, FANCI, FANCL, FANCM, IRX5, MDM2, MRE11, MUTYH, NBN, PALB2, PARP1, PIK3CA, PRKDC, PTEN, RAD50, RAD51B, RAD51C, RAD51D, RAD54L, RPA1, SEM1, TP53*), związanych z rozwojem dziedzicznego raka jajnika (panel Ion AmpliSeq™ Comprehensive Ovarian Cancer Research Panel (Thermo Fisher Scientific) + *CRNDE, IRX5* i *CEBPA*, (SeqCap EZ Enrichment System (Roche)) oraz przy użyciu panelu KAPA HyperPETE Hot Spot Panel (*AKT1, ALK, APC, ATM, BRAF, BRCA1, CDKN2A, CTNNB1, EGFR, ERBB2, ESR1, FBXW7, FGFR1, FGFR2, FGFR3, GNA11, GNAQ, GNAS, HRAS, IDH1, IDH2, JAK2, KIT, KRAS, NF1, NRAS, NTRK3, PDGFRA, PIK3CA, POLE, PTCH1, PTEN, RET, STK11, TP53, TSC1, TSC2*) (Roche), w którym znajdowały się tzw. gorące punkty w genomie („hot-spot"), będące często pojawiającymi się zmianami genetycznymi w licznych nowotworach.

- Analiza DNA techniką NGS na platformach iSeq100 i NovaSeq 6000 (Illumina) w trybie sparowanych końców. Ocena jakości wyników sekwencjonowania narzędziami FASTQC i Trimmomatic. Mapowanie do sekwencji referencyjnej programami STAR i HISAT2, ocena jakości mapowania programami SAMTOOLS, GATK i QUALIMAP. Identyfikacja mutacji i polimorfizmów o silnym/krytycznym (HIGH) lub umiarkowanym (MODERATE) wpływie na funkcje kodowanych białek (wg bazy ENSEMBL) programem Variant Effect Predictor (VEP) (ENSEMBL). Analiza bioinformatyczna i statystyczna (ocena istotności statystycznej zmian częstości występowania mutacji w poszczególnych genach pomiędzy BOTS, lgOvCa i hgOvCa testem Chi-kwadrat i/lub testem dokładnym Fishera) przy użyciu autorskich programów napisanych w językach Bash, R i Python przez dr. Łukasza Szafrona. W analizach bioinformatycznych wszystkie warianty genetyczne występujące rzadziej niż w 10%, odczytów zostały odfiltrowane. Zmiany takie mogły wynikać z błędów polimerazy DNA. Gdyby nawet nie były one błędami, to i tak nie udałoby się ich potwierdzić

sekwencjonowaniem Sangera (zbyt niska częstość ich występowania uniemożliwiłaby ich dostrzeżenie na chromatogramie).

- Potwierdzenie wybranych wariantów genetycznych metodą gradientowego PCR w połączeniu z analizą produktów na żelu agarozowym oraz sekwencjonowaniem Sangera z wykorzystaniem własnoręcznie zaprojektowanych starterów. Amplifikacji DNA dokonano przy użyciu polimerazy AmpliTaq Gold (Thermo Fisher Scientific). Do enzymatycznego oczyszczanie produktów PCR wykorzystano zestaw ExoSAP-IT (Thermo Fisher Scientific). Sekwencjonowanie DNA metodą Sangera przeprowadzono z użyciem zestawu BigDye Terminator v3.1 Cycle Sequencing Kit (Thermo Fisher Scientific), a do oczyszczania produktu po sekwencjonowaniu użyto zestawu ExTerminator (A&A Biotechnology). Odczytu wyników sekwencjonowania dokonano na sekwenatorze 3500 Genetic Analyzer (Thermo).

- Izolacja białka całkowitego. Lizaty białkowe uzyskano poprzez homogenizację tkanki w buforze RIPA (Thermo) z dodatkiem inhibitorów proteaz/fosfataz (Halt Protease Inhibitor Cocktail; Thermo). Pomiaru stężenia białka dokonano za pomocą metody kolorymetrycznej BCA (Sigma), z wykorzystaniem białka BSA (ang. *bovine serum albumin*) jako wzorca do krzywej standardowej. Poziom absorbancji mierzono na spektrofotometrze przy długości 540 nm.

- Analizy SDS-PAGE oraz Western Blot dla białek NBN, CHEK2, TP53, FANCI, FAND2, CHEK1. Jako kontroli ładowania użyto membran wybarwionych 0,1% PonceauS (Sigma) w 5% roztworze kwasu octowego, oraz przeciwciał skierowanych przeciwko β-aktynie (Thermo) i winkulinie (Thermo). Oba białka są budulcami cytoszkieletu. Sygnał chemiluminescencyjny dla wszystkich białek sczytywany był na aparacie UVP ChemStudio Imaging System (Analytik Jena).

- Konwersja bisulfidowa DNA z wykorzystaniem zestawu EZ DNA Methylation Kit (ZymoResearch).

- Ocena jakości konwersji bisulfidowej dla kilku przypadków raków jajnika i BOT poprzez wykonanie metylo-specyficznego PCR z primerami komplementarnymi do regionu promotorowego genu *CRNDE*. Amplifikacji DNA dokonano przy użyciu polimerazy AmpliTaq Gold (Thermo Fisher Scientific). Do enzymatycznego oczyszczanie produktów PCR wykorzystano zestaw ExoSAP-IT (Thermo Fisher Scientific). Sekwencjonowanie DNA metodą Sangera przeprowadzono z użyciem zestawu BigDye Terminator v3.1 Cycle

Sequencing Kit (Thermo Fisher Scientific), a do oczyszczania produktu po sekwencjonowaniu użyto zestawu ExTerminator (A&A Biotechnology). Odczytu wyników sekwencjonowania dokonano na sekwenatorze 3500 Genetic Analyzer (Thermo).

- Hybrydyzacja DNA po konwersji bisulfidowej do mikromacierzy metylacyjnych Infinium® Methylation EPIC (Illumina) (zgodnie z protokołem przygotowanym przez producenta mikromacierzy, we współpracy z dr hab. Roksaną Iwanicką-Nowicką). Odczyt wyników z wykorzystaniem skanera mikromacierzy iScan (Illumina). Analiza bioinformatyczna i statystyczna w środowisku R z wykorzystaniem narzędzi dostępnych w pakiecie Bioconductor (dr Łukasz Szafron)

- Potwierdzenie zmian metylacyjnych w wybranych miejscach genomu metodą gradientowego metylo-specyficznego PCR w połączeniu z analizą produktów na żelu agarozowym oraz sekwencjonowaniem Sangera z wykorzystaniem własnoręcznie zaprojektowanych starterów (przy użyciu w.w. zestawów i maszyn).

Wyniki

Publikacja 1)

An Analysis of Genetic Polymorphisms in 76 Genes Related to the Development of Ovarian Tumors of Different Aggressiveness

W badaniach z wykorzystaniem paneli genowych skupiono się na analizie dwóch typów wariantów genetycznych: SNP (polimorfizmów jednonukleotydowych, *ang. single-nucleotide polymorphisms*) oraz non-SNP (głównie insercje, delecje i duplikacje, *ang. non-single-nucleotide polymorphisms*). Warianty były również rozpatrywane na podstawie ich wpływu na strukturę/funkcję kodowanego białka. Tym samym wyróżniono dwie główne grupy polimorfizmów: o umiarkowanym ("MODERATE") oraz silnym ("HIGH") wpływie na strukturę/funkcję kodowanych białek. Obie grupy wariantów były analizowane zarówno osobno, jak i łącznie. Do zmian o umiarkowanym wpływie zostały zaklasyfikowane: warianty zmiany sensu (skutkujące powstaniem innego aminokwasu, ang. *missense variants*), insercje i delecje niezmieniające ramki odczytu (trzynukleotydowe lub będące wielokrotnością trójki). Do zmian o charakterze "HIGH" zaliczono: insercje oraz delecje niebędące wielokrotnością trójki (najczęściej były to zmiany jednonukleotydowe), przedwczesne pojawienie się kodonu STOP, utrata kodonu START lub STOP, obecność wariantów w miejscach splicingowych na końcu 3' oraz 5'.

Z wykorzystaniem panelu 44 genów zidentyfikowano łącznie 85 unikatowych, wcześniej nieopisanych wariantów genetycznych (71 SNP i 14 non-SNP). Biorąc pod uwagę wszystkie grupy guzów oraz wszystkie typy wariantów (SNP i non-SNP, zarówno o umiarkowanym, jak i silnym wpływie na strukturę/funkcję kodowanego białka) najczęściej zmienionymi genami były *BRCA1, BRCA2, FANCA, SEM1* oraz *TP53*. Przy uwzględnieniu wariantów o jedynie silnym wpływie ("HIGH"), największą częstością zmian, wyłącznie w grupie hgOvCa, charakteryzowały się geny *BRCA1* oraz *TP53*. Co ciekawe liczba SNP, przede wszystkim o charakterze "MODERATE", była istotnie wyższa w grupie BOT bez mutacji *BRAF* V600E w porównaniu do wszystkich pozostałych grup guzów. Z kolei guzy BOT.V600E charakteryzowały się istotnie niższą liczbą takich SNP niż hgOvCa. Jednakże w grupie hgOvCa liczba wariantów genetycznych wyłącznie o silnym wpływie (zarówno SNP, jak i non-SNP) była istotnie wyższa w porównaniu do pozostałych grup nowotworów (poza porównaniem lgOvCa vs hgOvCa dla SNP o charakterze „HIGH").

W przypadku panelu „hot-spot" odkryto 82 unikatowe, wcześniej nieopisane warianty genetyczne (75 nowych SNP i 7 nowych non-SNP). Biorąc pod uwagę wszystkie grupy guzów oraz wszystkie typy wariantów (SNP i non-SNP, „HIGH" i „MODERATE") najczęściej zmienionymi genami były *PTCH1* (we wszystkich grupach guzów) i *TP53* (głównie w hgOvCa). Przy porównaniu obu paneli genowych, wyniki uzyskane w panelu „hot-spot" różniły się od wyników uzyskanych dla panelu 44-genów pod względem częstości występowania SNP o charakterze „MODERATE", lub „HIGH" i „MODERATE" analizowanych wspólnie w grupie BOT. W panelu „hot-spot" liczba takich SNP w BOT była istotnie niższa niż w obu grupach raków. Natomiast w panelu 44-genowym SNP o ww. charakterze występowały istotnie częściej w BOT w porównaniu do pozostałych grup guzów. Taka rozbieżność wynika m.in. z 10-krotnie wyższego pokrycia genomu w panelu 44-genów (ok. 360 tys. bp) w porównaniu do panelu hot-spot (ok.36 tys. bp), który uwzględniał tylko miejsca, gdzie występują znane, powtarzające się w różnych nowotworach mutacje. Jednak te rozbieżności między dwoma panelami genowymi nie występowały gdy brano pod uwagę tylko SNP o silnym wpływie lub wszystkie warianty non-SNP o charakterze "HIGH" lub „HIGH" i "MODERATE". W tym przypadku, w obu panelach genowych, zmiany te występowały istotnie częściej w grupie hgOvCa w porównaniu do BOTS.

Wszystkie warianty SNP i non-SNP przypadające na dany na gen i na daną próbkę zostały również zsumowane i zbinaryzowane (porównanie braku (0) i obecności jakiegokolwiek wariantu genetycznego (1) w analizowanym genie w badanej próbce). Analizy statystyczne przeprowadzone po zastosowaniu tego algorytmu (przy użyciu testów Chi kwadrat i dokładnego Fishera) wykazały, że genem najbardziej różnicującym mniej agresywne nowotwory (BOT, BOT.V600E i lgOvCa) od najbardziej agresywnych (hgOvCa) był *TP53,* który był istotnie częściej zmutowany w hgOvCa. Wyniki te uzyskano dla obu paneli oraz obu grup polimorfizmów (zarówno „MODERATE" jak i „HIGH" i „MODERATE" analizowanych wspólnie). Jedyny wyjątek od tej reguły został znaleziony dla zmian o silnym wpływie w porównaniu lgOvCa vs. hgOvCa w panelu „hot-spot", gdzie nie zaobserwowano istotności statystycznej. Powodem była zapewne niewielka liczebności grupy lgOvCa oraz obecność w jednym przypadku lgOvCa dwóch zmian SNP o charakterze HIGH (chr17:g.7674921C>A, p.Glu204Ter i chr17:g.7676218C>A, p.Glu51Ter). Zgodnie z literaturą, warianty w genie *TP53* nie występują/występują bardzo rzadko w BOTS oraz lgOvCa (15,27). Nasze badania to potwierdziły. Warianty w *TP53* praktycznie nie wystąpiły w tych nowotworach. Wyjątkiem były dwie próbki BOT (zmiany w *TP53* dla tych BOT zidentyfikowane zostały w obu panelach genowych) oraz 1 przypadek lgOvCa z ww. dwoma wariantami SNP o charakterze „HIGH" (tylko w panelu „hot-spot"). Żadnego z tych SNP obecnego w lgOvCa nie znaleziono w

panelu 44-genowym, prawdopodobnie ze względu na niewielką częstość ich występowania (odsetek zmian w danym miejscu w genomie), wynoszącą odpowiednio 11% i 14%, oraz odmienną technikę wzbogacania DNA (sondy Sequence Capture w panelu 44 genów oraz technika PETE (ang. Primer Extension Target Enrichment) w panelu „hot-spot").

Innymi genami, o których warto wspomnieć, są *BRCA1* i *BRCA2*. W panelu 44 genów zarówno *BRCA1* jak i *BRCA2* były częściej zmienione w BOT niż w hgOvCa (głównie dla wariantów "MODERATE"). Jednakże właściwie wszystkie te warianty miały charakter zmian jednonukleotydowych (SNP). Gdy pod uwagę były brane tylko warianty o silnym wpływie na strukturę/funkcję kodowanych białek ("HIGH"), ich liczba była istotnie wyższa w hgOvCa w porównaniu do pozostałych grup guzów (tylko dla *BRCA1*, nie dla *BRCA2*) w obu panelach. Warto zaznaczyć, że w samym panelu "hot-spot", gen *BRCA2* nie został uwzględniony, podczas gdy liczba polimorfizmów w *BRCA1* była istotnie wyższa w hgOvCa niż w BOT, niezależnie od tego, czy uwzględniono tylko warianty o silnym wpływie ("HIGH"), czy wszystkie warianty genetyczne ("HIGH"/"MODERATE"). W panelu analizującym „hot-spoty" nie stwierdzono żadnych zmian w *BRCA1* zarówno o umiarkowanym, jak i o silnym wpływie w grupach BOT i lgOvCa. Jeden SNP o charakterze "MODERATE" (chr17:g.43057132C>A) był znaleziony w jednej próbce BOT.V600E. Wyniki uzyskane dla panelu 44 genów są zgodne z wynikami zawartymi w pracy z 2020 r., gdzie na dużej grupie pacjentów z guzami jajnika stwierdzono, że częstość zmian w genach *BRCA1/2* jest podobna w hgOvCa i BOTS (odpowiednio 30,9% i 28,9%) (28). Niemniej wyniki uzyskane w panelu „hot-spot" zgadzają się z obecnym stanem wiedzy, który mówi, że zmiany w genach *BRCA1/2* prowadzące do upośledzenia działania funkcji BRCA1 i BRCA2 występują głównie w zaawansowanych rakach jajnika (3). Należy też pamiętać, że rozbieżności w wynikach uzyskanych dla każdego z paneli mogą być spowodowane powyżej opisanymi różnicami w pokryciu genomu (10-krotnie większy obszar pokrycia dla panelu 44 genów), oraz różnymi technikami tworzenia bibliotek wykorzystywanymi w obu panelach.

Na uwagę zasługuje również gen *KRAS*, w którym warianty o umiarkowanym lub silnym/umiarkowanym wpływie na kodowane białko, różnicowały najlepiej BOT (bez mutacji *BRAF* V600E) od wszystkich innych grup nowotworów z wyjątkiem lgOvCa. *KRAS* był częściej zmutowany w BOT i lgOvCa niż w grupach BOT.V600E lub hgOvCa. Potwierdza to podobieństwo molekularne między tymi dwiema grupami guzów. Jednocześnie taki wynik pokazuje, że w BOT bez wariantu V600E w genie *BRAF*, obecne są mutacje aktywujące w *KRAS*. Dla grupy lgOvCa charakterystyczna była również większa częstość zmutowania w dwóch innych genach, *ATM* i *NRAS*. *ATM* był częściej zmieniony w lgOvCa niż w grupie BOT.V600E, ale ta prawidłowość

ograniczała się tylko do wariantów o umiarkowanym wpływie (p = 0,036). Jeśli chodzi o *NRAS*, przede wszystkim zmiany typu "MODERATE" występowały istotnie częściej w lgOvCa niż w trzech pozostałych grupach nowotworów.

Podobnie do *KRAS*, geny kodujące białka zaangażowane w ubikwitynację były częściej zmienione w grupie BOT i odróżniały te guzy od raków jajnika. W dwóch genach zaangażowanych w ubikwitynację (*FANCB* i *SEM1)* warianty o charakterze "MODERATE" były zidentyfikowane częściej w BOT niż w rakach (*SEM1*) lub tylko w porównaniu do hgOvCa (*FANCB*). Warianty w tych dwóch genach nie różnicowały BOT od BOT.V600E.

W analizie regresji przeprowadzonej dla obu paneli genowych skupiono się tylko na wynikach, które były zgodne dla analiz jedno i wieloczynnikowych. Z obu paneli genowych, po uwzględnieniu wartości pod krzywą ROC (AUC, służącą do oceny zdolności dyskryminacyjnych modeli) oraz wartości p, najlepszym markerem dla raków jajnika były zmiany w genie *FANCI*. Gen ten jest doskonałym kandydatem na marker prognostyczny u pacjentek z zaawansowanym rakiem jajnika, w którym nie stwierdzono akumulacji białka TP53. Obecność wariantów w *FANCI* była lepszym predyktorem wznowy niż choroba resztkowa (RT, ang. *residual tumor*) (HR 40,02 i p = 0,0022 dla *FANCI* vs HR 34,1 i p = 0,0077 dla RT >= 2cm oraz HR 22,77 i p = 0,01 dla RT < 2cm), co czyni go negatywnym markerem prognostycznym. Poza *FANCI* obiecującymi markerami prognostycznymi dla hgOvCa były *FANCF* i *TSC2*. Natomiast obecność wariantów w *BRCA2* była wartościowym predyktorem odpowiedzi na leczenie. Dla grupy BOTS jedynym genem, który został zidentyfikowany w analizach regresji, był *PARP1*. Niemniej okazał się on również przydatnym markerem prognostycznym. Warianty w tym genie wpływały na zwiększone ryzyko wznowy (HR 6,02, p = 0,01). Co więcej, model dla tego genu odznaczał się bardzo dobrymi właściwościami dyskryminacyjnymi (AUC dla modelu jednoczynnikowego: 85%, wieloczynnikowego: 88,1%. Czułość na poziomie 1, natomiast specyficzność = 0,729).

W celu potwierdzenia wpływu wybranych wariantów genetycznych na ekspresję odpowiadających im białek przeprowadzono analizy Western blot (WB) dla:

- NBN (wariant non-SNP: chr8:g.89971217_89971221del; p.Lys219AsnfsTer16)

- CHEK2 (wariant non-SNP: chr22:g.28695869del; p.Thr367MetfsTer15)

- TP53 (warianty zmiany sensu (SNP) skutkujące akumulacją białka: chr17:g.7675085C>T; p.Cys176Tyr, chr17:g.7673824C>G; p.Gly266Arg, chr17:g.7676040C>G; p.Arg110Pro, chr17:g.7673776G>A; p.Arg282Trp)

- TP53 (warianty non-SNPs: chr17:g.7674900dup; p.Thr211AsnfsTer5, chr17:g.7670686del; p.Arg342GlufsTer3, 3chr17:g.7674241del; p.Cys242AlafsTer5, chr17:g.7676078del; p.Pro98LeufsTer25, chr17:g.7676041_7676042insTTTC; p.Arg110GlufsTer40.

- FANCI (SNP: 89285210C>T; p.Leu605Phe)

- FANCD2 (ocena ekspresji FANCD2 w próbkach z ww. wariantem FANCI p.Leu605Phe, oraz niezależne przeanalizowanie ekspresji FANCD2 z obecnym SNP: chr3:g.10073349G>T; p.Gly901Val)

- CHEK1 (SNP: chr11:g.125625996G>A; p.Trp79Ter)

W próbkach posiadających wyżej wymienione warianty non-SNP w genach *NBN*, *CHEK2* oraz *TP53* zaobserwowano obniżoną ekspresję/brak ekspresji białek kodowanych przez te geny. Dla próbek z wariantami zmiany sensu w genie *TP53* zaobserwowano zwiększony sygnał dla białka TP53. Natomiast dla białek FANCI, FANCD2 oraz CHEK1 uzyskano nietypowe wyniki. Guzy z wariantem p.Leu605Phe w FANCI, w których nie stwierdzono dodatkowo obecności żadnych wariantów polimorficznych w genach *BRCA1/2*, nie wykazywały ekspresji zmutowanego FANCI. Inaczej sytuacja wyglądała w próbkach z jakimikolwiek wariantami w genach *BRCA1/2*. W takim przypadku ekspresja zmutowanego FANCI była wysoka. Ponadto ta sama analiza WB ujawniła korelację między ekspresją białek FANCI i FANCD2 (będącego partnerem molekularnym FANCI (29)), niezależnie od tego, czy w *FANCD2* występowały jakiekolwiek warianty genetyczne. Obecność najczęściej występującego wariantu chr3:g.10073349G>T (p.Gly901Val) w *FANCD2* również nie korelowała z jego ekspresją. Wyniki z analiz WB uzyskane dla FANCI, razem z wynikami regresji, jednoznacznie wskazują na istotną rolę, jaką FANCI odgrywa u pacjentek z rakiem jajnika i pokazują, że działanie tego genu/białka uzależnione jest od tła molekularnego, przede wszystkim od aktywności kluczowych supresorów BRCA1/2 i TP53.

Ciekawy wynik uzyskano również dla SNP w genie *CHEK1* (chr11:g.125625996G>A, p.Trp79Ter), prowadzącego do powstania przedwczesnego kodonu terminacyjnego. W guzach, w których zmiana ta występowała z dużą częstością zaobserwowano niespodziewanie wysoką ekspresję białka CHEK1 (im wyższy odsetek zmienionego allelu, tym silniejszy sygnał dla CHEK1). Na podstawie dostępnych danych literaturowych oraz naszych własnych badań nie sposób jednoznacznie stwierdzić, czy CHEK1 pełni funkcję onkogenu czy supresora w guzach jajnika. Niemniej jednak dalsze badania jego wariantów wydają się interesujące w kontekście potencjalnych terapii ukierunkowanych z użyciem preksasertybu, selektywnego inhibitora CHEK1. Badania wykazały, że jego zastosowanie, jako pojedynczego leku lub w połączeniu z inhibitorami PARP,

wydłużało przeżycie pacjentów z hgOvCa (30). Ta kombinacja inhibitorów może być potencjalnie przydatna w leczeniu guzów granicznych, ponieważ, jak wyżej wspomniano, polimorfizmy w *PARP1* zostały zidentyfikowane w naszych badaniach jako negatywny marker prognostyczny w BOTS. Dodatkowo niektóre z naszych BOTS zawierały opisany powyżej wariant CHEK1 p.Trp79Ter.

Publikacja 2)

The Diversity of Methylation Patterns in Serous Borderline Ovarian Tumors and Serous Ovarian Carcinomas

W tym badaniu, ze względu na wysokie koszty eksperymentu, wykorzystano wyłącznie część pierwotnych guzów jajnika typu surowiczego. Badanie obejmowało analizę pojedynczych miejsc metylacji (CpG/DMP, ang. *differentially methylated probes*), całych regionów genomu, niezależnych od lokalizacji genów (DMR, ang. *differentially methylated regions*) oraz funkcjonalnych regionów genowych (złożonych z CpG w obrębie promotorów (proksymalnego i dystalnego), egzonów, intronów, cds (ang. *coding sequence*), lncRNA, a także 3' i 5' UTRów). Ponadto skupiono się na analizie metylacyjnej w obrębie obu nici DNA jednocześnie, jak również niezależnie dla poszczególnych nici (+ i -).

W pierwszej kolejności przeanalizowano status metylacji genów osi TP53-MDM2-CDKN1A. W grupie lgOvCa (zgodnie z obecnym stanem wiedzy) nie zaobserwowano akumulacji białka TP53, która jest częstym zjawiskiem w zaawansowanych rakach jajnika (hgOvCa) (31). Jednak ponieważ zmiany metylacyjne mogą poprzedzać wystąpienie mutacji (22,23), naszym celem było sprawdzenie, czy metylacja *TP53*, jak również jego bezpośrednich partnerów (*MDM2* i *CDKN1A*) jest istotnie zmieniona w mniej zaawansowanych guzach (BOTS i lgOvCa). W lgOvCa zaobserwowano hipermetylację w prawie każdym regionie *TP53* (największe zmiany były widoczne w promotorach i pierwszym egzonie, czyli regionach mających najsilniejszy wpływ na późniejszą ekspresję białka (32,33)). Co więcej, metylacja wszystkich egzonów *TP53* była istotnie wyższa w lgOvCa w porównaniu do hgOvCa. W przypadku onkogenu MDM2 zaobserwowano odwrotny efekt, ale tylko w porównaniach hgOvCa vs BOTS, i tylko w regionie bliższego promotora. Jeśli chodzi o *CDKN1A*, który koduje białko supresorowe p21, wbrew oczekiwaniom zaobserwowano niższe poziomy metylacji w obrębie proksymalnego promotora i pierwszego egzonu w lgOvCa i hgOvCa w porównaniu z BOTS. Co ciekawe, pierwszy egzon genu *CDKN1A* był bardziej hipometylowany w lgOvCa niż w hgOvCa. Ponadto nie zidentyfikowano różnic w metylacji w żadnym z trzech wyżej wymienionych genów między BOT a BOT.V600E.

Całościowa analiza miejsc metylacyjnych (zarówno CpG jak i DMR) wykazała globalną hipometylację genomu w rakach (szczególnie w hgOvCa) w porównaniu do mniej złośliwych guzów. Zgodnie z obecnym stanem wiedzy najwięcej różnic metylacyjnych (zarówno w liczbie CpG jak i DMR) zaobserwowano pomiędzy lgOvCa a hgOvCa oraz pomiędzy BOT a hgOvCa. Co ciekawe, grupa BOT.V600E cechowała się najniższą liczbą istotnie zmienionych CpG i DMR w

porównaniu do wszystkich pozostałych grup guzów. Co więcej, w grupie BOT.V600E zaobserwowano hipometylację genomu w porównaniu z BOT. Mogłoby to sugerować ich większą aktywność metaboliczną i agresywność. Przy analizie DMR, które różnicowały poszczególne grupy guzów, zaobserwowano, że 10 kolejnych, najbardziej zmienionych DMRów różnicujących BOT (bez mutacji *BRAF* V600E) od lgOvCa, znajdowało się na tym samym obszarze genomu na chromosomie 6 o wielkości 3,5 mln par zasad, obejmującym region MHC (ang. *major histocompatibility complex*). W żadnym z 5 pozostałych porównań guzów nie zaobserwowano takiego zjawiska.

Analizy ontologiczne wykazały kilka głównych grup procesów, które występowały we wszystkich porównaniach guzów. Były to procesy związane z różnicowaniem/rozwojem, adhezją, układem nerwowym, cyklem komórkowym oraz metabolizmem RNA. Zaobserwowano również terminy ontologiczne charakterystyczne tylko dla wybranych grup guzów, i tak np. procesy związane z metabolizmem kwasów tłuszczowych i adipogenezy były wzbogacone w geny hipermetylowane tylko w grupie BOT, a procesy związane z białkiem KRAS oraz EMT (przejściem epitelialno-mezenchymalnym, ang. *epithelial-mesenchymal transition*) były charakterystyczne dla porównania lgOvCa vs hgOvCa (hipermetylacja genów zaangażowanych w te procesy była charakterystyczna dla grupy lgOvCa).

W analizach regresji ponownie skupiono się na wynikach zgodnych dla analiz jedno i wieloczynnikowych. Ze względu na ogromną liczbę uzyskanych DMRów, które mogłyby zostać potencjalnymi markerami, zdecydowano się zastosować filtrowanie istotności statystycznej w poszczególnych analizach (w rakach, dla analiz regresji Cox'a i logistycznej były to odpowiednio wartości $p < 0.0005$ i $p < 0.005$. Natomiast ze względu na mniejszą liczbę przypadków, w BOTS zdecydowano się wszędzie zostawić wartość $p < 0,05$). Tym sposobem uzyskano listę kilkudziesięciu najbardziej obiecujących genów, których zmieniona metylacja istotnie wpływała na przeżycie i wznowę (hgOvCa), odpowiedź na leczenie (hgOvCa) i ryzyko wystąpienia mikroinwazji/wszczepów (BOTS). Dla BOTS nie uzyskano żadnych znamiennych wyników dla analiz prognostycznych. W BOTS najlepszymi zdolnościami dyskryminacyjnymi charakteryzowały się DMRy w obrebie genów *BAIAP3, IL34, WNT10A, NEU1* i *SLC44A4*. Natomiast w hgOvCa były to DMRy w genach *HMOX1, TCN2, PES1, RP1-56J10.8, ABR, NCAM1, RP11-629G13.1, AC006372.4* i *NPTXR* oraz w jednym regionie międzygenowym na chromosomie 16 (pojedynczy CpG na nici (-); chr16:g.(−)880831–880831).

Publikacja 3) Edytorial

Special Issue: Biomarkers and Early Detection Strategies of Ovarian Tumors

Praca stanowi wprowadzenie do specjalnego wydania czasopisma International Journal of Molecular Sciences, jak również zawiera podsumowanie aktualnej wiedzy nt. występowania, czynników ryzyka, prewencji, diagnostyki oraz leczenia (chemioterapia oraz terapie ukierunkowane) raków jajnika.

Wnioski

- Analiza wariantów polimorficznych z wykorzystaniem 2 paneli genowych uwidoczniła wiele genów, które różnicują wszystkie grupy analizowanych guzów. Poza mutacjami w genach *TP53* i *BRCA1,* które istotnie częściej występowały w najbardziej zaawansowanych rakach jajnika, wykazano, że warianty polimorficzne w innych genach wydają się odgrywać ważną rolę w BOT (*KRAS*) i w lgOvCa (*KRAS* i *NRAS*), ale nie w hgOvCa, co po raz kolejny dowodzi, że guzy graniczne i lgOvCa są ze sobą molekularnie spokrewnione. Ponadto, geny zaangażowane w ubikwitynację (*SEM1, FANCB*) również były istotnie częściej zmienione w grupie BOT. Poza wariantami w *KRAS* i *BRAF,* żaden z przebadanych genów nie różnicował BOT od BOT.V600E.

- Znaleziono markery prognostyczne o dużych zdolnościach dyskryminacyjnych dla BOTS i hgOvCa. Dla hgOvCa najlepszym markerem były zmiany w genie *FANCI,* natomiast dla BOTS była to obecność SNP w genie *PARP1*. Co więcej, wartość genu *FANCI* jako markera, jak również ekspresja białka FANCI*,* były związane ze statusem kluczowych supresorów TP53 i BRCA1/2.

- Hipometylacja genomu zwiększa się wraz ze wzrastającą agresywnością guzów jajnika, będąc najsilniejszą w hgOvCa. Grupa guzów BOT.V600E odbiega pod względem metylacji nie tylko od raków, ale również od BOT bez mutacji *BRAF* V600E. W guzach tych zaobserwowano najmniejszą liczbę CpG i DMR o znamiennie zmienionej metylacji w porównaniu ze wszystkimi innymi grupami.

- Pomimo nielicznych mutacji (dwóch SNP zidentyfikowanych wyłącznie w panelu „hot-spot") oraz braku akumulacji białka TP53 w grupie lgOvCa, metylacja tego genu jest istotnie wyższa w tej grupie guzów, nie tylko w porównaniu z BOTS, ale również z hgOvCa. Może to oznaczać, że w lgOvCa inaktywacja supresora TP53 dokonuje się przede wszystkim na drodze epigenetycznej, a nie w wyniku mutacji.

- Zmiany metylacyjne w genach związanych z układem odpornościowym (i mikrośrodowiskiem guza) prawdopodobnie odgrywają kluczową rolę w transformacji guzów granicznych do lgOvCa, gdyż 10 najbardziej zmienionych DMR, w porównaniu BOT vs lgOvCa, znajdowało się na 3,5-milionowym obszarze genomu na chromosomie 6 (region MHC). Co więcej, jednym z markerów o najlepszych zdolnościach dyskryminacyjnych w grupie BOTS były zmiany metylacyjne w obrębie genu *IL34,*

37

kodującego interleukinę 34, wpływającą na różnicowanie makrofagów w kierunku immunosupresyjnej populacji TAM (ang. *tumor-associated macrophages*). Hipermetylacja DMRów w obrębie *IL34* (która najprawdopodobniej prowadzi do zmniejszonej ekspresji IL34), była korzystnym czynnikiem predykcyjnym, zmniejszającym ryzyko powstania mikroinwazji i wszczepów w guzie.

- Poza wspomnianą wyżej *IL34*, zmiany metylacyjne w wielu innych genach okazały się dobrymi markerami predykcyjnymi (zarówno dla hgOvCa, jak i BOTS) lub prognostycznymi (hgOvCa).

Bibliografia

1. Arora, T. *et al.* (2022) *Ovarian Cancer*, StatPearls Publishing.
2. Chan, J.K. *et al.* (2022) Symptoms of Women With High-Risk, Early-Stage Ovarian Cancer. *Obstet. Gynecol.*, **139**, 157.
3. Guo, T. *et al.* (2021) <p>Cellular Mechanism of Gene Mutations and Potential Therapeutic Targets in Ovarian Cancer</p>. *Cancer Manag. Res.*, **13**, 3081–3100.
4. Babaier, A. *et al.* (2022) Low-Grade Serous Carcinoma of the Ovary: The Current Status. *Diagnostics*, **12**, 458.
5. Wong, K.-K. *et al.* (2022) Integrated multi-omic analysis of low-grade ovarian serous carcinoma collected from short and long-term survivors. *J. Transl. Med.*, **20**, 606.
6. Hauptmann, S. *et al.* (2017) Ovarian borderline tumors in the 2014 WHO classification: evolving concepts and diagnostic criteria. *Virchows Arch.*, **470**, 125–142.
7. Seong, S.J. *et al.* (2015) Controversies in borderline ovarian tumors. *J. Gynecol. Oncol.*, **26**, 343–349.
8. Bourdel, N. *et al.* (2021) Borderline ovarian tumors: French guidelines from the CNGOF. Part 2. Surgical management, follow-up, hormone replacement therapy, fertility management and preservation. *J. Gynecol. Obstet. Hum. Reprod.*, **50**, 101966.
9. Timor-Tritsch, I.E. *et al.* (2019) New sonographic marker of borderline ovarian tumor: microcystic pattern of papillae and solid components. *Ultrasound Obstet. Gynecol. Off. J. Int. Soc. Ultrasound Obstet. Gynecol.*, **54**, 395–402.
10. Englisz, A. *et al.* (2024) Sensitivity and Specificity of Selected Biomarkers and Their Combinations in the Diagnosis of Ovarian Cancer. *Diagnostics*, **14**, 949.
11. Niu, L. *et al.* (2021) Recurrence characteristics and clinicopathological results of borderline ovarian tumors. *BMC Womens Health*, **21**, 134.
12. Shih, K. *et al.* (2011) Risk factors for recurrence of ovarian borderline tumors. *Gynecol. Oncol.*, **120**, 480–484.
13. Bjørge, T. *et al.* (2004) BRCA1 mutations in ovarian cancer and borderline tumours in Norway: a nested case–control study. *Br. J. Cancer*, **91**, 1829–1834.
14. Lakhani, S.R. *et al.* (2004) Pathology of Ovarian Cancers in BRCA1 and BRCA2 Carriers. *Clin. Cancer Res.*, **10**, 2473–2481.
15. Singer, G. *et al.* (2005) Patterns of p53 mutations separate ovarian serous borderline tumors and low- and high-grade carcinomas and provide support for a new model of ovarian carcinogenesis: a mutational analysis with immunohistochemical correlation. *Am. J. Surg. Pathol.*, **29**, 218–224.
16. Mayr, D. *et al.* (2006) KRAS and BRAF mutations in ovarian tumors: a comprehensive study of invasive carcinomas, borderline tumors and extraovarian implants. *Gynecol. Oncol.*, **103**, 883–887.
17. Grisham, R.N. *et al.* (2013) BRAF Mutation is Associated with Early Stage Disease and Improved Outcome in Patients with Low-Grade Serous Ovarian Cancer. *Cancer*, **119**, 548–554.
18. Śmiech, M. *et al.* (2020) Emerging BRAF Mutations in Cancer Progression and Their Possible Effects on Transcriptional Networks. *Genes*, **11**, 1342.
19. Szafron, L.A. *et al.* (2024) The Clinical Significance of CRNDE Gene Methylation, Polymorphisms, and CRNDEP Micropeptide Expression in Ovarian Tumors. *Int. J. Mol. Sci.*, **25**, 7531.
20. Stemke-Hale, K. *et al.* (2013) Frequency of mutations and polymorphisms in borderline ovarian tumors of known cancer genes. *Mod. Pathol. Off. J. U. S. Can. Acad. Pathol. Inc*, **26**, 10.1038/modpathol.2012.194.

21. Ogrodniczak, A. *et al.* (2022) Association of recurrent mutations in BRCA1, BRCA2, RAD51C, PALB2, and CHEK2 with the risk of borderline ovarian tumor. *Hered. Cancer Clin. Pract.*, **20**, 11.

22. Heery, R. *et al.* (2021) DNA methylation variation along the cancer epigenome and the identification of novel epigenetic driver events. *Nucleic Acids Res.*, **49**, 12692–12705.

23. Hanson, H.E. *et al.* (2022) The Mutagenic Consequences of DNA Methylation within and across Generations. *Epigenomes*, **6**, 33.

24. Shih, I.-M. *et al.* (2010) Distinct DNA methylation profiles in ovarian serous neoplasms and their implications in ovarian carcinogenesis. *Am. J. Obstet. Gynecol.*, **203**, 584.e1-584.e22.

25. Zeller, C. *et al.* (2013) The DNA Methylomes of Serous Borderline Tumors Reveal Subgroups With Malignant- or Benign-Like Profiles. *Am. J. Pathol.*, **182**, 668–677.

26. Woroniecka, R. *et al.* (2022) Cryptic MYC insertions in Burkitt lymphoma: New data and a review of the literature. *PloS One*, **17**, e0263980.

27. Testa, U. *et al.* (2018) Ovarian Cancers: Genetic Abnormalities, Tumor Heterogeneity and Progression, Clonal Evolution and Cancer Stem Cells. *Medicines*, **5**, 16.

28. Lhotova, K. *et al.* (2020) Multigene Panel Germline Testing of 1333 Czech Patients with Ovarian Cancer. *Cancers*, **12**, 956.

29. Longerich, S. *et al.* (2014) Regulation of FANCD2 and FANCI monoubiquitination by their interaction and by DNA. *Nucleic Acids Res.*, **42**, 5657.

30. Neizer-Ashun, F. *et al.* (2021) Reality CHEK: Understanding the biology and clinical potential of CHK1. *Cancer Lett.*, **497**, 202–211.

31. Cole, A.J. *et al.* (2016) Assessing mutant p53 in primary high-grade serous ovarian cancer using immunohistochemistry and massively parallel sequencing. *Sci. Rep.*, **6**, 26191.

32. Chmelarova, M. *et al.* (2013) Methylation in the p53 promoter in epithelial ovarian cancer. *Clin. Transl. Oncol. Off. Publ. Fed. Span. Oncol. Soc. Natl. Cancer Inst. Mex.*, **15**, 160–163.

33. Brenet, F. *et al.* (2011) DNA Methylation of the First Exon Is Tightly Linked to Transcriptional Silencing. *PLoS ONE*, **6**, e14524.

Publikacje omówione w niniejszej rozprawie

Article

An Analysis of Genetic Polymorphisms in 76 Genes Related to the Development of Ovarian Tumors of Different Aggressiveness

Laura A. Szafron [1], Piotr Sobiczewski [2], Agnieszka Dansonka-Mieszkowska [3], Jolanta Kupryjanczyk [4] and Lukasz M. Szafron [1,*]

[1]   Maria Sklodowska-Curie National Research Institute of Oncology, 02-781 Warsaw, Poland; laura.szafron@gmail.com
[2]   Department of Gynecological Oncology, Maria Sklodowska-Curie National Research Institute of Oncology, 02-781 Warsaw, Poland
[3]   Cancer Molecular and Genetic Diagnostics Department, Maria Sklodowska-Curie National Research Institute of Oncology, 02-781 Warsaw, Poland
[4]   Department of Cancer Pathomorphology, Maria Sklodowska-Curie National Research Institute of Oncology, 02-781 Warsaw, Poland
*   Correspondence: lukszafron@gmail.com

Abstract: Borderline ovarian tumors (BOTS) are rare neoplasms of intermediate aggressiveness between cystadenomas and low-grade ovarian cancers (lgOvCa), which they share some molecular resemblances with. In contrast to the most frequent and well-described high-grade ovarian carcinomas (hgOvCa), the molecular background of BOTS and lgOvCa is less thoroughly characterized. Here, we aimed to analyze genetic variants in crucial tumor suppressors and oncogenes in BOTS (with or without the *BRAF* V600E mutation), lgOvCa, and hgOvCa in two gene panels using next-generation sequencing. Then, we verified the existence of selected polymorphisms by Sanger sequencing. Finally, Western blot analyses were carried out to check the impact of the selected polymorphisms on the expression of the corresponding proteins. Our study contributes to the molecular characterization of ovarian neoplasms, demonstrating divergent polymorphic patterns pointing to distinct signaling pathways engaged in their development. Certain mutations seem to play an important role in BOTS without the *BRAF* V600E variant (*KRAS*) and in lgOvCa (*KRAS* and *NRAS*), but not in hgOvCa. Additionally, based on multivariable regression analyses, potential biomarkers in BOTS (*PARP1*) and hgOvCa (*FANCI*, *BRCA2*, *TSC2*, *FANCF*) were identified. Noteworthy, for some of the analyzed genes, such as *FANCI*, *FANCD2*, and *FANCI*, *FANCF*, *TSC2*, the status of BRCA1/2 and TP53, respectively, turned out to be crucial. Our results shed new light on the similarities and differences in the polymorphic patterns between ovarian tumors of diverse aggressiveness. Furthermore, the biomarkers identified herein are of potential use as predictors of the prognosis and/or response to therapy.

Keywords: ovarian cancer; borderline ovarian tumor; DNA sequence variant; NGS; Western blot; *TP53*; *RAS*; *BRAF*; *BRCA1/2*

1. Introduction

Ovarian carcinoma (OvCa) is a common and complex malignant disease with a generally poor outcome and an exceptionally high mortality worldwide [1]. There are two main types of OvCa: high-grade (hgOvCa) and low-grade (lgOvCa) ovarian carcinomas. The former is the most common type, characterized by extreme genomic instability, chromosomal rearrangements, and frequently mutated genes, especially those encoding tumor suppressor proteins, such as *TP53*, *BRCA1*, and *BRCA2* [2]. By contrast, lgOvCa is a rare ovarian tumor characterized by a younger age at diagnosis, relative chemoresistance, and prolonged survival compared to its high-grade counterpart. Additionally, lgOvCa do not bear or rarely have mutations in *TP53* and *BRCA1/2* [3,4], and they (especially those of the serous subtype) share molecular resemblances with borderline ovarian tumors (BOTS) [5].

BOTS are regarded as neoplasms that are less aggressive than invasive carcinomas. They are also a rare entity (about 15% of epithelial ovarian neoplasms) and have relatively low malignant potential. In contrast to OvCa, BOTS predominantly occur in women at a reproductive age, are usually diagnosed at a lower FIGO stage, and have better survival rates. Despite these advantages, BOTS are difficult to diagnose preoperatively by imaging methods because there are no specific criteria to distinguish them from their malignant counterparts with high confidence [6]. Additionally, following the complete removal of the tumor, even 20% of BOTS may recur. Most BOTS recur as borderline tumors; however, in about 30% of patients with peritoneal implants, OvCa develops [5,7,8]. In contrast to hgOvCa, in BOTS, mutations in *TP53* and *BRCA1/2* are rare [9–11], whereas the most frequently mutated genes are *BRAF* and *KRAS* (especially in BOTS of the serous subtype). Mutations in these genes are sometimes also found in serous lgOvCa, while, in patients with hgOvCa, their occurrence is rare [12,13]. In addition to *KRAS*, *BRAF*, *BRCA1/2*, and *TP53*, a few studies have also investigated the frequency of *PIK3CA*, *EGFR*, *CTNNB1*, *RAD51C*, *PALB2*, *CHEK2*, and *PTEN* mutations in BOTS compared to invasive ovarian carcinomas [14,15]. Nevertheless, data on the polymorphic status of tumor suppressors and oncogenes in BOTS remain scarce. OvCa are far better genetically characterized than BOTS. Still, there are discrepancies as to the clinical significance of some molecular markers that need to be dispelled.

Therefore, in BOTS without the *BRAF* V600E variant (here referred to as BOT), in BOTS harboring this genetic variant (BOT.V600E), and in lgOvCa and hgOvCa, we aimed to characterize the polymorphic status of 76 genes using two next-generation sequencing (NGS) gene panels. The first one comprised oncogenes and tumor suppressor genes involved in the development of hereditary ovarian cancer (41 genes) plus *CRNDE*, *IRX5*, and *CEBPA*. The second panel contained hot spots in genes frequently mutated in sporadic human cancers (37 genes), most of which were missing in the first gene panel. Except for the thorough examination of gene polymorphisms and their association with various clinicopathological parameters with the use of uni- and multivariable regression models, our workflow involved the confirmation of selected gene variants by Sanger sequencing, and also the verification of whether there is a correlation between the presence of the given polymorphism and the expression alterations of the corresponding protein. Hence, this work may contribute to a better understanding of the ovarian tumor molecular landscape and lay grounds for the discovery of new biomarkers.

2. Results

2.1. Distribution of Genetic Polymorphisms in Different Tumor Groups

After the NGS and bioinformatic analyses, we obtained a list of genetic variants with a high or moderate impact on the corresponding protein's structure and function. Genetic alterations with these impacts were either analyzed in combination or separately to determine whether the variants with distinct impacts exhibit concordant or discordant effects on the ovarian tumor outcome. Additionally, two questions need to be clarified. Firstly, in the 44-gene panel, one extra oncogene, the investigation of which was unintended, *KCNMB3* [16], was enriched. This was probably because its locus partially overlaps that of the *PIK3CA* gene, which was originally included in the panel and encoded by the opposite DNA strand. Similarly, in the hot-spot panel, one extra gene, *FBXW7-AS1*, was enriched, being an antisense transcript of the *FBXW7* gene [17], present in the hot-spot panel. Secondly, polymorphisms in the *CRNDE* gene (enriched in the 44-gene panel) were earlier described in another paper by our team [18], and therefore they will not be addressed in this article.

When using the 44-gene panel in the entire group of ovarian tumors, we discovered 85 unique, previously undescribed variants (71 new SNPs and 14 new non-SNPs). The list of all the detected variants is presented in a supplementary file named Supplement-variants.xlsx. The cumulative frequency of all the detected genetic variants (SNPs and non-SNPs combined) in different groups of tumors is presented in Figure 1A,B (variants with a high or moderate

(A) or only a high (B) impact) and Figure S1A (variants with a moderate impact only). In Figures 1C–F and S1C,E, relevant box plots, depicting the overall frequency of SNP and non-SNP variants separately in different ovarian tumor groups, are shown. These box plots are additionally supplemented with detailed statistical tests. Furthermore, the mean counts of either SNP or non-SNP alterations per gene per tumor group are also presented in Figure S2A–F. When considering all the variants together (Figure 1A), the most frequently altered genes (the fraction of altered samples in at least one group >0.5) were *BRCA1*, *BRCA2*, *FANCA*, *SEM1*, and *TP53*. However, if only high-impact variants are considered (Figure 1B), the highest frequencies of genetic alterations (>0.3) were present in the *BRCA1* and *TP53* genes, and in the hgOvCa group only. By contrast, the number of SNPs with a high/moderate (Figure 1C) or only a moderate (Figure S1C) impact on a protein structure/function was significantly higher in the BOT without the *BRAF* V600E mutation compared to all the remaining tumor groups. Moreover, the same analysis revealed that the BOT.V600E tumors were characterized by a significantly lower number of SNPs than hgOvCa. Noteworthy, in hgOvCa, the number of high-impact genetic variants (either SNPs or non-SNPs) was significantly elevated compared to all the other tumor groups, except for SNPs with a high impact in the lgOvCa vs. hgOvCa comparison (Figure 1D–F). Remarkably, the numbers of non-SNPs with only a moderate impact on a protein structure/function did not significantly differentiate any ovarian tumor groups (Figure S1E), conceivably due to the low frequency of these variants (six such changes were found in only three genes, *ATRX*, *CHEK1*, and *PTEN* (Figure S2D), exclusively in nine hgOvCa tumors (see Supplement-variants.xlsx)).

For the hot-spot panel, we discovered 82 unique, not previously described genetic variants (75 new SNPs and 7 new non-SNPs). Their list can be found in Supplement-variants.xlsx. The cumulative frequency of all the detected variants (SNPs and non-SNPs combined) in all the genes in every group of tumors is presented in Figure 2A,B (variants with a high or moderate (A) or only a high (B) impact) and Figure S1B (variants with a moderate impact only). In Figures 2C–F and S1D,F, relevant box plots, depicting the overall frequency of SNP and non-SNP variants separately in different ovarian tumor groups, are shown. These box plots are additionally supplemented with detailed statistical tests. Furthermore, mean counts of either SNP or non-SNP alterations per gene per tumor group are also presented in Figure S2G–L. When considering high and moderate variants together, and with SNPs and non-SNPs combined (Figure 2A), the most frequently altered genes (the fraction of altered samples in at least one group > 0.5) were *PTCH1* (altered in all tumor groups) and *TP53* (altered mainly in hgOvCa). Interestingly, genetic variants in the *BRCA1* gene were less frequently identified in the hot-spot panel than in the 44-gene panel. Nevertheless, if only the high-impact variants are considered, the mutational profiles of *BRCA1* and *TP53*, detected with both panels, were similar, revealing the high frequency of genetic alterations within these genes in OvCa, especially in hgOvCa (Figures 1B and 2B). Notably, in the hot-spot panel, we also detected two variants in the *TP53* gene in one lgOvCa sample (chr17:g.7674921C>A, p.Glu204Ter and chr17:g.7676218C>A, p.Glu51Ter). Neither of these SNPs were found in the 44-gene panel, probably due to their low frequencies, equaling 11% and 14%, respectively. It needs to be mentioned here that, in our bioinformatic workflow, all sequence variants less frequent than 10% were filtered out to eliminate alterations resulting from DNA polymerase errors and those too rare to both elicit an evident clinical effect and be successfully validated by Sanger sequencing.

When only SNPs are taken into account, the results for the hot-spot panel importantly differ from those obtained for the 44-gene panel with respect to the frequency of non-high-impact SNPs in the BOT group. In the hot-spot panel, the number of such SNPs in BOT was significantly lower than in both OvCa groups (Figures 2C and S1D). By contrast, in the 44-gene panel, non-high-impact SNPs in BOT were much more abundant than in all the remaining tumor groups (Figures 1C and S1C). Yet, this divergence disappeared when either high-impact SNPs or all non-SNPs were considered (Figures 1D–F and 2D–F), revealing the increased frequency of genetic alterations in hgOvCa compared to BOTS in both panels.
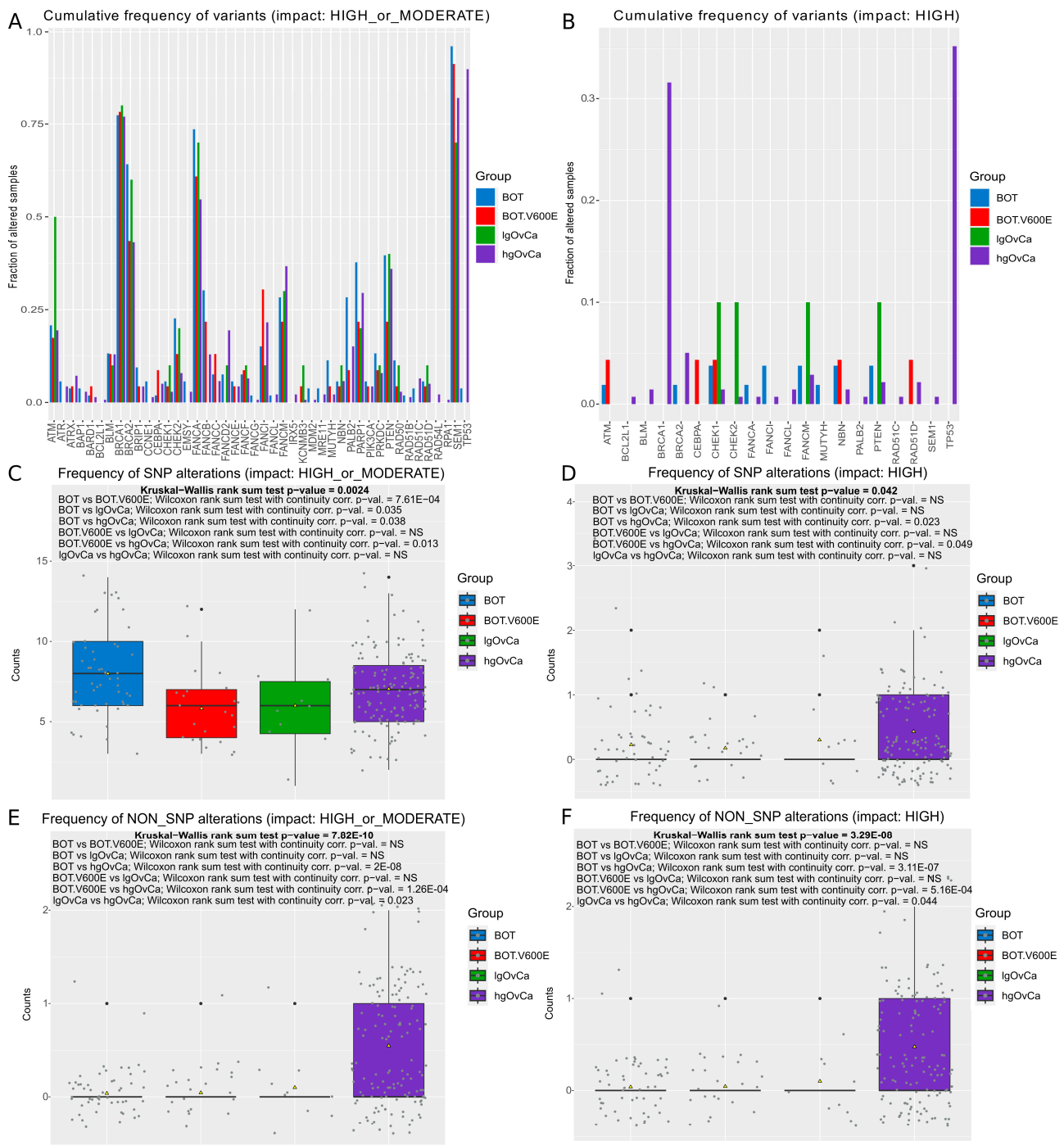
Figure 1. SNP and non-SNP variants—44-gene panel. (**A**,**B**) The cumulative frequency of all variants per gene in each tumor group ((**A**)—variants with a high or moderate impact, (**B**)—only the variants with a high impact). (**C–F**) Box plots demonstrating differences in the numbers of genetic variants between the analyzed groups of tumors for SNPs ((**C**) a high or moderate impact, (**D**) only a high impact) and non-SNPs ((**E**) a high or moderate impact, (**F**) only a high impact). Each box plot is additionally supplemented with the Kruskal–Wallis rank sum test (showing whether there is any statistically significant difference between the analyzed sets of variants) and the Wilcoxon rank sum test with continuity correction (the post hoc test applied to determine which tumor groups differed from each other). NS: not significant. Group sizes: BOT: *n* = 53; BOT.V600E: *n* = 23; lgOvCa: *n* = 10; hgOvCa: *n* = 139.
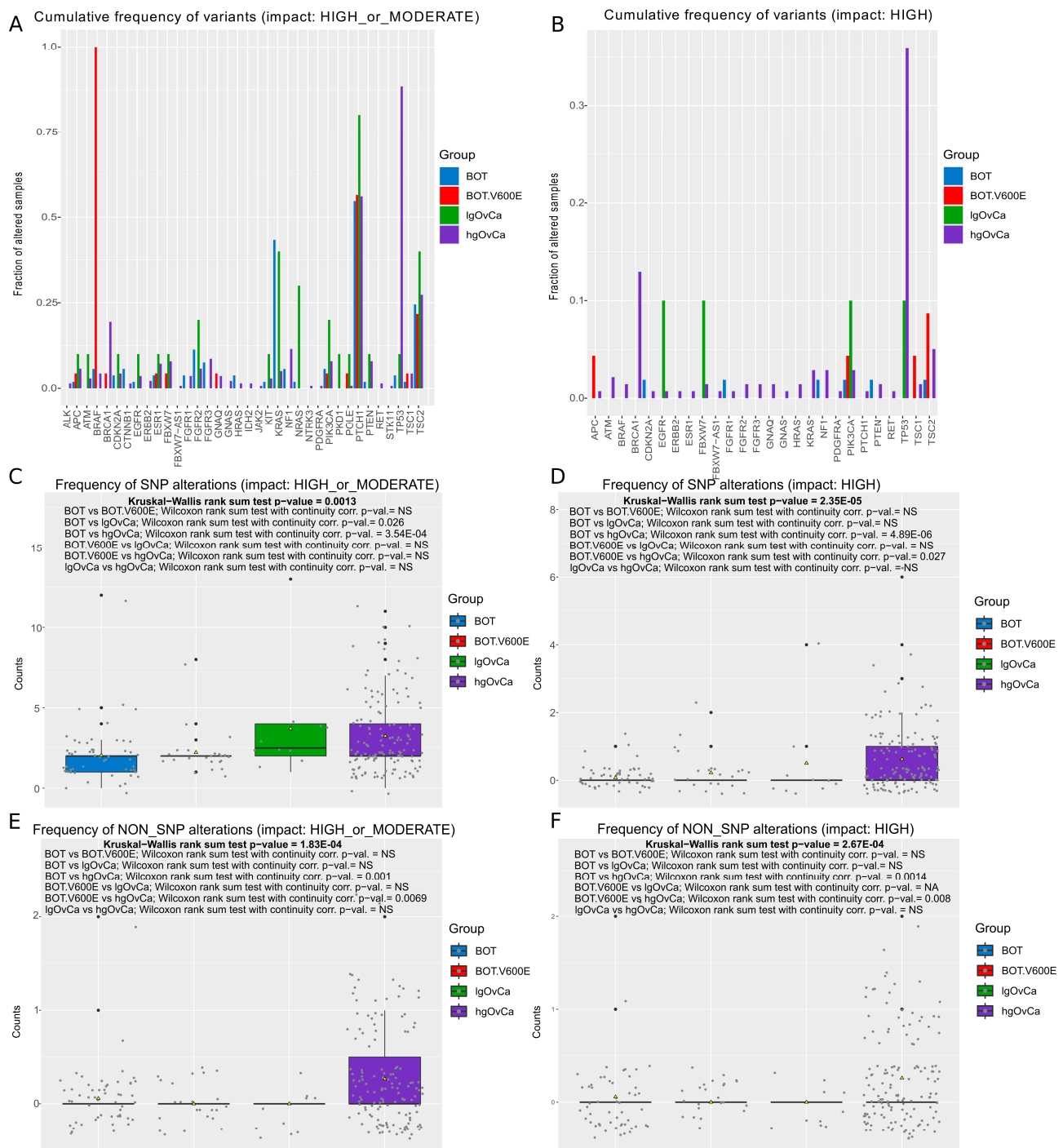
Figure 2. SNP and non-SNP variants—hot-spot gene panel. (**A**,**B**) Cumulative frequency of all variants (SNPs and non-SNPs combined) per gene in each tumor group ((**A**)—variants with a high or moderate impact, (**B**)—only the variants with a high impact). (**C**–**F**) Box plots demonstrating differences in the numbers of genetic variants between the analyzed groups of tumors for SNPs ((**C**) a high or moderate impact, (**D**) only a high impact) and non-SNPs ((**E**) a high or moderate impact, (**F**) only a high impact). Each box plot is additionally supplemented with the Kruskal–Wallis rank sum test (showing whether there is any statistically significant difference between the analyzed sets of variants) and the Wilcoxon rank sum test with continuity correction (the post hoc test applied to determine which tumor groups differed from each other). NS: not significant. Group sizes: BOT: *n* = 53; BOT.V600E: *n* = 23; lgOvCa: *n* = 10; hgOvCa: *n* = 139.

All SNP and non-SNP variants per gene per sample were summed and binarized (at least one variant present vs. no alteration). The subsequent statistical analysis of this dataset, shown in Table 1, revealed that *TP53* was the most differentiating gene between less aggressive tumors (BOT, BOT.V600E, and lgOvCa) and hgOvCa (in the latter, it was more frequently mutated), regardless of the gene panel and the variant impact. The only exception to this rule was found for high-impact alterations in the lgOvCa vs. hgOvCa comparison in the hot-spot panel, where no statistical significance was observed.

Table 1. Genetic variants with a high or moderate impact significantly differentiating ovarian tumor groups, identified with two gene panels.

			44-GENE PANEL			
			Impact HIGH or MODERATE			
			Group Comparison and *p*-Value			
Gene	**BOT vs. BOT.V600E**	**BOT vs. lgOvCa**	**BOT vs. hgOvCa**	**BOT.V600E vs. lgOvCa**	**BOT.V600E vs. hgOvCa**	**lgOvCa vs. hgOvCa**
TP53			5.67×10^{-31} (↑hgOvCa)		1.23×10^{-18} (↑hgOvCa)	1.8×10^{-9} (↑hgOvCa)
FANCB			9.71×10^{-3} (↑BOT)			
SEM1		2.51×10^{-2} (↑BOT)	1.01×10^{-2} (↑BOT)			
FANCA			2.61×10^{-2} (↑BOT)			
FANCD2			4.97×10^{-2} (↑hgOvCa)		1.52×10^{-2} (↑hgOvCa)	
BRCA2			1.47×10^{-2} (↑BOT)			
CHEK2			1.04×10^{-2} (↑BOT)			
MUTYH			1.44×10^{-2} (↑BOT)			
RAD50			2.83×10^{-2} (↑BOT)			
			Impact MODERATE			
			Group Comparison and *p*-Value			
Gene	**BOT vs. BOT.V600E**	**BOT vs. lgOvCa**	**BOT vs. hgOvCa**	**BOT.V600E vs. lgOvCa**	**BOT.V600E vs. hgOvCa**	**lgOvCa vs. hgOvCa**
TP53			3.48×10^{-14} (↑hgOvCa)		6.97×10^{-9} (↑hgOvCa)	1.64×10^{-4} (↑hgOvCa)
BRCA1			2.76×10^{-2} (↑BOT)			
FANCB			9.71×10^{-3} (↑BOT)			
SEM1		2.51×10^{-2} (↑BOT)	1.01×10^{-2} (↑BOT)			
MUTYH			3.8×10^{-2} (↑BOT)			
BRCA2			3.83×10^{-3} (↑BOT)			
CHEK2			5.94×10^{-3} (↑BOT)			
FANCA			2.61×10^{-2} (↑BOT)			
FANCD2			4.97×10^{-2} (↑hgOvCa)		1.52×10^{-2} (↑hgOvCa)	
RAD50			2.83×10^{-2} (↑BOT)			
PALB2			4.31×10^{-2} (↑BOT)			
ATM				3.62×10^{-2} (↑lgOvCa)		
			Impact HIGH			
			Group Comparison and *p*-Value			
Gene	**BOT vs. BOT.V600E**	**BOT vs. lgOvCa**	**BOT vs. hgOvCa**	**BOT.V600E vs. lgOvCa**	**BOT.V600E vs. hgOvCa**	**lgOvCa vs. hgOvCa**
TP53			1.25×10^{-8} (↑hgOvCa)		1.47×10^{-4} (↑hgOvCa)	3.08×10^{-2} (↑hgOvCa)

Table 1. *Cont.*

| BRCA1 | | | 1.25 × 10⁻⁷ (↑hgOvCa) | | 6.01 × 10⁻⁴ (↑hgOvCa) | 3.4 × 10⁻² (↑hgOvCa) |

HOT-SPOT PANEL

Impact HIGH or MODERATE

Group Comparison and *p*-Value

Gene	BOT vs. BOT.V600E	BOT vs. lgOvCa	BOT vs. hgOvCa	BOT.V600E vs. lgOvCa	BOT.V600E vs. hgOvCa	lgOvCa vs. hgOvCa
TP53			1.01 × 10⁻²⁹ (↑hgOvCa)		7.62 × 10⁻¹⁸ (↑hgOvCa)	2.35 × 10⁻⁷ (↑hgOvCa)
BRAF	1.52 × 10⁻¹⁶ (↑BOT.V600E)			1.08 × 10⁻⁸ (↑BOT.V600E)	1.08 × 10⁻²³ (↑BOT.V600E)	
NRAS		1.1 × 10⁻² (↑lgOvCa)		2.2 × 10⁻² (↑lgOvCa)		2.22 × 10⁻⁴ (↑lgOvCa)
BRCA1			1.08 × 10⁻⁴ (↑hgOvCa)			
FBXW7			3.67 × 10⁻² (↑hgOvCa)			
KRAS	6.44 × 10⁻⁵ (↑BOT)		2.58 × 10⁻¹⁰ (↑BOT)	5.13 × 10⁻³ (↑lgOvCa)		2.77 × 10⁻³ (↑lgOvCa)

Impact MODERATE

Group Comparison and *p*-Value

Gene	BOT vs. BOT.V600E	BOT vs. lgOvCa	BOT vs. hgOvCa	BOT.V600E vs. lgOvCa	BOT.V600E vs. hgOvCa	lgOvCa vs. hgOvCa
TP53			2.27 × 10⁻¹⁵ (↑hgOvCa)		1.66 × 10⁻⁹ (↑hgOvCa)	8.26 × 10⁻⁵ (↑hgOvCa)
BRAF	1.52 × 10⁻¹⁶ (↑BOT.V600E)			1.08 × 10⁻⁸ (↑BOT.V600E)	1.08 × 10⁻²⁴ (↑BOT.V600E)	
NRAS		1.1 × 10⁻² (↑lgOvCa)		2.2 × 10⁻² (↑lgOvCa)		2.22 × 10⁻⁴ (↑lgOvCa)
KRAS	6.44 × 10⁻⁵ (↑BOT)		1.41 × 10⁻¹¹ (↑BOT)	5.13 × 10⁻³ (↑lgOvCa)		1.11 × 10⁻³ (↑lgOvCa)

Impact HIGH

Group Comparison and *p*-Value

Gene	BOT vs. BOT.V600E	BOT vs. lgOvCa	BOT vs. hgOvCa	BOT.V600E vs. lgOvCa	BOT.V600E vs. hgOvCa	lgOvCa vs. hgOvCa
TP53			5.84 × 10⁻⁹ (↑hgOvCa)		1.35 × 10⁻⁴ (↑hgOvCa)	
BRCA1			3.98 × 10⁻³ (↑hgOvCa)			

p-values of the applicable (chi-squared or Fisher's exact) test are included, followed by an arrow and the name of the group in which a given gene was more frequently altered (both written in brackets). In case of a lack of statistical significance, the corresponding cell is empty.

Two other genes worth mentioning here are *BRCA1* and *BRCA2*, since, in this study, their mutational profiles seemed to depend not only on the gene panel used but also on the impact that the genetic alterations had on the structure and function of the proteins encoded by these genes. In the 44-gene panel, both aforementioned genes turned out to be more frequently altered in BOT than in hgOvCa if moderate-impact variants were considered. This regularity also persisted if high-impact alterations in the *BRCA2* gene were included. By contrast, only high-impact *BRCA1* variants occurred much more frequently in hgOvCa than in all the other ovarian tumor groups (Table 1). In the hot-spot panel, the *BRCA2* gene was not included, while the number of polymorphisms in *BRCA1* was significantly higher in hgOvCa than in BOT, irrespective of whether only high-impact or all genetic variants were taken into account.

In this study, *KRAS* was the gene in which high- or moderate-impact variants most strongly differentiated BOT from all the other tumor groups, except lgOvCa. In two other genes, involved in ubiquitination, *FANCB* and *SEM1*, moderate-impact variants were identified significantly more frequently in BOT than in OvCa (*SEM1*) or hgOvCa (*FANCB*). Of note, the variants in these two genes did not differentiate BOT from BOT.V600E. Moreover, from among 76 different genes investigated in the two panels in the present study, *BRAF* was the only one that was more frequently mutated in the BOT.V600E tumors compared to all the other groups.

Genetic changes in the *KRAS* gene occurred frequently not only in BOT but also in lgOvCa compared to BOT.V600E and hgOvCa. Apart from *KRAS*, variants in two other genes, *ATM* and *NRAS*, predominated in lgOvCa. ATM was more frequently altered in lgOvCa than in the BOT.V600E group, yet this regularity was confined to the moderate-impact variants only. As for *NRAS*, moderate-impact alterations in this gene prevailed in lgOvCa in comparison with the three remaining tumor groups.

For the confirmation of polymorphisms in the selected genes, we used gradient PCR combined with Sanger sequencing. With this technique, we managed to successfully verify one previously identified variant in the *TP53* gene (chr17:g.7670658_7670659insA, p.Lys351Ter) [19] and seven new variants (SNPs and non-SNPs) with either a moderate or high impact on a protein's structure/function. The verification results and the detailed description of each analyzed polymorphism are presented in Figure S3.

2.2. Regression Analyses

Using the 44-gene panel, we identified that the genetic variants in *PARP1* were of prognostic value and had a significant impact on BOTS patients' RFS (Table 2 and Figure 3A–D). Notably, no genetic variants in the genes investigated in this study were identified as good predictors of the occurrence of microinvasions or implants within the tumor masses in BOTS. In hgOvCa, the only marker found to be predictive of response to chemotherapy were genetic variants in *BRCA2*. Polymorphisms in this gene positively affected both the CR and PS in patients with tumors without the TP53 protein accumulation, either treated with TP or irrespective of the chemotherapeutic regimen used (Table 2 and Figure 3I). The genetic variants in *BRCA2* revealed their favorable prognostic value as well by decreasing the risk of death in the whole group of patients, in the subgroup treated with TP, and in patients with tumors without TP53 accumulation. The *FANCF* gene was discovered here as another marker of a good prognosis in hgOvCa, as its polymorphisms diminished the risk of death in the TP-treated patients with tumors lacking the TP53 accumulation. By contrast, in the same group of patients, the *FANCI* gene was identified as a negative prognostic factor, elevating the risk of relapse (Table 2 and Figure 3E–H).

In the hot-spot panel, no genetic variants of prognostic or predictive importance were found for BOTS. For hgOvCa, we discovered a single adverse prognostic marker, *TSC2*. Genetic variants in this gene increased the risk of death in patients treated with the TP regimen, whose tumors exhibited the accumulation of the TP53 protein (Table 2).

Of note, the regression analysis was not performed for lgOvCa patients due to the small size of this cohort ($n = 10$), making multivariable statistical inference impossible. Nevertheless, it is worth emphasizing here that in the randomization (chi-squared and Fisher's exact) tests, described in Section 2.1, we managed to obtain statistically significant results for comparisons involving lgOvCa, which proved that the statistical power of these tests was high enough despite the rarity of lgOvCa tumors in our experimental setup.

Table 2. The results of multivariable Cox and logistic regression analyses for the models with good discriminating capabilities (assessed based on their AUC values) that matched with corresponding univariable tests.

44-Gene Panel		
BOTS		
RFS/relapse in the whole group of patients (full table)	**HR [95% Cl]**	***p*-value**
PARP1	6.82 [1.584–29.39]	0.01
hgOvCa		
DFS/relapse in the subgroup of patients treated with TP and without *TP53* accumulation in tumors	**HR [95% Cl]**	***p*-value**
FANCI	40.02 [3.784–423.133]	0.0022
Residual tumor <2 cm vs. no residual tumor (0 cm)	22.77 [2.061–251.608]	0.01
Residual tumor ≥2 cm vs. no residual tumor (0 cm)	34.1 [2.547–456.619]	0.0077
CR in the subgroup of tumors without *TP53* accumulation	**OR [95% Cl]**	***p*-value**
BRCA2	7.06 [1.328–37.581]	0.022
OS/death in the whole group of patients (full table)	**HR [95% Cl]**	***p*-value**
BRCA2	0.58 [0.399–0.85]	0.005
Residual tumor <2 cm vs. no residual tumor (0 cm)	2.85 [1.654–4.903]	1.6×10^{-4}
Residual tumor ≥2 cm vs. no residual tumor (0 cm)	3.75 [2.058–6.821]	1.55×10^{-5}
OS/death in patients with tumors without TP53 accumulation	**HR [95% Cl]**	***p*-value**
BRCA2	0.42 [0.204–0.865]	0.019
Residual tumor ≥2 cm vs. no residual tumor (0 cm)	4.63 [1.348–15.883]	0.015
OS/death in the subgroup of patients treated with TP	**HR [95% Cl]**	***p*-value**
BRCA2	0.53 [0.337–0.84]	0.007
Residual tumor <2 cm vs. no residual tumor (0 cm)	2.97 [1.616–5.471]	4.6×10^{-4}
Residual tumor ≥2 cm vs. no residual tumor (0 cm)	3.94 [1.944–7.986]	1.4×10^{-4}
CR in the subgroup of patients treated with TP and without TP53 accumulation in tumors	**OR [95% Cl]**	***p*-value**
BRCA2	6.73 [1.047–43.239]	0.045
PS in the subgroup of tumors without *TP53* accumulation	**OR [95% Cl]**	***p*-value**
BRCA2	8.23 [1.509–44.836]	0.015
PS in the subgroup of patients treated with TP and without TP53 accumulation in tumors	**OR [95% Cl]**	***p*-value**
BRCA2	8.33 [1.251–55.476]	0.028
OS/death in the subgroup of patients treated with TP and without TP53 accumulation in tumors	**HR [95% Cl]**	***p*-value**
FANCF	0.15 [0.024–0.976]	0.047
Residual tumor <2 cm vs. no residual tumor (0 cm)	3.69 [1.159–11.74]	0.027
Residual tumor ≥2 cm vs. no residual tumor (0 cm)	7.75 [1.84–32.595]	0.005
Hot-Spot Panel		
hgOvCa		
OS/death in the subgroup of patients treated with TP and with TP53 accumulation in tumors	**HR [95% Cl]**	***p*-value**
TSC2	2.52 [1.191–5.329]	0.016
Residual tumor <2 cm vs. no residual tumor (0 cm)	2.86 [1.312–6.249]	0.008
Residual tumor ≥2 cm vs. no residual tumor (0 cm)	2.61 [1.104–6.146]	0.029

The best models, the discriminating capabilities of which are shown in Figure 3, are underlined. AUC values for each model are provided in a file named Supplement-matching regression.xlsx. RFS—relapse-free survival; OS—overall survival; DFS—disease-free survival; TP—taxane/platinum chemotherapy; CR—complete remission; PS—platinum sensitivity; HR—hazard ratio; OR—odds ratio; CI—confidence interval.
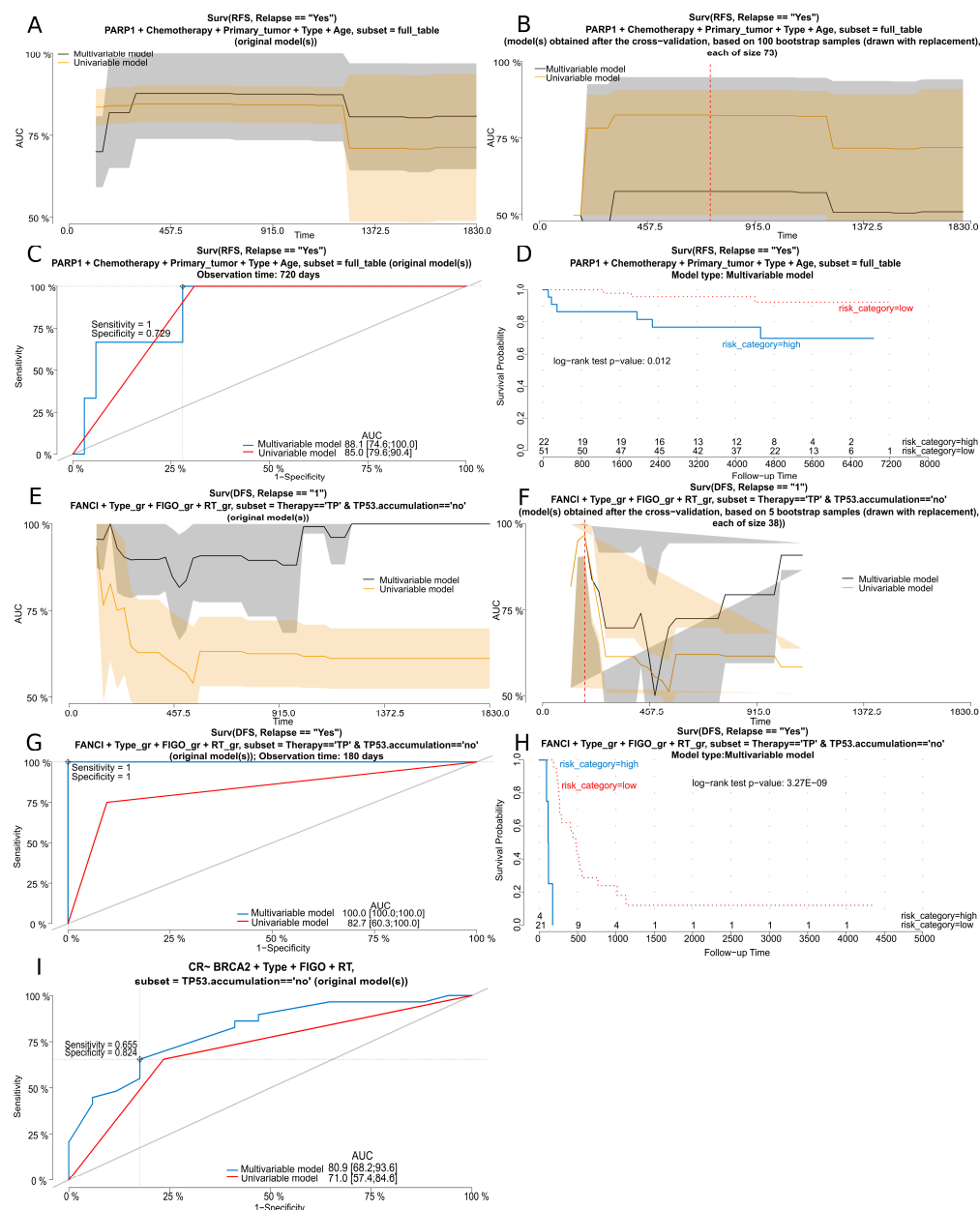
Figure 3. Cox and logistic regression analyses for selected genes. (**A–H**) Cox regression analysis results for the *PARP1* gene (RFS) in the whole BOTS group (**A–D**) and for the *FANCI* gene (DFS) in the subgroup of hgOvCa patients treated with the TP regimen and without *TP53* accumulation in their tumors (**E–H**). (**I**) Logistic regression analysis results for the *BRCA2* gene (CR) in the subgroup of hgOvCa patients without TP53 accumulation in their tumors. (**A**,**B**,**E**,**F**) AUC plots for uni- and multivariable Cox regression models obtained before (**A**,**E**) and after (**B**,**F**) a bootstrap-based cross-validation of the original dataset. The red dashed line indicates the same time point that was used to draw the time-dependent ROC curves (**C**,**G**). Optimal cutoff points for these ROC curves were calculated for the multivariable models based on the Youden index. Discrimination sensitivity and specificity values for cutoff points, determined for ROC curves in (**C**,**G**), are also provided. (**D**,**H**) Kaplan–Meier survival curves obtained for the patients divided into two categories (risk higher (high) or lower (low) than for the ROC curves' (**C**,**G**) estimated cutoff point, based on the risk of relapse, calculated using the multivariable models. The Kaplan–Meier curves are supplemented with the results of the log-rank test as well. (**I**) ROC curves for uni- and multivariable logistic regression models. An optimal cutoff point for these ROC curves was calculated for the multivariable model based on the Youden index. Discrimination sensitivity and specificity values for this cutoff point are also provided. RFS—recurrence-free survival; DFS—disease-free survival; RT—residual tumor size; CR—complete remission; TP—taxane/platinum chemotherapy.

2.3. Assessment of Relationship between Selected Gene Polymorphisms and Expression of Corresponding Proteins

To evaluate, on the protein level, the effects of the genetic alterations found in this study, we analyzed the expression of several proteins encoded by genes with SNP and non-SNP variants. The Western blot (WB) results are presented in Figures 4 and 5. We observed a lower or no signal on a membrane for non-SNP frameshift polymorphisms detected in the following: *NBN* (chr8:g.89971217_89971221del, p.Lys219AsnfsTer16; Figure 4A); *CHEK2* (chr22:g.28695869del, p.Thr367MetfsTer15; Figure 4C); and *TP53* (chr17:g.7674900dup, p.Thr211AsnfsTer5; chr17:g.7670686del, p.Arg342GlufsTer3; chr17:g.7674241del, p.Cys242AlafsTer5; chr17:g.7676078del, p.Pro98LeufsTer25; chr17:g.7676041_7676042insTTTC, p.Arg110GlufsTer40; Figure 4E). Additionally, we analyzed some samples with *TP53* missense mutations (with a moderate impact) (chr17:g.7675085C>T, p.Cys176Tyr; chr17:g.7673824C>G, p.Gly266Arg; chr17:g.7676040C>G, p.Arg110Pro; chr17:g.7673776G>A, p.Arg282Trp), for which we observed TP53 accumulation and a strong signal on a membrane (Figure 4E). Interestingly, for *CHEK1* with a STOP-gain variant (chr11:g.125625996G>A, p.Trp79Ter; Figure 4G), a higher percentage of altered reads resulted in increased CHEK1 expression.

Moreover, we found out that the expression of FANCI and its protein partner, FANCD2, was mutually correlated and likely dependent on the presence of genetic variants in the *BRCA1/2* genes. Tumor cases with the *FANCI* chr15:g.89285210C>T (p.Leu605Phe) variant did not show any specific pattern of FANCI expression (Figure 5A). However, the same samples had a similar pattern of FANCD2 expression (Figure 5B), regardless of whether they harbored variants in *FANCD2* (Figure 5G). Yet, the occurrence of FANCD2 expression seemed to depend on the presence of *BRCA1/2* genetic alterations (Figure 5G). In the absence of sequence variants in these two genes, no signal for altered FANCI, and concomitantly for FANCD2, was observed on membranes (compare Figure 5G and Figure 5A,B). Additionally, we tested whether the most frequent variant in *FANCD2* (chr3:g.10073349G>T; p.Gly901Val) affected the FANCD2 expression, which revealed no relationship (Figure 5E,H).
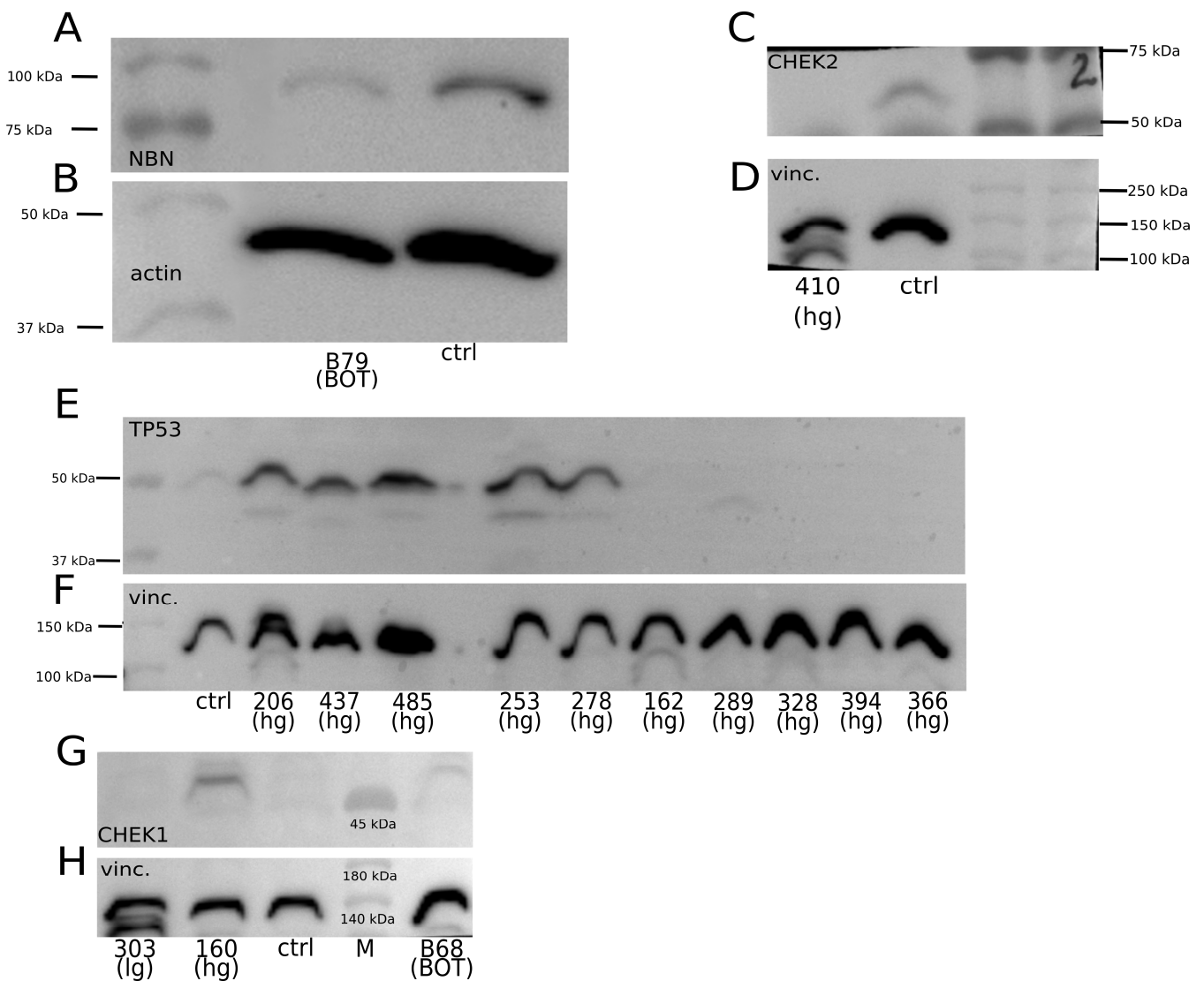
Figure 4. Selected genetic variants and their impact on the expression of corresponding proteins. (**A**) *NBN* chr8:g.89971217_89971221del (p.Lys219AsnfsTer16): 20% of reads with this sequence alteration (altered reads) in the B79 BOT sample. (**C**) *CHEK2* chr22:g.28695869del (p.Thr367MetfsTer15): 72% of altered reads in the 410 hgOvCa sample. (**E**) *TP53* missense variants: 206: chr17:g.7675085C>T (p.Cys176Tyr), 437: chr17:g.7673824C>G (p.Gly266Arg), 485: chr17:g.7676040C>G (p.Arg110Pro), 253: chr17:g.7673776G>A (p.Arg282Trp), 278: chr17:g.7673776G>A (p.Arg282Trp); TP53 non-SNPs with a HIGH impact: 162: chr17:g.7674900dup (p.Thr211AsnfsTer5), 289: chr17:g.7670686del (p.Arg342GlufsTer3), 328: chr17:g.7674241del (p.Cys242AlafsTer5), 394: chr17:g.7676078del (p.Pro98LeufsTer25), 366: chr17:g.7676041_7676042insTTTC (p.Arg110GlufsTer40). Altered reads: 206—64%; 437—72%; 485—71%; 253—84%; 278—63%; 162—67%; 289—52%; 328—43%; 394—40%; 366—50%. (**G**) *CHEK1* chr11:g.125625996G>A (p.Trp79Ter) in all three tumors. Altered reads: 303—18%; 160—69%; B68—49%. (**B**) Actin as a loading control, detected with a rabbit polyclonal anti-actin Ab, and (**D,F,H**) vinculin as a loading control, detected with a rabbit polyclonal anti-vinculin Ab. M—protein marker; vinc.—vinculin; ctrl—normal ovary; hg—hgOvCa; lg—lgOvCa; Ab—antibody.
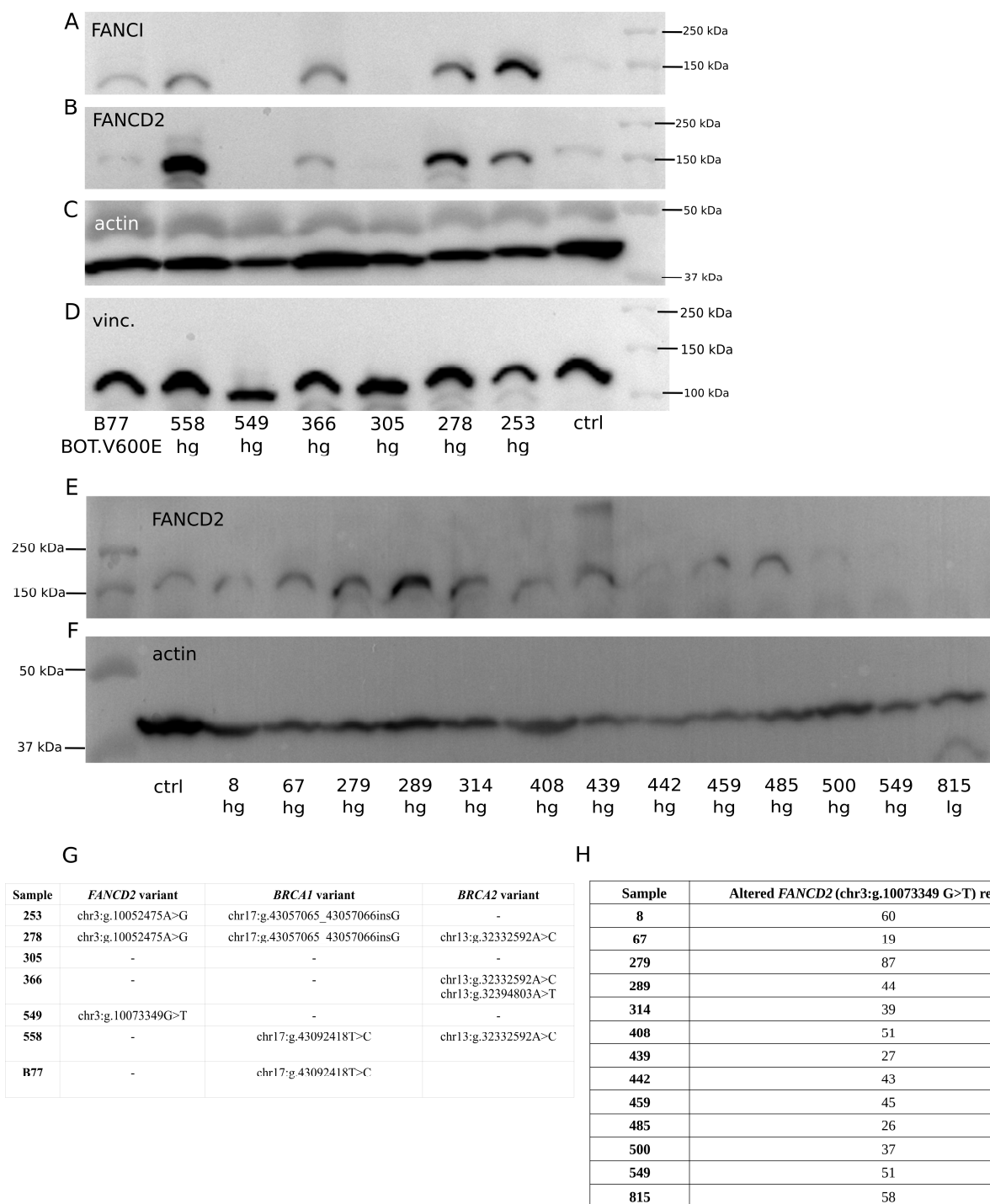
Figure 5. Frequent genetic variants in the *FANCI* and *FANCD2* genes and their impact on the expression of corresponding proteins. (**A**) the *FANCI* chr15:g.89285210C>T (p.Leu605Phe) variant; altered reads: B77—51%, 558—92%, 549—85%, 366—45%, 305—86%, 278—33%, 253—32%. No relationship between the percentage of altered reads and the protein level was observed. (**B**) FANCD2 expression for the same cases as in (**A**). (**E**) Expression of FANCD2 in the cases with the most frequently occurring *FANCD2* variant: chr3:g.10073349G>T (p.Gly901Val). No relationship between the presence of this variant, the percentage of altered reads (**H**), and the protein level was observed. (**G**) A table showing the occurrence of *FANCD2* and *BRCA1/2* variants in samples with the *FANCI* chr15:g.89285210C>T variant. (**C,D,F**) Loading controls. A rabbit polyclonal anti-actin or anti-vinculin primary antibody was used to detect actin (**C,F**) and vinculin (**D**), respectively. Ctrl—normal ovary; hg—hgOvCa; lg—lgOvCa.

3. Discussion

The aim of this study was the analysis of genetic variants in crucial tumor suppressors and oncogenes in ovarian tumors of different aggressiveness. We not only evaluated the polymorphic status of these genes in large, thoroughly characterized cohorts of OvCa and BOTS, but we also found predictive and/or prognostic markers for both tumor groups and analyzed the functional role of selected polymorphisms regarding their influence on the expression of the corresponding proteins.

Unexpectedly, our NGS results, obtained for the 44-gene panel, showed that the number of SNPs with a high or moderate or only moderate impact on the structure and/or function of the corresponding proteins was higher in BOT compared to BOT.V600E, lgOvCa, or hgOvCa. Conversely, when analyzing only hot spots in selected genes, the frequency of SNP variants with these impacts was significantly lower in BOT than in both OvCa groups. This apparent discrepancy may be explained by the fact that the two panels investigated in this study contained different sets of genes. As proven in the present study, the list of genes from the 44-gene panel more frequently mutated in BOT compared to the other tumor groups (*FANCB*, *SEM1*, *FANCA*, *BRCA2*, *CHEK2*, *MUTYH*, *RAD50*) was much longer than analogically altered genes in the hot-spot panel (*KRAS* only). Additionally, the hot-spot panel was designed to investigate well-known genetic alterations. By contrast, in the 44-gene panel, an approximately 10 times bigger region of the genome was covered, enabling the detection of rare genetic variants, usually omitted in, e.g., diagnostic approaches. Nevertheless, when only polymorphisms with a high impact on a protein function and/or structure were considered, the number of genetic variants identified in both panels was the highest in hgOvCa, thus supporting the general knowledge about ovarian carcinomas [20,21].

The mutational status of *TP53* can be considered one of the best markers differentiating hgOvCa (frequent mutations in *TP53*) from BOTS (no or very rare mutations) [11,22,23] and lgOvCa (relatively rare mutations) [24]. In line with these reports, TP53 was one of the most frequently altered genes in the present study, mainly in hgOvCa. By contrast, no variants in *TP53* were found in our lgOvCa cases, besides two poorly covered high-impact SNPs in one lgOvCa specimen. Interestingly, these SNPs were detected only in the hot-spot panel, making use of a novel NGS hybridization capture technology (known as Primer Extension Target Enrichment, KAPA HyperPETE, Roche), offering much better sequencing coverage uniformity than the older hybridization-based capture approach (KAPA HyperCap, Roche), utilized in the 44-gene panel [25]. As for BOTS, the only two missense variants in *TP53* found in this study were observed in two BOT samples of a mucinous subtype. This outcome aligns with the current state of the knowledge too, given that Kang et al. reported TP53 mutations in 19.4% of mucinous BOTS, which was associated with a higher risk of recurrence [26]. Consistently, one of our two *TP53* mutation-bearing BOT patients had progression to OvCa. Noteworthy, herein, we also managed to confirm our NGS results for *TP53* on the protein level by observing both the lack of TP53 in samples with high-impact non-SNP variants and TP53 accumulation in tumors harboring *TP53* missense SNPs. These results are in line with our previous immunohistochemical evaluation of TP53 expression [27].

According to the literature, alongside genetic aberrations in *TP53*, mutations in *BRCA1/2* are also frequent in hgOvCa [24,28] and are rare in BOTS and lgOvCa [3,9,10,24]. Our results obtained with the 44-gene panel do not seem fully consistent with the literature, as we found variants in *BRCA1/2* genes in many non-high-grade ovarian tumors. However, it needs to be emphasized that, except for one SNP in a single BOT, these were only moderate-impact variants. These variants accounted for the significantly higher number of genetic alterations found in *BRCA1/BRCA2* in BOT compared to hgOvCa. Yet, when only high-impact variants were considered, *BRCA1* (but not *BRCA2*) was, as expected, more frequently altered in hgOvCa in comparison with all the remaining tumor groups. By contrast, in the hot-spot panel, which concentrated on well-established variants only and omitted most of the poorly investigated genetic alterations, no *BRCA1* polymorphisms with a high/moderate impact were found in BOT or lgOvCa, and only a single moderate-impact

variant was present in one BOT.V600E sample. As a consequence, when only commonly analyzed hot spots in the *BRCA1* gene were taken into account, our statistical workflow corroborated the generally acknowledged predominance of sequence variants in this gene in hgOvCa compared to BOT. Still, according to a recent NGS study, carried out on big cohorts (containing 1333 OvCa and 152 BOTS patients), the prevalences of *BRCA1/2* mutations are similar in hgOvCa and BOTS (30.9% and 28.9%, respectively) [29]. Thus, this paper seems to corroborate our finding, made with the 44-gene panel, that lots of genetic alterations in *BRCA1* are detectable in BOTS if high-throughput sequencing techniques (not limited to known hot spots only) are applied. As for *BRCA2*, similarly to *BRCA1*, the moderate-impact variants of this gene prevailed in BOT compared to hgOvCa. Conversely, we revealed no differences in the frequencies of high-impact *BRCA2* polymorphisms between the investigated groups of ovarian tumors. Nevertheless, *BRCA2* emerged in this study as a promising, favorable predictive and prognostic marker in hgOvCa. The presence of sequence variants in *BRCA2* improved the patient OS, CR, and PS, especially in tumors without TP53 accumulation. Although this outcome may seem odd, given the tumor suppressor capabilities of this gene, a similar phenomenon was earlier observed in small-cell lung cancer [30], where the authors of the cited research reported a link between the occurrence of *BRCA2* mutations and the higher sensitivity of tumors to chemotherapy. In line with these findings, data obtained in vitro also provided strong evidence for the better response of BRCA-deficient tumors to platinum drugs, which was further confirmed by ex vivo studies, where *BRCA* mutation carriers exhibited better survival and longer disease-free intervals upon treatment with platinum drugs [31]. As BRCA1/BRCA2 proteins are responsible for the repair of double-strand DNA breaks (DSBs), the presence of pathogenic variants in *BRCA2* leads to the impaired activity of its protein product and thus increases the risk of a DSB in a tumor cell. If such a cell expresses functional TP53 (no TP53 accumulation is observed), apoptosis is induced [32], thus ameliorating the outcome of platinum-based treatment, as shown herein.

As for genetic alterations characteristic of less aggressive ovarian tumors, the genes with the highest number of polymorphisms in BOTS and lgOvCa compared to hgOvCa were *KRAS*, *BRAF*, and *NRAS*, which is in line with the scientific literature [13,33–36]. Given that BOTS with the *BRAF* V600E variant occurred in much younger patients than those lacking this mutation [18], here, both these groups of tumors were analyzed separately. Interestingly, *KRAS* was more frequently mutated in BOT and lgOvCa than in either BOT.V600E or hgOvCa, while the frequencies of *KRAS* variants in lgOvCa and BOT were comparable. This confirms the molecular resemblance between these two tumor groups. Simultaneously, such an outcome demonstrates that in BOTS without the *BRAF* V600E variant (being the most frequent polymorphism in this gene, found in this study in about 72% of *BRAF*-deficient tumors), KRAS-activating mutations are present. The KRAS-dependent cancer-promoting mechanism hinges mainly on mutations in the Gly12(G12)-coding region of the gene [37,38], which, in our research, predominated in BOT and lgOvCa alike. By contrast, none of the *KRAS* polymorphisms, which we found in a few hgOvCa tumors, affected Gly12. Furthermore, it is worth mentioning that all three of our BOT cases with *BRAF* variants other than V600E (i.e., K601E, G466R, and G466V) simultaneously harbored *KRAS* G12 variants. This suggests that out of all the *BRAF* polymorphisms, only *BRAF* V600E exerts a sufficiently strong cancer-promoting effect to act independently of *KRAS* mutations [39]. As for *NRAS* variants, their prevalence differentiated lgOvCa from all the other tumor groups investigated in our study. This outcome supports the finding of others that mutations in *NRAS* are found in serous lgOvCa but not, or rarely, in serous BOTS [40]. Similarly to activating mutations in *KRAS*, their counterparts in *NRAS* also speed up tumor progression. Moreover, such variants are found in recurrent serous lgOvCa too [41,42]. In this context, it is worth mentioning that one of our serous BOT samples with microinvasions harbored the NRAS-activating variant (p.Gln61Arg) [43], which occurred most frequently in our lgOvCa group as well. The presence of such a mutation in a BOT sample not only constitutes further confirmation of the molecular similarity between BOT and lgOvCa [5,44]

but also implies that this BOT tumor might have transformed and recurred as lgOvCa if it had not been completely excised. According to the literature, in advanced ovarian carcinomas, *NRAS* mutations are rare [45]. Consistently, we did not identify such genetic alterations in our hgOvCa series. Of note, mutations in the *KRAS*, *NRAS*, and *BRAF* genes have also been reported in other human malignancies, e.g., colorectal and endometrial cancers [46–49].

Genes encoding proteins involved in ubiquitination were also more frequently altered in BOT and differentiated these tumors from OvCa (but not from BOT.V600E). One of these genes, *SEM1*, which codes for a 26S proteasome subunit [17], was very often altered in all the tumor groups. Although the most frequent variant, found in all the tumor groups, p.Gln59Pro is widespread in the human population (maximum allele frequency (AF_{max}) of 0.88); still, the overall number of *SEM1* variants was significantly higher in BOT than in either lgOvCa or hgOvCa. Nowadays, no scientific reports on the role of this polymorphism in tumors are available. For the second gene, *FANCB*, which encodes a DNA repair-involved protein required for FANCD2 ubiquitination [17], literature data concerning OvCa are scarce, while its function in BOTS has not been studied so far. *FANCB* missense mutations were shown to cause the instability of the catalytic module and Fanconi Anemia (FA) core complex dysfunction. By contrast, SNPs in the *FANCB* 3′UTR did not affect the expression or function of the protein [50]. Given that all the *FANCB* polymorphisms found in our research were located in the coding sequence of the gene, their occurrence may likely impair the FANCB function, as proven in the study cited above. Interestingly, according to the current state of the knowledge, the *FANCB* role in cancer seems discrepant. On the one hand, no mutations in this gene in hereditary breast/ovarian cancers were found [51] and no associations between *FANCB* and the development of *BRCA1/2*-negative familial cancers were demonstrated [50]. On the other hand, Matta et al. [50] unraveled the relationship between the expression of *FANCB* and breast cancer in older patients with decreased DNA repair capacities. In this context, our results appear to shed new light on the clinical importance of *FANCB*, showing that this gene may play more important roles in BOTS than in OvCa.

Our regression analysis revealed genetic variants in *PARP1* as a marker of a poor prognosis in BOTS. This gene encodes a protein activated by DNA damage, regulating the function of many tumor suppressors, including TP53 [52]. In the literature, the data on the *PARP1* role in BOTS are limited; however, its meaning in OvCa has been profoundly investigated [53,54]. Consequently, PARP inhibitors have been approved for the maintenance treatment of recurrent platinum-sensitive *BRCA1/2*-deficient OvCa. Yet, newer data demonstrated therapeutic benefits in tumors beyond those with *BRCA1/2* mutations [55]. Remarkably, the most frequent *PAPR1* polymorphism in all the groups of tumors analyzed herein, p.Val762Ala, was different from that causing resistance to olaparib, one of the PARP inhibitors [56]. Despite its predominance in the human population (AF_{max} around 45%), the p.Val762Ala variant was previously shown to be associated with several types of cancer, including gallbladder cancer [57,58]. The same polymorphism also increased the risk of breast cancer among the Saudi and Asian populations, simultaneously decreasing this risk among Caucasians [59]. Interestingly, though other scientists reported that *PARP1* expression in serous OvCa is higher than in BOTS [60], in our hgOvCa series, this gene was neither more frequently altered nor identified as a potential biomarker.

Polymorphisms in two other genes encoding proteins involved in the FA pathway, FANCF and FANCI, were identified herein as promising outcome predictors in hgOvCa. Noteworthy, variants in *FANCI* exhibited significantly better discriminative capabilities than those in *FANCF*, as assessed based on the AUC values. The FANCI protein forms a heterodimer with FANCD2, which is subsequently monoubiquitinated by the FA core complex. Such a heterodimer localizes to the damaged chromatin and promotes interstrand crosslink repair [50]. In our analyses, the presence of variants in the *FANCI* gene increased the risk of recurrence in the TP-treated patients with tumors lacking the TP53 accumulation. When the literature data are considered, the role of *FANCI* seems ambiguous, as this gene

has been reported to play both oncogenic and tumor suppressor roles [61,62]. Moreover, *FANCI* was recently proposed as a new OvCa-predisposing gene in carriers of the *FANCI* p.Leu605Phe variant [63], the frequency of which turned out to be significantly higher in OvCa-prone families with normal *BRCA1/2* genes [64]. In vitro studies revealed that the Leu605Phe isoform of FANCI was expressed at a reduced level and conferred sensitivity on HeLa and OvCa cells to cisplatin but not to a PARP inhibitor [64]. Consistently, our WB analyses revealed that tumors with the *FANCI* p.Leu605Phe variant and normal *BRCA1/2* genes did not express mutated FANCI, in contrast to *BRCA1/2*-deficient tumors, where FANCI expression was detected. Additionally, the same WB analysis unraveled the correlation between the expression of the FANCI and FANCD2 proteins. All these results clearly suggest that the role of *FANCI* depends on the molecular background in the cell controlled by crucial tumor suppressors, such as BRCA1/2 and TP53.

Our last result worth discussing deals with *CHEK1* for the nonsense variant in which (chr11:g.125625996G>A, p.Trp79Ter) we observed the unexpectedly high expression of the CHEK1 protein. Interestingly, both molecular phenomena seemed to be positively correlated (the higher the percentage of the altered allele, the stronger the signal for CHEK1 on a membrane). The SNP in question is located in the first exon/5′UTR region of *CHEK1*. If the longest isoform of CHEK1 (XP_011540862.1) is considered, the discussed polymorphism leads to the formation of a premature stop codon. In such a case, the utilization of an alternative start codon located downstream from the newly formed stop codon may not only restore the CHEK1 expression as a shorter isoform but concomitantly affect its levels in the cell. Consistently, according to the literature, short CHEK1 isoforms may occur due to alternative splicing or protein cleavage [65]. The role of *CHEK1* in tumorigenesis is ambiguous. Initially, CHEK1 was thought to be a tumor suppressor because of the role it plays in the DNA damage response and cell cycle checkpoint response [66]. However, no evidence of homozygous loss of function *CHEK1* mutants in human cancers was found. Moreover, the *CHEK1* gene was overexpressed in several solid tumors, and its expression was correlated with the tumor grade and disease recurrence [67]. In step with these findings, the complete loss of *CHEK1* suppresses chemically induced carcinogenesis, whereas tumor cells with increased levels of *CHEK1* may acquire survival advantages due to the ability to resist chemotherapy-induced DNA damage. As a result, reduced survival rates of patients with high *CHEK1* expression were reported in bladder, brain, lung, ovary, and breast cancers [67]. Although our results do not elucidate whether CHEK1 acts more like an oncogene or suppressor in ovarian tumors, further investigation of its variants appears interesting in the context of potential targeted therapies with Prexasertib, a selective CHEK1 inhibitor. Its application, either as a single agent or in combination with PARP inhibitors, stimulated tumor regression and prolonged hgOvCa patient survival [68]. This combination of inhibitors could be of potential use in BOTS, since *PARP1* polymorphisms were identified herein as a negative prognostic marker in these tumors, while some BOTS also harbored the above-described *CHEK1* p.Trp79Ter variant.

Finally, as with every study, this one also has some limitations that ought to be mentioned here. Although we managed to identify numerous genetic variants, due to financial and time-related constraints, the functional validation was only performed for a small subset of these polymorphisms. Thus, the clinical significance of many identified variants, listed in the Supplement-variants.xlsx file, remains unclear and should be addressed in future research. Furthermore, it needs to be emphasized that in our bioinformatic workflow, all sequence variants less frequent than 10% were filtered out. This approach was utilized to reduce the rate of false-positive hits, yet, hypothetically, some rare, clinically important polymorphisms may have been excluded from the analysis too. The next limitation worth bringing up results from the fact that we analyzed bulk tumor samples, which are just a part of the entire tumor microenvironment, the complexity and heterogeneity of which might not have been fully captured due to the constraints of the experimental setup applied in this study. Also, in terms of the tumor complexity and heterogeneity, we are aware that the loading controls in our Western blot experiments sometimes differed between lysates

from distinct OvCa samples analyzed on the same gel. This inconsistency was not caused by any laboratory error or imprecision but, rather, is related to the vast biodiversity of ovarian tumors, especially high-grade OvCa, which results from the genomic and proteomic instability of such malignancies [69]. In the present study, to diminish the risk of drawing false conclusions, the concentration of all the protein lysates was not only assessed by Ponceau S red staining but was also precisely measured and normalized with the BCA method and a standard curve for bovine serum albumin (BSA). In the end, the present research was performed on a retrospective (not prospective) cohort of patients, collected for 20 years, meticulously followed up, and carefully checked for the compatibility of all the clinicopathological parameters. This approach, though widely used, could introduce some hardly definable biases and limit the ability to control for potential confounding factors.

4. Materials and Methods

4.1. Patients and Clinicopathological Parameters

In this study, a retrospective set of 225 non-consecutive ovarian tumor samples was used, including 76 BOTS (61 of the serous type and 15 of other histological types), 10 lgOvCa (9 of the serous type and 1 of another type), and 139 hgOvCa (113 of the serous type and 26 of other types). All the samples were collected from an ethnically uniform cohort of patients of central European origin, hospitalized at the Maria Sklodowska-Curie National Research Institute of Oncology, Warsaw, Poland, in the years 1995–2015. The corresponding medical records were critically reviewed by at least two physicians. Out of 76 BOTS, 21 were collected as snap-frozen samples, whereas the remaining 55 specimens were available in the form of formalin-fixed, paraffin-embedded (FFPE) blocks only. By contrast, all our OvCa samples were snap-frozen. The detailed clinicopathological characteristics for the BOTS and OvCa are presented in Supplementary Tables S1 and S2, respectively. For two lgOvCa, the information on the applied chemotherapy was missing, which was one of the grouping variables in our study. Therefore, these samples were excluded from Table S2. As for the evaluation of the clinical endpoints, all surviving patients had at least a 3-year follow-up. The specimens were carefully selected to meet the following criteria: an adequate staging procedure (stages were assessed for all cancers and primary BOTS) according to the recommendations by the International Federation of Gynecologists and Obstetricians (FIGO) [70], tumor tissue from the first laparotomy available, availability of clinical data including patient age and follow-up, as well as tumor histological type and grade and residual tumor size. Noteworthy, all BOT patients were characterized by no residual disease. All tumors were uniformly histopathologically reviewed and classified according to the new WHO criteria [5,71]. Additionally, a complete evaluation of the genetic variants in the *TP53* gene (for all tumors) and the TP53 protein status (for cancers only) was performed by either next-generation sequencing or with the PAb1801 mouse monoclonal antibody (1:500, Sigma-Genosys, Cambridge, UK), as described previously [27]. Most BOT patients (*n* = 60) did not undergo any chemical treatment. The remaining individuals suffering from BOTS (*n* = 16) received chemotherapy, administered either pre- or postoperatively. All carcinomas were excised from previously untreated patients. A total of 35 OvCa patients were treated postoperatively with platinum/cyclophosphamide (PC), while 112 of them underwent the taxane/platinum (TP) treatment after a surgical intervention. In BOTS, the relapse-free survival time (RFS) and the presence of microinvasions or implants within the tumor masses were used as dependent variables determining the disease outcome. The chemotherapy administration status was used as an independent logical variable in the multivariable statistical analyses. Other covariates taken into account in the multivariable statistical inference in BOTS were a logical variable determining whether the tumor was primary, the tumor histological type, and the patient age (continuous variable). In addition, BOTS were analyzed in the entire cohort of patients, and in subgroups comprising either BOT.V600E or BOT specimens only, since the presence of the *BRAF* V600E mutation was previously found to be significantly correlated with the lower age of patients diagnosed with BOTS [18]. For cancers, the overall survival (OS) and disease-free survival (DFS) of

patients were used as dependent prognostic variables, while the platinum sensitivity (PS) and complete remission (CR) served as dependent factor variables predictive of the tumors' response to treatment. CR was defined as the disappearance of all clinical and biochemical symptoms of ovarian cancer assessed after completion of the first-line chemotherapy and confirmed four weeks later [72]. DFS was assessed only for the patients who achieved CR. As for the independent variables used in the statistical analyses in cancers, the histological type and clinical stage of the tumors along with the residual tumor size were taken into account as factor variables in the multivariable statistical models. Noteworthy, due to the small size of the lgOvCa subgroup, only hgOvCa samples were subjected to the regression analyses performed in the present study. The hgOvCa were investigated in either the entire set of samples or in subgroups depending on the chemotherapy regimen used (PC/TP) and/or the TP53 accumulation status. Notably, two of the above-mentioned lgOvCa samples excluded from Table S2 were taken into account in the entire bioinformatic workflow presented herein, except for the Cox and logistic regression analyses, which required detailed clinicopathological information.

4.2. DNA Isolation and Quality Assessment

Genomic DNA (gDNA) from snap-frozen sections was isolated using the QIAmp DNA Mini Kit (Qiagen; Hilden, Germany), whereas gDNA from FFPE blocks was extracted on the MagCore Nucleic Acid Extractor machine using the MagCore Genomic DNA FFPE One-Step Kit (RBC Biosciences, Xinbei City, Taiwan). gDNA concentrations were measured on the Qubit 4 Fluorometer (Thermo Fisher Scientific (Thermo), Waltham, MA, USA) using the Qubit dsDNA HS Assay Kit (Thermo). Before the construction of the NGS libraries, the gDNA quality was assessed using our in-house-developed method based on the comparison of the real-time quantitative PCR (qPCR) efficiency for two amplicons of different lengths, described in the paper by Woroniecka et al. [73].

4.3. Construction of Total gDNA Libraries; 44-Gene Panel Enrichment and Verification; NGS Sequencing

For the libraries' construction, 120–500 ng of gDNA was used. Libraries were created using the KAPA Hyperplus Kit (Roche, Basel, Switzerland) according to the protocol provided by the producer. The verification of the libraries' size was made on 2100 Bioanalyzer (Agilent Technologies, Santa Clara, CA, USA). Total gDNA libraries were then enriched in exonic sequences of the following 44 genes: *ATM, ATR, ATRX, BAP1, BARD1, BCL2L1, BLM, BRCA1, BRCA2, BRIP1, CCNE1, CEBPA, CHEK1, CHEK2, CRNDE, EMSY, FANCA, FANCB, FANCC, FANCD2, FANCE, FANCF, FANCG, FANCI, FANCL, FANCM, IRX5, MDM2, MRE11, MUTYH, NBN, PALB2, PARP1, PIK3CA, PRKDC, PTEN, RAD50, RAD51B, RAD51C, RAD51D, RAD54L, RPA1, SEM1*, and *TP53*, using the SeqCap EZ Hybridization&Wash Kit with biotinylated hybridization probes (Roche). Out of these genes, 41 were involved in hereditary ovarian carcinoma development (as stated in the description of the Ion AmpliSeq™ Comprehensive Ovarian Cancer Research Panel, Thermo). The remaining three genes, *CRNDE, IRX5*, and *CEBPA*, were added by our team to further extend the functionality of this panel. The whole enriched region covered ca 360,000 bp in the genome. The verification of the DNA enrichment was performed by qPCR with four pairs of primers designed by Roche. The list of primers and the results of the enrichment evaluation for each primer pair are presented in Figure S4A–D,F. The NGS libraries were sequenced on the NovaSeq 6000 Platform (Illumina, San Diego, CA, USA) in the paired-end mode (2×100 bp for DNA obtained from frozen material or 2×75 bp for DNA isolated from FFPE blocks). The resultant BAM files were deposited in the European Nucleotide Archive (ENA) database (data acc. no. PRJEB75542).

4.4. Hot-Spot Panel Enrichment and Verification; NGS Sequencing

For the hot-spot analysis, total gDNA libraries, also employed for the 44-gene panel, were used. The enrichment in 37 genes frequently mutated in sporadic human cancers

(*AKT1, ALK, APC, ATM, BRAF, BRCA1, CDKN2A, CTNNB1, EGFR, ERBB2, ESR1, FBXW7, FGFR1, FGFR2, FGFR3, GNA11, GNAQ, GNAS, HRAS, IDH1, IDH2, JAK2, KIT, KRAS, NF1, NRAS, NTRK3, PDGFRA, PIK3CA, POLE, PTCH1, PTEN, RET, STK11, TP53, TSC1, TSC2*) was performed using the KAPA HyperPETE Hot Spot Panel (Roche). The whole enriched region covered approximately 36,000 bp in the human genome. The verification of the gDNA enrichment was performed using qPCR with one pair of our in-house-designed primers for *TP53* exon 4. For the enrichment verification results and PCR primer sequences, refer to Figure S4E,F. The NGS libraries were sequenced on the iSeq100 platform (Illumina) in the paired-end mode (2×150 bp for DNA obtained from frozen material or 2×100 bp for DNA isolated from FFPE blocks). The resultant BAM files were deposited in the ENA database (data acc. no. PRJEB75531).

4.5. Bioinformatic Analyses

The quality of our NGS data (FASTQ files) was assessed with the FASTQC app (v. 0.12.1) and then optimized with Trimmomatic (v. 0.39). Mapping to the reference human genome (hg38) was performed using the HISAT2 aligner (v. 2.2.1). Afterward, the mapping quality was evaluated with the Samtools (v. 1.6), Genome Analysis Toolkit (v. v4.5.0.0), and Qualimap (v. 2.3) apps. Next, our in-house-developed software, SeqDepth_checker (v. 1.0, downloadable from https://github.com/lukszafron, LMS_gh, accessed on 29 May 2024), was utilized to evaluate the mean sequencing read coverage depths for each region enriched in every gene. If the mean coverage depth for a given region was lower than 5, this region was excluded from further analyses to diminish the risk of considering unevenly enriched DNA regions as non-mutated in samples with poor enrichment. The obtained BAM files were subsequently analyzed with bcftools software (v. 1.18) to create VCF files with the AD tag. Next, the variants were subjected to two-step filtering. First, variants less frequent than 10% were filtered out based on the AD tag, using the VAF checker app (version: 1.0), a program available for download at LMS_gh. Then, the vcf-annotate app from the VCFtools package (version: 0.1.16) was employed to filter out variants that did not meet the following criteria: all filters with default values applied, except for MinAB = 2 (a minimum number of alternate bases of 2), Qual = 20 (minimum sequence quality of 20), MinMQ = 20 (minimum mapping quality of 20), and MinDP = 5 (minimum sequence coverage depth of 5). Subsequently, the obtained VCF files were divided with bcftools into two subsets, SNPs and non-SNPs, containing SNP variants vs. all other sequence alterations, i.e., indels (insertions, deletions), mnps (multi-nucleotide polymorphisms), bnd (breakpoints), and others, respectively. Next, the variant identification and effect prediction analysis was carried out using the Ensembl Variant Effect Predictor (VEP) app (v. 109) and the merged Ensembl and RefSeq databases [74]. The obtained tab-delimited CSV files (VEP output tables) were further analyzed consecutively with two R programs developed by LMS, vep.r (v. 2.2) and vep.comparison.r (v. 2.2), both available for download at LMS_gh. Ensembl VEP divides sequence variants into four categories: high, moderate, low, and modifier, based on their expected impact on the transcript and protein sequences. For details, refer to the Ensembl web page [75]. The two aforementioned R apps were utilized first to filter out all variants characterized by low or modifier impacts and then to exclude all variants except those that either had a known adverse clinical significance (determined with the CLIN_SIG tag) or negatively affected the protein structure and function (as assessed by either the SIFT or PolyPhen algorithms). The new, previously unidentified sequence variants (with an empty "Existing_variation" field in the VEP output table), variants for which all three "CLIN_SIG", "SIFT" and "PolyPhen" fields were empty, or those with a maximum allele frequency (MAX_AF) lower than 0.01, were also included in the final report generated by the vep.r app. The analyses were carried out independently for SNP and non-SNP variants. Subsequently, these results were combined with the binarization of sequence alterations for every gene (sequence variants with a high or moderate impact present (1) vs. absent (0)). Afterward, to identify genes with significantly different frequencies of sequence alterations between the investigated groups of ovarian tumors,

statistical inference with the chi-squared test or the Fisher's exact test (depending on the sizes of the analyzed subgroups) was carried out, followed by the data visualization. This final step of the analysis was performed with the vep.comparison.r script. A list of all polymorphic variants for each sample is presented in Supplement-variants.xlsx.

All genes containing variants identified in our bioinformatic analyses were subsequently subjected to detailed statistical inference with the use of univariable and multivariable Cox proportional hazards models (package: survival, v. 3.5.7) to assess the value of these genes as potential novel prognostic biomarkers. All Cox models were also checked with respect to the proportionality of hazards for each variable used. The prediction of the treatment response was carried out by generating univariable and multivariable logistic regression models (packages: stats., v. 4.0.2, and rms, v. 6.0.1). The dependent, independent, and grouping variables (different for BOTS and hgOvCa) are described above in the section entitled Patients and Clinicopathological Parameters. In order to verify the discriminating capabilities of the created Cox and logistic regression models, we performed their cross-validation in new datasets, generated from the original data by bootstrapping (with replacement) and a subsequent comparison of the areas under ROC curves (AUCs) between the original and bootstrapped datasets, using the riskRegression package (v. 2023.12.21) [76]. The R script written to automate the above-mentioned statistical inference and subsequent visualization of the results (regression.analyses.r, v. 1.2) is downloadable from LMS_gh.

In order to identify the best potential biomarkers, we performed a matching of our regression analyses' results. In this step, each univariable model was compared with its multivariable counterpart, and the models were considered matched when the analyzed genes and groups of tumors were the same, when both *p*-values were <0.05, when both HR/OR values were either higher or lower than 1, and, concomitantly, when the discriminating capabilities of both models were good enough (AUC values >0.65). Notably, in this paper, only the models that matched are presented.

4.6. Verification of Selected Polymorphisms

In this study, the following selected genetic variants (with coordinates consistent with the hg38 human genome assembly) in 8 genes were verified by gradient PCR and Sanger sequencing: *MUTYH*, chr1:45332673del; *BRCA2*, chr17:43093093_43093096del; *FANCE*, chr6:g.35456000T>G; *FANCI*, chr15:g.89295051C>T; *FANCM*, chr14:g.45187852C>G; *PRKDC*, chr8:g.47779009C>T; *RAD51D*, chr17:g.35106436del; and *TP53*, chr17:g.7670658_7670659insA, COSV99037094. The PCR reactions employed either the AmpliTaq Gold™ DNA Polymerase (Thermo) or the Phusion Green High-Fidelity DNA Polymerase (Thermo)) and in-house-designed sets of primers (Table S3). PCR products were analyzed by agarose gel electrophoresis using the Simply Safe reagent (EurX, Gdansk, Poland) for DNA visualization. Gels were documented on the UVP ChemStudio Imaging System (Analityk Jena, Jena, Germany). Afterward, specific PCR products of expected lengths were cleaned with ExoSAP-IT (Thermo) and sequenced using the appropriate primer and the BigDye Terminator v 3.1 Cycle Sequencing Kit (Thermo). Sanger sequencing products were then cleaned with the ExTerminator Kit (A&A Biotechnology, Gdansk, Poland) and analyzed on the 3500 Genetic Analyzer (Thermo).

4.7. Protein Concentration Measurement

Total protein lysates were obtained by incubating tumor samples with the RIPA buffer supplemented with the Halt Protease Inhibitor Cocktail (Thermo). Next, the concentration of each lysate was evaluated with the BCA assay (Sigma Aldrich, Saint Louis, MO, USA), using BSA (Thermo) in amounts ranging from 0 to 25 µg per well as a standard curve. The absorbance at 540 nm was measured on the Victor 3 spectrophotometer (model: 1420-012, Perkin Elmer, Waltham, MA, USA). The negative control wells, containing only the BCA solution, were used as blank samples in this experiment.

4.8. Western Blot (WB) Analyses

WB analyses were performed for selected variants in genes coding for the TP53, NBN, CHEK1, CHEK2, FANCI, and FANCD2 proteins. Each WB experiment was preceded by WB tests confirming the specificity of the used primary antibodies (Abs). Except for lysates prepared from tumors, we also used a lysate prepared from a normal ovary as a control. For each experiment, 15–20 μg of a protein lysate was added per well. An electrophoretic separation of proteins was performed in 10–12% polyacrylamide gels (40% stock solution with the acrylamide to bis-acrylamide ratio equaling 37.5:1, BioRad, Hercules, CA, USA). To estimate the molecular weights of proteins, we used either the Broad Range Prestained Protein Marker (Proteintech, Rosemont, IL, USA) or the Precision Plus Protein Standard (BioRad). Depending on the protein being analyzed, either 0.2 μm nitrocellulose (Amersham™ Protran®, Cytiva, Marlborough, MA, USA) or 0.2 μm PVDF (Thermo) membranes were used. The transfer buffer was composed of 25 mM Tris (Sigma Aldrich), 192 mM Glycine (Sigma Aldrich), and 5–10% (*v/v*) methanol (Sigma Aldrich). Protein transfer was performed overnight (4 °C, 27 mA) or for 1–1.25 h (4 °C, 300 mA). For the membrane blocking, a 5% solution of skimmed milk (SM Gostyn, Gostyn, Poland) in the 1xTBST buffer (Tris-buffered saline (0.05 M Tris and 0.15 M NaCl) with 0.1% Tween-20 detergent (Sigma)) was used. As loading controls, Ponceau S red (Sigma Aldrich) staining, rabbit anti-β-actin Ab (1:100) (Thermo), and rabbit anti-vinculin Ab (1:500) (Thermo) were applied. Most primary Abs against selected proteins were purchased from Proteintech and were polyclonal antibodies developed in rabbits. By contrast, the primary mouse anti-TP53 antibody (Calbiochem, San Diego, CA, USA) was monoclonal. Chemiluminescence signals were detected on the UVP ChemStudio Imaging System (Analytik Jena, Jena, Germany) using either the goat anti-rabbit HRP-conjugated secondary Ab (Thermo) or the goat anti-mouse HRP-conjugated secondary Ab (Proteintech) and the SignalBright Max Chemiluminescent Substrate (Proteintech). A detailed description of the WB conditions for each protein is presented in Table S4.

5. Conclusions

In this study, we examined the role of polymorphic variants in the most important oncogenes and suppressors in BOTS, lgOvCa, and hgOvCa. Our work contributes to the elucidation of the molecular landscape of various ovarian neoplasms, demonstrating completely divergent mutation profiles and molecular pathways engaged in their development. Certain mutations seem to play an important role in BOTS without the *BRAF* V600E variant (*KRAS*) and in lgOvCa (*KRAS* and *NRAS*), but not in hgOvCa, once again proving that advanced OvCa are molecularly distinct from less aggressive ovarian neoplasms. Additionally, based on multivariable regression analyses utilizing detailed clinicopathological data, potential biomarkers in BOTS (*PARP1*) and hgOvCa (*FANCI*, *BRCA2*, *TSC2*, *FANCF*) were identified. Noteworthy, for some of the analyzed genes, such as *FANCI*, *FANCD2*, and *FANCI*, *FANCF*, *TSC2*, the status of BRCA1/2 and TP53, respectively, turned out to be crucial. Although thorough mechanistic insight is necessary to fully investigate the molecular background of each genetic variant reported herein and to understand its clinical importance, still, our work sheds new light on the similarities and differences in the polymorphic patterns between ovarian tumors of diverse aggressiveness. Thus, it forms a valuable foundation for future research.

Institutional Review Board Statement: This study was conducted according to the guidelines of the Declaration of Helsinki and was approved in writing by the Institutional Review Board of the Maria Sklodowska-Curie National Research Institute of Oncology (nos. 49/2003 and 39/2007).

Informed Consent Statement: Informed consent was obtained from all subjects involved in this study.

Data Availability Statement: All data are available in the main text or Supplementary Materials.

References

1. Arora, T.; Mullangi, S.; Lekkala, M.R. *Ovarian Cancer*; StatPearls Publishing: Treasure Island, FL, USA, 2022.
2. Guo, T.; Dong, X.; Xie, S.; Zhang, L.; Zeng, P.; Zhang, L. Cellular Mechanism of Gene Mutations and Potential Therapeutic Targets in Ovarian Cancer. *CMAR* **2021**, *13*, 3081–3100. [CrossRef]
3. Babaier, A.; Mal, H.; Alselwi, W.; Ghatage, P. Low-Grade Serous Carcinoma of the Ovary: The Current Status. *Diagnostics* **2022**, *12*, 458. [CrossRef]
4. Wong, K.-K.; Bateman, N.W.; Ng, C.W.; Tsang, Y.T.M.; Sun, C.S.; Celestino, J.; Nguyen, T.V.; Malpica, A.; Hillman, R.T.; Zhang, J.; et al. Integrated Multi-Omic Analysis of Low-Grade Ovarian Serous Carcinoma Collected from Short and Long-Term Survivors. *J. Transl. Med.* **2022**, *20*, 606. [CrossRef]
5. Hauptmann, S.; Friedrich, K.; Redline, R.; Avril, S. Ovarian Borderline Tumors in the 2014 WHO Classification: Evolving Concepts and Diagnostic Criteria. *Virchows Arch.* **2017**, *470*, 125–142. [CrossRef] [PubMed]
6. Seong, S.J.; Kim, D.H.; Kim, M.K.; Song, T. Controversies in Borderline Ovarian Tumors. *J. Gynecol. Oncol.* **2015**, *26*, 343–349. [CrossRef]
7. Niu, L.; Tian, H.; Xu, Y.; Cao, J.; Zhang, X.; Zhang, J.; Hou, J.; Lv, W.; Wang, J.; Xin, L.; et al. Recurrence Characteristics and Clinicopathological Results of Borderline Ovarian Tumors. *BMC Women's Health* **2021**, *21*, 134. [CrossRef]
8. Shih, K.; Zhou, Q.; Huh, J.; Morgan, J.; Iasonos, A.; Aghajanian, C.; Chi, D.; Barakat, R.; Abu-Rustum, N. Risk Factors for Recurrence of Ovarian Borderline Tumors. *Gynecol. Oncol.* **2011**, *120*, 480–484. [CrossRef]
9. Bjørge, T.; Lie, A.K.; Hovig, E.; Gislefoss, R.E.; Hansen, S.; Jellum, E.; Langseth, H.; Nustad, K.; Tropé, C.G.; Dørum, A. BRCA1 Mutations in Ovarian Cancer and Borderline Tumours in Norway: A Nested Case–Control Study. *Br. J. Cancer* **2004**, *91*, 1829–1834. [CrossRef]
10. Lakhani, S.R.; Manek, S.; Penault-Llorca, F.; Flanagan, A.; Arnout, L.; Merrett, S.; McGuffog, L.; Steele, D.; Devilee, P.; Klijn, J.G.M.; et al. Pathology of Ovarian Cancers in BRCA1 and BRCA2 Carriers. *Clin. Cancer Res.* **2004**, *10*, 2473–2481. [CrossRef]
11. Singer, G.; Stöhr, R.; Cope, L.; Dehari, R.; Hartmann, A.; Cao, D.-F.; Wang, T.-L.; Kurman, R.J.; Shih, I.-M. Patterns of P53 Mutations Separate Ovarian Serous Borderline Tumors and Low- and High-Grade Carcinomas and Provide Support for a New Model of Ovarian Carcinogenesis: A Mutational Analysis with Immunohistochemical Correlation. *Am. J. Surg. Pathol.* **2005**, *29*, 218–224. [CrossRef]
12. Mayr, D.; Hirschmann, A.; Löhrs, U.; Diebold, J. KRAS and BRAF Mutations in Ovarian Tumors: A Comprehensive Study of Invasive Carcinomas, Borderline Tumors and Extraovarian Implants. *Gynecol. Oncol.* **2006**, *103*, 883–887. [CrossRef]
13. Grisham, R.N.; Iyer, G.; Garg, K.; Delair, D.; Hyman, D.M.; Zhou, Q.; Iasonos, A.; Berger, M.F.; Dao, F.; Spriggs, D.R.; et al. BRAF Mutation Is Associated with Early Stage Disease and Improved Outcome in Patients with Low-Grade Serous Ovarian Cancer. *Cancer* **2013**, *119*, 548–554. [CrossRef]
14. Stemke-Hale, K.; Shipman, K.; Kitsou-Mylona, I.; de Castro, D.G.; Hird, V.; Brown, R.; Flanagan, J.; Hani Gabra, H.; Mills, G.B.; Agarwal, R.; et al. Frequency of Mutations and Polymorphisms in Borderline Ovarian Tumors of Known Cancer Genes. *Mod. Pathol.* **2013**, *26*, 544–552. [CrossRef]
15. Ogrodniczak, A.; Menkiszak, J.; Gronwald, J.; Tomiczek-Szwiec, J.; Szwiec, M.; Cybulski, C.; Dębniak, T.; Huzarski, T.; Tołoczko-Grabarek, A.; Byrski, T.; et al. Association of Recurrent Mutations in BRCA1, BRCA2, RAD51C, PALB2, and CHEK2 with the Risk of Borderline Ovarian Tumor. *Hered. Cancer Clin. Pract.* **2022**, *20*, 11. [CrossRef]
16. Ko, E.-A.; Kim, Y.-W.; Lee, D.; Choi, J.; Kim, S.; Seo, Y.; Bang, H.; Kim, J.-H.; Ko, J.-H. Expression of Potassium Channel Genes Predicts Clinical Outcome in Lung Cancer. *Korean J. Physiol. Pharmacol. Off. J. Korean Physiol. Soc. Korean Soc. Pharmacol.* **2019**, *23*, 529. [CrossRef]
17. Stelzer, G.; Rosen, N.; Plaschkes, I.; Zimmerman, S.; Twik, M.; Fishilevich, S.; Stein, T.I.; Nudel, R.; Lieder, I.; Mazor, Y.; et al. The GeneCards Suite: From Gene Data Mining to Disease Genome Sequence Analyses. *Curr. Protoc. Bioinform.* **2016**, *54*, 1.30.1–1.30.33. [CrossRef]
18. Szafron, L.A.; Iwanicka-Nowicka, R.; Podgorska, A.; Bonna, A.M.; Sobiczewski, P.; Kupryjanczyk, J.; Szafron, L.M. The Clinical Significance of CRNDE Gene Methylation, Polymorphisms, and CRNDEP Micropeptide Expression in Ovarian Tumors. *Int. J. Mol. Sci.* **2024**, *25*, 7531. [CrossRef]

19. Griffith, O.L.; Spies, N.C.; Anurag, M.; Griffith, M.; Luo, J.; Tu, D.; Yeo, B.; Kunisaki, J.; Miller, C.A.; Krysiak, K.; et al. The Prognostic Effects of Somatic Mutations in ER-Positive Breast Cancer. *Nat. Commun.* **2018**, *9*, 3476. [CrossRef]

20. Vias, M.; Morrill Gavarró, L.; Sauer, C.M.; Sanders, D.A.; Piskorz, A.M.; Couturier, D.-L.; Ballereau, S.; Hernando, B.; Schneider, M.P.; Hall, J.; et al. High-Grade Serous Ovarian Carcinoma Organoids as Models of Chromosomal Instability. *eLife* **2023**, *12*, e83867. [CrossRef]

21. Smith, P.; Bradley, T.; Gavarró, L.M.; Goranova, T.; Ennis, D.P.; Mirza, H.B.; De Silva, D.; Piskorz, A.M.; Sauer, C.M.; Al-Khalidi, S.; et al. The Copy Number and Mutational Landscape of Recurrent Ovarian High-Grade Serous Carcinoma. *Nat. Commun.* **2023**, *14*, 4387. [CrossRef]

22. Kupryjanczyk, J.; Bell, D.A.; Dimeo, D.; Beauchamp, R.; Thor, A.D.; Yandell, D.W. P53 Gene Analysis of Ovarian Borderline Tumors and Stage I Carcinomas. *Hum. Pathol.* **1995**, *26*, 387–392. [CrossRef]

23. Katabuchi, H.; Tashiro, H.; Cho, K.R.; Kurman, R.J.; Hedrick Ellenson, L. Micropapillary Serous Carcinoma of the Ovary: An Immunohistochemical and Mutational Analysis of P53. *Int. J. Gynecol. Pathol.* **1998**, *17*, 54–60. [CrossRef]

24. Testa, U.; Petrucci, E.; Pasquini, L.; Castelli, G.; Pelosi, E. Ovarian Cancers: Genetic Abnormalities, Tumor Heterogeneity and Progression, Clonal Evolution and Cancer Stem Cells. *Medicines* **2018**, *5*, 16. [CrossRef]

25. KAPA HyperPETE. Available online: https://sequencing.roche.com/us/en/products/product-category/primer-extension-based-target-enrichment.html (accessed on 7 June 2024).

26. Kang, E.Y.; Cheasley, D.; LePage, C.; Wakefield, M.J.; da Cunha Torres, M.; Rowley, S.; Salazar, C.; Xing, Z.; Allan, P.; Bowtell, D.D.L.; et al. Refined Cut-off for TP53 Immunohistochemistry Improves Prediction of TP53 Mutation Status in Ovarian Mucinous Tumors: Implications for Outcome Analyses. *Mod. Pathol.* **2021**, *34*, 194–206. [CrossRef]

27. Kupryjańczyk, J.; Szymańska, T.; Madry, R.; Timorek, A.; Stelmachów, J.; Karpińska, G.; Rembiszewska, A.; Ziółkowska, I.; Kraszewska, E.; Debniak, J.; et al. Evaluation of Clinical Significance of TP53, BCL-2, BAX and MEK1 Expression in 229 Ovarian Carcinomas Treated with Platinum-Based Regimen. *Br. J. Cancer* **2003**, *88*, 848–854. [CrossRef]

28. Ghezelayagh, T.S.; Pennington, K.P.; Norquist, B.M.; Khasnavis, N.; Radke, M.R.; Kilgore, M.R.; Garcia, R.L.; Lee, M.; Katz, R.; Leslie, K.K.; et al. Characterizing TP53 Mutations in Ovarian Carcinomas with and without Concurrent BRCA1 or BRCA2 Mutations. *Gynecol. Oncol.* **2021**, *160*, 786–792. [CrossRef]

29. Lhotova, K.; Stolarova, L.; Zemankova, P.; Vocka, M.; Janatova, M.; Borecka, M.; Cerna, M.; Jelinkova, S.; Kral, J.; Volkova, Z.; et al. Multigene Panel Germline Testing of 1333 Czech Patients with Ovarian Cancer. *Cancers* **2020**, *12*, 956. [CrossRef]

30. Flis, M.; Krawczyk, P.; Drogoń, I.; Kurek, K.; Kieszko, R.; Milanowski, J. The Effectiveness of Chemotherapy in Small Cell Lung Cancer Patients with BRCA2 Gene Mutation and Schwartz-Bartter Syndrome. *Oncol. Clin. Pr.* **2019**, *15*, 120–123. [CrossRef]

31. Mylavarapu, S.; Das, A.; Roy, M. Role of BRCA Mutations in the Modulation of Response to Platinum Therapy. *Front. Oncol.* **2018**, *8*, 16. [CrossRef]

32. Roy, R.; Chun, J.; Powell, S.N. BRCA1 and BRCA2: Different Roles in a Common Pathway of Genome Protection. *Nat. Rev. Cancer* **2011**, *12*, 68–78. [CrossRef]

33. Moujaber, T.; Etemadmoghadam, D.; Kennedy, C.J.; Chiew, Y.-E.; Balleine, R.L.; Saunders, C.; Wain, G.V.; Gao, B.; Hogg, R.; Srirangan, S.; et al. BRAF Mutations in Low-Grade Serous Ovarian Cancer and Response to BRAF Inhibition. *JCO Precis. Oncol.* **2018**, *2*, 1–14. [CrossRef]

34. Auner, V.; Kriegshäuser, G.; Tong, D.; Horvat, R.; Reinthaller, A.; Mustea, A.; Zeillinger, R. KRAS Mutation Analysis in Ovarian Samples Using a High Sensitivity Biochip Assay. *BMC Cancer* **2009**, *9*, 111. [CrossRef]

35. Garziera, M.; Roncato, R.; Montico, M.; De Mattia, E.; Gagno, S.; Poletto, E.; Scalone, S.; Canzonieri, V.; Giorda, G.; Sorio, R.; et al. New Challenges in Tumor Mutation Heterogeneity in Advanced Ovarian Cancer by a Targeted Next-Generation Sequencing (NGS) Approach. *Cells* **2019**, *8*, 584. [CrossRef]

36. Mutations in the KRAS Gene in Ovarian Tumors—PubMed. Available online: https://pubmed.ncbi.nlm.nih.gov/19995707/ (accessed on 14 January 2024).

37. Merz, V.; Gaule, M.; Zecchetto, C.; Cavaliere, A.; Casalino, S.; Pesoni, C.; Contarelli, S.; Sabbadini, F.; Bertolini, M.; Mangiameli, D.; et al. Targeting KRAS: The Elephant in the Room of Epithelial Cancers. *Front. Oncol.* **2021**, *11*, 638360. [CrossRef]

38. Zhu, C.; Guan, X.; Zhang, X.; Luan, X.; Song, Z.; Cheng, X.; Zhang, W.; Qin, J.-J. Targeting KRAS Mutant Cancers: From Druggable Therapy to Drug Resistance. *Mol. Cancer* **2022**, *21*, 159. [CrossRef]

39. Śmiech, M.; Leszczyński, P.; Kono, H.; Wardell, C.; Taniguchi, H. Emerging BRAF Mutations in Cancer Progression and Their Possible Effects on Transcriptional Networks. *Genes* **2020**, *11*, 1342. [CrossRef]

40. Hunter, S.M.; Anglesio, M.S.; Ryland, G.L.; Sharma, R.; Chiew, Y.-E.; Rowley, S.M.; Doyle, M.A.; Li, J.; Gilks, C.B.; Moss, P.; et al. Molecular Profiling of Low Grade Serous Ovarian Tumours Identifies Novel Candidate Driver Genes. *Oncotarget* **2015**, *6*, 37663–37677. [CrossRef]

41. Xing, D.; Suryo Rahmanto, Y.; Zeppernick, F.; Hannibal, C.G.; Kjaer, S.K.; Vang, R.; Shih, I.-M.; Wang, T.-L. Mutation of NRAS Is a Rare Genetic Event in Ovarian Low-Grade Serous Carcinoma. *Hum. Pathol.* **2017**, *68*, 87–91. [CrossRef]

42. Champer, M.; Miller, D.; Kuo, D.Y.-S. Response to Trametinib in Recurrent Low-Grade Serous Ovarian Cancer with NRAS Mutation: A Case Report. *Gynecol. Oncol. Rep.* **2019**, *28*, 26–28. [CrossRef]

43. Grill, C.; Larue, L. NRAS, NRAS, Which Mutation Is Fairest of Them All? *J. Investig. Dermatol.* **2016**, *136*, 1936–1938. [CrossRef]

44. McCluggage, W.G. Ovarian Borderline Tumours: A Review with Comparison of Serous and Mucinous Types. *Diagn. Histopathol.* **2014**, *20*, 333–350. [CrossRef]

45. Zhong, F.; Zhu, T.; Pan, X.; Zhang, Y.; Yang, H.; Wang, X.; Hu, J.; Han, H.; Mei, L.; Chen, D.; et al. Comprehensive Genomic Profiling of High-grade Serous Ovarian Carcinoma from Chinese Patients Identifies Co-occurring Mutations in the *Ras/Raf* Pathway with *TP53*. *Cancer Med.* **2019**, *8*, 3928–3935. [CrossRef]

46. Bożyk, A.; Krawczyk, P.; Reszka, K.; Krukowska, K.; Kolak, A.; Mańdziuk, S.; Wojas-Krawczyk, K.; Ramlau, R.; Milanowski, J. Correlation between KRAS, NRAS and BRAF Mutations and Tumor Localizations in Patients with Primary and Metastatic Colorectal Cancer. *Arch. Med. Sci. AMS* **2022**, *18*, 1221–1230. [CrossRef]

47. Alessandro, L.; Low, K.-J.E.; Abushelaibi, A.; Lim, S.-H.E.; Cheng, W.-H.; Chang, S.-K.; Lai, K.-S.; Sum, Y.W.; Maran, S. Identification of NRAS Diagnostic Biomarkers and Drug Targets for Endometrial Cancer-An Integrated in Silico Approach. *Int. J. Mol. Sci.* **2022**, *23*, 14285. [CrossRef]

48. Sideris, M.; Emin, E.I.; Abdullah, Z.; Hanrahan, J.; Stefatou, K.M.; Sevas, V.; Emin, E.; Hollingworth, T.; Odejinmi, F.; Papagrigoriadis, S.; et al. The Role of KRAS in Endometrial Cancer: A Mini-Review. *Anticancer Res.* **2019**, *39*, 533–539. [CrossRef]

49. He, M.; Breese, V.; Hang, S.; Zhang, C.; Xiong, J.; Jackson, C. BRAF V600E Mutations in Endometrial Adenocarcinoma. *Diagn. Mol. Pathol. Am. J. Surg. Pathol. Part B* **2013**, *22*, 35–40. [CrossRef]

50. Gianni, P.; Matenoglou, E.; Geropoulos, G.; Agrawal, N.; Adnani, H.; Zafeiropoulos, S.; Miyara, S.J.; Guevara, S.; Mumford, J.M.; Molmenti, E.P.; et al. The Fanconi Anemia Pathway and Breast Cancer: A Comprehensive Review of Clinical Data. *Clin. Breast Cancer* **2022**, *22*, 10–25. [CrossRef]

51. Del Valle, J.; Rofes, P.; Moreno-Cabrera, J.M.; López-Dóriga, A.; Belhadj, S.; Vargas-Parra, G.; Teulé, À.; Cuesta, R.; Muñoz, X.; Campos, O.; et al. Exploring the Role of Mutations in Fanconi Anemia Genes in Hereditary Cancer Patients. *Cancers* **2020**, *12*, 829. [CrossRef]

52. Gajewski, S.; Hartwig, A. PARP1 Is Required for ATM-Mediated P53 Activation and P53-Mediated Gene Expression after Ionizing Radiation. *Chem. Res. Toxicol.* **2020**, *33*, 1933–1940. [CrossRef]

53. Zuo, W.-W.; Zhao, C.-F.; Li, Y.; Sun, H.-Y.; Ma, G.-M.; Liu, Y.-P.; Kang, S. High Expression of PARP1 in Tumor and Stroma Cells Predicts Different Prognosis and Platinum Resistance in Patients With Advanced Epithelial Ovarian Cancer. *Front. Oncol.* **2022**, *12*, 931445. [CrossRef]

54. Hockings, H.; Miller, R.E. The Role of PARP Inhibitor Combination Therapy in Ovarian Cancer. *Ther. Adv. Med. Oncol.* **2023**, *15*, 17588359231173183. [CrossRef]

55. Miller, R.E.; El-Shakankery, K.H.; Lee, J.-Y. PARP Inhibitors in Ovarian Cancer: Overcoming Resistance with Combination Strategies. *J. Gynecol. Oncol.* **2022**, *33*, e44. [CrossRef]

56. Wang, S.S.Y.; Jie, Y.E.; Cheng, S.W.; Ling, G.L.; Ming, H.V.Y. PARP Inhibitors in Breast and Ovarian Cancer. *Cancers* **2023**, *15*, 2357. [CrossRef]

57. Anjali, K.; Singh, D.; Kumar, P.; Kumar, T.; Narayan, G.; Singh, S. PARP1 Rs1136410 (A/G) Polymorphism Is Associated with Early Age of Onset of Gallbladder Cancer. *Eur. J. Cancer Prev.* **2022**, *31*, 311–317. [CrossRef]

58. Li, H.; Zha, Y.; Du, F.; Liu, J.; Li, X.; Zhao, X. Contributions of PARP-1 Rs1136410 C>T Polymorphism to the Development of Cancer. *J. Cell. Mol. Med.* **2020**, *24*, 14639–14644. [CrossRef]

59. Ma, X.-B.; Wang, X.-J.; Wang, M.; Dai, Z.-M.; Jin, T.-B.; Liu, X.-H.; Kang, H.-F.; Lin, S.; Xu, P.; Dai, Z.-J. Impact of the PARP1 Rs1136410 and Rs3219145 Polymorphisms on Susceptibility and Clinicopathologic Features of Breast Cancer in a Chinese Population. *Transl. Cancer Res.* **2016**, *5*. [CrossRef]

60. Postawski, K.; Monist, M.; Keith, G. PARP-1 Activity in Normal and Cancerous Human Endometrium and Its Relationship with Quantity of Abasic Sites (AP). *Ginekol. Pol.* **2011**, *82*, 16–21.

61. Zhang, X.; Lu, X.; Akhter, S.; Georgescu, M.-M.; Legerski, R.J. FANCI Is a Negative Regulator of Akt Activation. *Cell Cycle* **2016**, *15*, 1134–1143. [CrossRef]

62. Cai, Z.; Duan, Y.; Li, W.; Liu, Z.; Gong, Z.; Hong, S.; He, X.; Xuanyuan, X.; Chen, Y.; Bi, X.; et al. FANCI Serve as a Prognostic Biomarker Correlated with Immune Infiltrates in Skin Cutaneous Melanoma. *Front. Immunol.* **2023**, *14*, 1295831. [CrossRef]

63. Fierheller, C.T.; Alenezi, W.M.; Serruya, C.; Revil, T.; Amuzu, S.; Bedard, K.; Subramanian, D.N.; Fewings, E.; Bruce, J.P.; Prokopec, S.; et al. Molecular Genetic Characteristics of FANCI, a Proposed New Ovarian Cancer Predisposing Gene. *Genes* **2023**, *14*, 277. [CrossRef]

64. Fierheller, C.T.; Guitton-Sert, L.; Alenezi, W.M.; Revil, T.; Oros, K.K.; Gao, Y.; Bedard, K.; Arcand, S.L.; Serruya, C.; Behl, S.; et al. A Functionally Impaired Missense Variant Identified in French Canadian Families Implicates FANCI as a Candidate Ovarian Cancer-Predisposing Gene. *Genome Med.* **2021**, *13*, 186. [CrossRef] [PubMed]

65. Zhang, Y.; Hunter, T. Roles of Chk1 in Cell Biology and Cancer Therapy. *Int. J. Cancer* **2014**, *134*, 1013–1023. [CrossRef]

66. McNeely, S.; Beckmann, R.; Bence Lin, A.K. CHEK Again: Revisiting the Development of CHK1 Inhibitors for Cancer Therapy. *Pharmacol. Ther.* **2014**, *142*, 1–10. [CrossRef] [PubMed]

67. Fadaka, A.O.; Bakare, O.O.; Sibuyi, N.R.S.; Klein, A. Gene Expression Alterations and Molecular Analysis of CHEK1 in Solid Tumors. *Cancers* **2020**, *12*, 662. [CrossRef]

68. Neizer-Ashun, F.; Bhattacharya, R. Reality CHEK: Understanding the Biology and Clinical Potential of CHK1. *Cancer Lett.* **2021**, *497*, 202–211. [CrossRef]

69. Morden, C.R.; Farrell, A.C.; Sliwowski, M.; Lichtensztejn, Z.; Altman, A.D.; Nachtigal, M.W.; McManus, K.J. Chromosome Instability Is Prevalent and Dynamic in High-Grade Serous Ovarian Cancer Patient Samples. *Gynecol. Oncol.* **2021**, *161*, 769–778. [CrossRef]

70. Creasman, W.J. Announcement, FIGO Stages 1988, Revisions. *Gynecol. Oncol.* **1989**, *35*, 125–127.

71. Mehra, P.; Aditi, S.; Prasad, K.M.; Bariar, N.K. Histomorphological Analysis of Ovarian Neoplasms According to the 2020 WHO Classification of Ovarian Tumors: A Distribution Pattern in a Tertiary Care Center. *Cureus* **2023**, *15*, e38273. [CrossRef]

72. Miller, A.B.; Hoogstraten, B.; Staquet, M.; Winkler, A. Reporting Results of Cancer Treatment. *Cancer* **1981**, *47*, 207–214. [CrossRef]

73. Woroniecka, R.; Rymkiewicz, G.; Szafron, L.M.; Blachnio, K.; Szafron, L.A.; Bystydzienski, Z.; Pienkowska-Grela, B.; Borkowska, K.; Rygier, J.; Kotyl, A.; et al. Cryptic MYC Insertions in Burkitt Lymphoma: New Data and a Review of the Literature. *PLoS ONE* **2022**, *17*, e0263980. [CrossRef]

74. McLaren, W.; Gil, L.; Hunt, S.E.; Riat, H.S.; Ritchie, G.R.S.; Thormann, A.; Flicek, P.; Cunningham, F. The Ensembl Variant Effect Predictor. *Genome Biol.* **2016**, *17*, 122. [CrossRef]

75. Calculated Consequences. Available online: https://www.ensembl.org/info/genome/variation/prediction/predicted_data.html (accessed on 3 July 2021).

76. Gerds, T.A.; Cai, T.; Schumacher, M. The Performance of Risk Prediction Models. *Biom. J.* **2008**, *50*, 457–479. [CrossRef]

The Diversity of Methylation Patterns in Serous Borderline Ovarian Tumors and Serous Ovarian Carcinomas

Laura A. Szafron [1,*], Roksana Iwanicka-Nowicka [2,3], Piotr Sobiczewski [4], Marta Koblowska [2,3], Agnieszka Dansonka-Mieszkowska [5], Jolanta Kupryjanczyk [6] and Lukasz M. Szafron [1,*]

[1] Maria Sklodowska-Curie National Research Institute of Oncology, 02-781 Warsaw, Poland
[2] Laboratory of Systems Biology, Faculty of Biology, University of Warsaw, 02-106 Warsaw, Poland; r.iwanicka@uw.edu.pl (R.I.-N.); marta@ibb.waw.pl (M.K.)
[3] Laboratory for Microarray Analysis, Institute of Biochemistry and Biophysics, Polish Academy of Sciences, 02-106 Warsaw, Poland
[4] Department of Gynecological Oncology, Maria Sklodowska-Curie National Research Institute of Oncology, 02-781 Warsaw, Poland; sobiczewskipiotr7@gmail.com
[5] Cancer Molecular and Genetic Diagnostics Department, Maria Sklodowska-Curie National Research Institute of Oncology, 02-781 Warsaw, Poland; agnieszka.dansonka-mieszkowska@nio.gov.pl
[6] Department of Cancer Pathomorphology, Maria Sklodowska-Curie National Research Institute of Oncology, 02-781 Warsaw, Poland; jolanta.kupryjanczyk@nio.gov.pl
[*] Correspondence: laura.szafron@gmail.com (L.A.S.); lukszafron@gmail.com (L.M.S.)

Simple Summary: In tumorigenesis, aberrant DNA methylation may be an earlier and stronger modifier of gene expression than mutations. Herein, 128 serous ovarian tumors were analyzed, including borderline ovarian tumors (BOTS) with (BOT.V600E) and without (BOT) the *BRAF* V600E mutation, low-grade (lg), and high-grade (hg) ovarian cancers (OvCa). The methylome of the samples was profiled with Infinium MethylationEPIC microarrays. Global, genome-wide hypomethylation positively correlated with the increasing aggressiveness of tumors, being the strongest in hgOvCa. Remarkably, the ten most significant differentially methylated regions (DMRs) in the genome, discriminating BOT from lgOvCa, encompassed the MHC region on chromosome 6. We also identified hundreds of DMRs potentially useful as predictive biomarkers in BOTS and hgOvCa. DMRs with the best discriminative capabilities overlapped the following genes: *BAIAP3*, *IL34*, *WNT10A*, *NEU1*, *SLC44A4,* and *HMOX1*, *TCN2*, *PES1*, *RP1-56J10.8*, *ABR*, *NCAM1*, *RP11-629G13.1*, *AC006372.4*, *NPTXR* in BOTS and hgOvCa, respectively. By identifying potential biomarkers, this study might improve ovarian tumor outcome.

Abstract: Background: Changes in DNA methylation patterns are a pivotal mechanism of carcinogenesis. In some tumors, aberrant methylation precedes genetic changes, while gene expression may be more frequently modified due to methylation alterations than by mutations. **Methods**: Herein, 128 serous ovarian tumors were analyzed, including borderline ovarian tumors (BOTS) with (BOT.V600E) and without (BOT) the *BRAF* V600E mutation, low-grade (lg), and high-grade (hg) ovarian cancers (OvCa). The methylome of the samples was profiled with Infinium MethylationEPIC microarrays. **Results**: The biggest number of differentially methylated (DM) CpGs and regions (DMRs) was found between lgOvCa and hgOvCa. By contrast, the BOT.V600E tumors had the lowest number of DM CpGs and DMRs compared to all other groups and, in relation to BOT, their genome was strongly downmethylated. Remarkably, the ten most significant DMRs, discriminating BOT from lgOvCa, encompassed the MHC region on chromosome 6. We also identified hundreds of DMRs, being of potential use as predictive biomarkers in BOTS and hgOvCa. DMRs with the best discriminative capabilities overlapped the following genes: *BAIAP3*, *IL34*, *WNT10A*, *NEU1*, *SLC44A4*, and *HMOX1*, *TCN2*, *PES1*, *RP1-56J10.8*, *ABR*, *NCAM1*, *RP11-629G13.1*, *AC006372.4*, *NPTXR* in BOTS and hgOvCa, respectively. **Conclusions**: The global genome-wide hypomethylation positively correlates with the increasing aggressiveness of ovarian tumors. We also assume that the immune system may play a pivotal role in the transition from BOTS to lgOvCa. Given that the BOT.V600E tumors had the lowest number of DM CpGs and DMRs compared to all other groups, when methylome is considered, such tumors might be placed in-between BOT and OvCa.

1. Introduction

Changes in DNA *methylation patterns are* a pivotal mechanism of carcinogenesis. In tumors, aberrant DNA methylation may be an earlier event than mutations. In some cancers, gene expression may even be more frequently modified due to methylation alterations than by mutations [1,2]. Borderline ovarian tumors (BOTS) exhibit intermediate aggressiveness between benign tumors and invasive carcinomas. They are a rare entity with relatively low malignant potential. In contrast to the majority of ovarian carcinomas, BOTS usually occur in women in reproductive age, are usually diagnosed at the low FIGO stage, and are characterized by better survival rates. Imaging methods (ultrasound, MRI) are useful to distinguish BOTS from OvCa preoperatively. However, the final diagnosis must be based on histopathological examination. Surgery with a complete resection is the cornerstone of BOTS treatment. Still, in young women considering procreation, a fertility-sparing surgical intervention is preferentially applied. Remarkably, chemotherapy is not recommended in BOTS [3,4]. Following the complete removal of the tumor, even 20% of BOTS may recur, usually as borderline tumors; however, in some patients, BOTS may recur as ovarian carcinomas [5–8]. Moreover, serous BOTS are closely related to serous low-grade carcinomas (lgOvCa), as they harbor similar genetic alterations [7,9]. By contrast, high-grade serous ovarian carcinomas (hgOvCa) are considered distinct ovarian neoplasms, molecularly unrelated to lgOvCa and BOTS [10]. Considering methylome changes, it was reported that serous hgOvCa form a separate cluster compared to BOTS and lgOvCa [11]. However, so far, methylation patterns of BOTS and lgOvCa of the serous type have been evaluated with low-resolution microarrays only. In addition, scientific data comparing ovarian tumors of diverse aggressiveness are still very scarce [11–14]. To fill out this gap, we aimed to obtain very detailed methylation profiles in such tumors. For this purpose, we performed the methylation analysis in non-consecutive primary serous ovarian tumors, obtained from previously untreated patients, using high throughput microarrays. This analysis was then validated by methylation-specific PCR combined with Sanger sequencing. Moreover, to investigate the biological role of the nominated biomarkers and assess their clinical usefulness, we carried out detailed DNA strand-specific and fold change-dependent ontology analyses, followed by the comprehensive statistical inference of all differentially methylated regions in the genome with multivariable regression models. Considering that the TP53 accumulation status has been previously shown to affect the clinical meaning of other molecular markers in our previous research on ovarian cancers [15,16], we decided to take this parameter into account in the present study. As to BOTS, we investigated these tumors in the context of the mutational status of the *BRAF* oncogene, which was demonstrated to be crucial for borderline ovarian tumors but not ovarian cancers [17,18]. Simultaneously, the presence of the *BRAF* V600E mutation turned out to be a negative clinical factor, associated with the earlier onset of BOTS in our previous research [19].

2. Materials and Methods

2.1. Patients and Clinicopathological Parameters

In the present study, a set of 128 non-consecutive, primary serous ovarian tumors of different aggressiveness was investigated. All the patients with these tumors were hospitalized at the Maria Sklodowska-Curie National Research Institute of Oncology, Warsaw, Poland in the years 1995–2015. Medical records of the patients were critically reviewed by at least two physicians. Our set of tumors included 25 BOTS (11 with and 14 without the *BRAF* V600E mutation, Table S1) and 103 OvCa (7 lgOvCa and 96 hgOvCa, Table S2). The specimens were selected to meet the following criteria: adequate staging procedure according to the recommendations by the International Federation of Gynecologists and

Obstetricians (FIGO), tumor tissue from the first laparotomy available, availability of clinical data including patient age and follow-up, as well as tumor histological type and grade, clinical stage, and residual tumor size. All tumors were uniformly histopathologically reviewed and re-classified according to new WHO criteria [7,20]. Additionally, a complete evaluation of genetic variants in the TP53 gene (for all tumors) and the TP53 protein status (for cancers only) was performed, as previously described, by either next-generation sequencing (NGS) [21] or with the mouse monoclonal antibody [15]. All the BOTS patients did not undergo any chemical treatment, whereas all OvCa were excised from previously untreated patients. Twenty-two ovarian cancer patients were treated postoperatively with platinum/cyclophosphamide (PC), while eighty-one underwent the taxane/platinum (TP) treatment after a surgical intervention. As to the evaluation of clinical endpoints, all surviving patients had at least a 3-year follow-up. In BOTS, RFS and the presence of microinvasions or non-invasive implants within the tumor masses were used as dependent variables determining the disease prognosis. As the covariates, taken into account in the multivariable statistical inference in BOTS, clinical stage according to FIGO (categorical variable), and patient age (continuous variable) were used. In addition, BOTS were analyzed in the entire cohort of patients, and subgroups comprising specimens with (BOT.V600E) or without (BOT) the *BRAF* V600E mutation, since the presence of this genetic alteration was previously found to be significantly correlated with the lower age of patients diagnosed with BOTS [19]. In cancers, OS and DFS were used as dependent prognostic variables, while PS and CR served as dependent factor variables predictive of response to treatment. CR was defined as the disappearance of all clinical and biochemical symptoms of ovarian cancer assessed after completion of the first-line chemotherapy and confirmed four weeks later. DFS was assessed only for the patients who achieved a CR. As to the independent variables used in multivariable statistical analyses in cancers, a FIGO stage of the tumors along with a residual tumor size were taken into account as factor covariates. Noteworthily, due to the small size of the lgOvCa subgroup, only hgOvCa samples were subjected to regression analyses performed in the present study. In such analyses, hgOvCa were investigated either as the entire group of specimens or in subgroups depending on the chemotherapy regimen used (PC or TP) and/or the TP53 accumulation status. The clinicopathological data were missing for one BOT.V600E specimen. Therefore, the relevant cohort described in Table S1 is smaller.

2.2. DNA Isolation and Quality Assessment

Our preliminary analyses revealed that the sample source (snap-frozen or FFPE) significantly affected hierarchical clustering of the data when overall differences in methylation patterns between the specimens were displayed on a heatmap (Figure S1). To eliminate this impact and reduce a potential bias in the methylation analysis results, each group of samples contained DNA isolated from both snap-frozen and FFPE sections (BOT: 4 snap-frozen, 10 FFPE, BOT.V600E: 4 snap-frozen, 7 FFPE, lgOvCa: 5 snap-frozen, 2 FFPE, and hgOvCa: 92 snap-frozen, 4 FFPE). Genomic DNA (gDNA) from snap-frozen sections was isolated using the QIAmp DNA Mini Kit (Qiagen; Hilden, Germany), whereas gDNA from FFPE blocks was extracted in the MagCore Nucleic Acid Extractor, using the MagCore Genomic DNA FFPE One-Step Kit (RBC Biosciences, Xinbei City, Taiwan). Before its hybridization to microarrays, gDNA quality was assessed using our in-house developed method based on the comparison of Real-Time quantitative PCR efficiency for two amplicons of different lengths, described in a paper by Woroniecka et al. [22].

2.3. DNA Bisulfite Conversion

High-quality gDNA isolated from tumors was subjected to a bisulfite conversion (EZ DNA Methylation Kit, Zymo Research; Irvine, CA, USA). Before and after the conversion, gDNA concentrations were measured on the Qubit 4 Fluorometer (Thermo Fisher Scientific; Waltham, MA, USA) using either the Qubit dsDNA HS Assay Kit or Qubit ssDNA Assay Kit, respectively (both kits were manufactured by Thermo Fisher Scientific). The bisulfite

conversion was carried out for 500–1000 ng of gDNA from snap-frozen tissue sections and 200–1000 ng of gDNA from FFPE blocks.

2.4. Microarray Profiling

Bisulfite-converted gDNA samples were subjected to microarray-based DNA methylation profiling with Infinium MethylationEPIC v1.0 BeadChip microarrays (Illumina; San Diego, CA, USA). For identifiers and genomic locations of over 850,000 methylation sites detectable with these microarrays, refer to Supplementary File: Illumina_Infinium_methyl_EPIC_array_ hg19_ext_attributes.xlsx. Hybridization was carried out according to the protocol provided by Illumina. The fluorescence signal was scanned with the iScan array scanner (Illumina).

2.5. Methylation-Specific PCR and Sanger Sequencing

Methylation changes at selected genomic sites were confirmed for three CpGs in three genes by methylation-specific PCR (employing the AmpliTaq Gold™ DNA Polymerase, Thermo Fisher Scientific) followed by Sanger sequencing, using the in-house designed primers: *DHDDS/HMGN2* (cg26108329, chr1:g.26797585 and cg05304531, chr1:g.26797576, Forward: TAATATGATTGGGGTATAGTAGAGGTGATT, Reverse: CACTAAATTAATCCCATC-TAATTTCTTAAA) and *SKI* (cg13488570, chr1:g.2222253, Forward: TTGTTGAGATATTT-TATTGGTTTGAGGGT, Reverse: AACTAATTCACCAAAAATCAAACTCAATTA). Each of the genomic positions mentioned above refers to the GRCh37 assembly of the human genome. PCR products were then analyzed by agarose gel electrophoresis using the Simply Safe reagent (EurX, Gdansk, Poland) for DNA visualization. Gels were documented on the UVP ChemStudio Imaging System (Analytik Jena, Jena, Germany). Afterward, the PCR products were cleaned with ExoSAP-IT (Thermo Fisher Scientific) and subjected to Sanger sequencing using the appropriate primer and the BigDye Terminator v. 3.1 Cycle Sequencing Kit (Thermo Fisher Scientific). Sanger sequencing products were then cleaned with the ExTerminator Kit (A&A Biotechnology, Gdansk, Poland) and analyzed on the 3500 Genetic Analyzer (Thermo Fisher Scientific). The conditions of methylation-specific PCR and Sanger sequencing reactions for each gene are presented in Table S3.

2.6. Bioinformatic and Statistical Analyses

All computations shown herein were run in the R environment (v. 4.3.2), using the GRCh37 (hg19) version of the human genome assembly as a reference. To ensure the highest standards of the methylation analysis, samples with poor hybridization quality were filtered out at the earliest step of the bioinformatic workflow. The hybridization quality was assessed by calculating the signal detection probability with the detectionP function (minfi package, v. 1.46.0). At least 85% of hybridization signals for each sample had to have p-values < 0.05 for the sample to remain in the analyses. All our samples passed that filter (Figure S2) and were submitted to the Gene Expression Omnibus (GEO) database (data acc. no. GSE267068). Apart from the samples, hybridization probes also underwent a three-step filtering, involving the detection probability cut-off (p-value < 0.05), filters of SNPs at CpG sites, and of cross-reactive probes. Due to the relatively poor quality of DNA isolated from FFPE blocks, we had to eliminate about 24% of the probes at the first filtering step to guarantee reliability of the final results. Therefore, the ultimate number of probes that passed all the filtering steps was 599,503 (69.24%). Subsequent bioinformatic analyses were performed in line with the workflow published by Maksimovic et al. [23] that was further improved by our team, as described in our previous work [19].

All differentially methylated regions (DMRs) identified in our bioinformatic analyses were subsequently subjected to detailed statistical inference with the use of univariable and multivariable Cox proportional hazards models (package: survival, v. 3.5-7) to assess the value of these DMRs as potential novel prognostic biomarkers. All Cox models were also checked with respect to proportionality of hazards for each variable used. The prediction of treatment response was carried out by generating univariable and multivariable logistic regression models (packages: stats. v. 4.0.2, and rms, v. 6.0-1). The dependent, independent,

and grouping variables used (different for BOTS and hgOvCa) were described above in the section entitled "Patients and clinicopathological parameters". In order to verify the discriminative capabilities of the created Cox and logistic regression models, we performed their cross-validation in new data sets, obtained from the original data by bootstrapping (with replacement), using the riskRegression package for R (v. 2023.12.21) [24]. Subsequently, areas under ROC curves (AUCs) between the original and bootstrapped data sets were compared.

To perform detailed gene ontology analyses, each CpG was assigned to the gene only when the CpG site was located on the same DNA strand as the coding sequence of the gene of interest. Furthermore, methylation alterations were analyzed either collectively or with regard to the direction of each change (i.e., hypermethylated genes were assessed independently of hypomethylated ones). The obtained lists of genes were then subjected to ontology analyses with the ShinyGO web app (v. 0.80), with the FDR cutoff set to 0.1 and the maximum pathway size of 2000.

3. Results

3.1. The Analysis of the MDM2/TP53/CDKN1A (p21) Axis

The *MDM2/TP53/CDKN1A* axis is a main pathway involved in the determination of genomic stability and the regulation of cell cycle progression [25]. Considering that methylation changes may precede mutations [2], and that the methylome of BOTS and lgOvCa has been poorly investigated so far, we intended to check whether methylation patterns in *TP53* and other genes in the aforementioned axis are different in BOTS and lgOvCa compared to hgOvCa. We focused mainly on methylation changes in promoters and first exons, as such alterations were proven to make the strongest impact on gene expression [26,27]. In Table S4, the complete list of CpGs in the *TP53*, *MDM2*, and *CDKN1A* gene regions analyzed herein is presented, whereas all significant methylation differences (average beta values) between the analyzed tumors groups for various regions of these genes are shown in Figures 1 and S3.

Overall, in the *TP53* tumor suppressor gene, we observed a tendency towards hypermethylation in carcinomas in comparison with BOTS (Figure 1A–C). Despite the fact that we found no *TP53* missense mutations and TP53 protein accumulation in our low-grade tumors [21], we observed hypermethylation in almost every region of this gene. The methylation of all *TP53* exons and also the first *TP53* exon only was even higher in lgOvCa than in hgOvCa (Figure 1C and Figure S3A). For *MDM2*, encoding an oncogenic protein, we observed an opposite effect. In the proximal promoter region of this gene, we found significantly lower methylation in hgOvCa compared to BOTS (Figure 1D). As to *CDKN1A*, which codes for the p21 tumor suppressor protein, we unexpectedly revealed lower methylation levels within the proximal promoter and 1st exon alike in carcinomas compared to BOTS (Figure 1E,F), especially when BOTS without the *BRAF* V600E variant were considered. Interestingly, the first exon of the *CDKN1A* gene was less methylated in lgOvCa than in hgOvCa.

Of note, no methylation differences in either of the above-mentioned three genes between BOT and BOT.V600E tumors were identified in the present study.
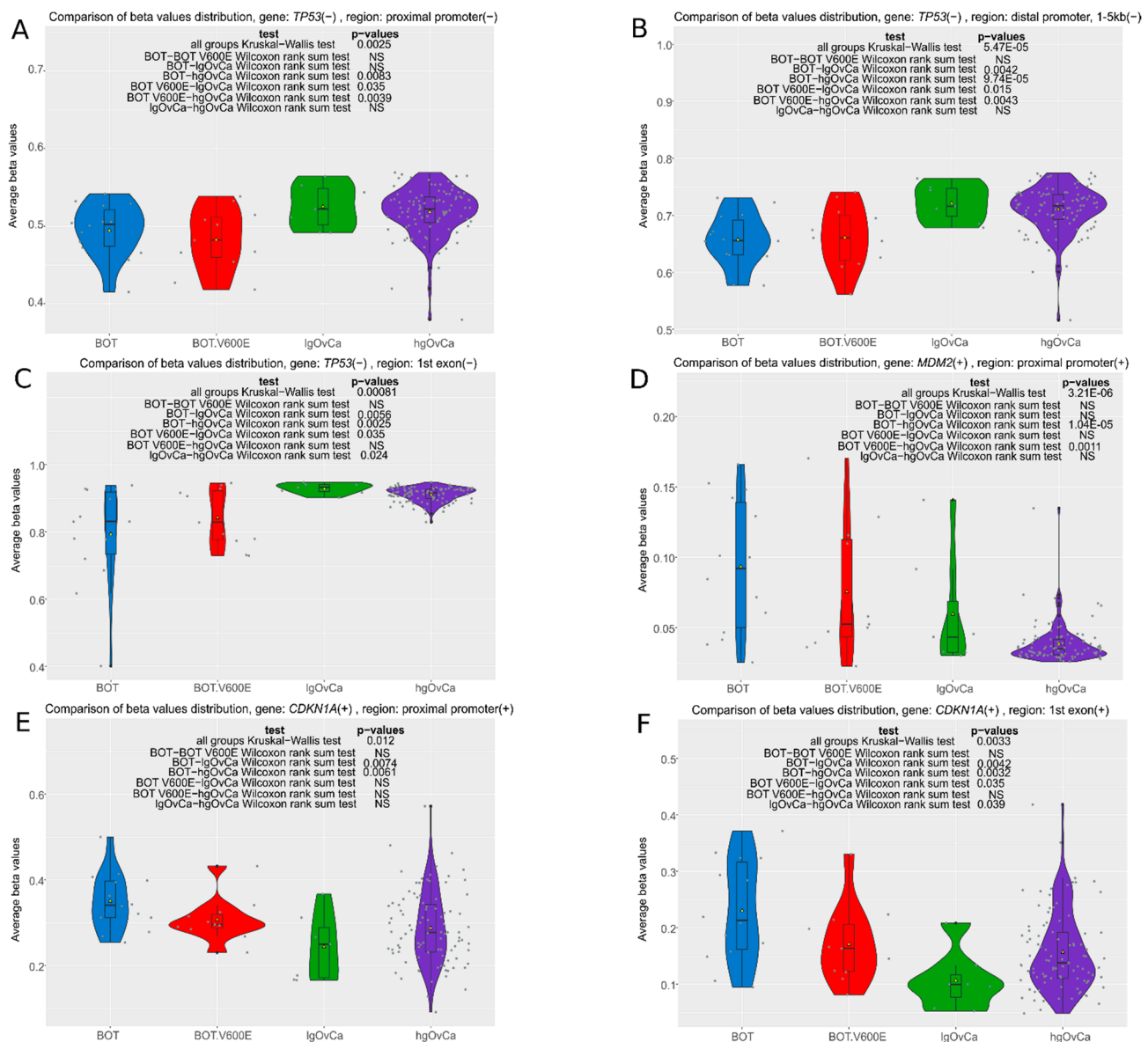
Figure 1. Violin plots of methylation changes (average beta values) in the promoter and first-exon regions of the *TP53*, *MDM2*, and *CDKN1A* genes (the remaining significant results are presented in Supplementary Figure S3). The values range from 0 to 1 (where 0 means no methylation and 1 denotes 100% methylation of CpGs detected in the region). Each analysis is supplemented with the results of two non-parametric statistical tests: the Kruskal–Wallis test (to determine overall methylation differences between the groups) and the Wilcoxon rank sum test to identify differences between particular groups; NS—non-significant result. Low p-values are displayed in exponential notation (e–n), in which e (exponent) multiplies the preceding number by 10 to the minus nth power.

3.2. Differences in Methylation Patterns Between Groups

The numbers of differentially methylated CpGs and differentially methylated regions (DMRs) in all inter-tumor-group comparisons are shown in Table 1. In general, global genome-wide hypomethylation positively correlated with the increasing aggressiveness of tumors and was especially evident in the hgOvCa group (the highest ratios of down-methylated/upmethylated CpGs and DMRs in hgOvCa vs. all the other tumor groups). Remarkably, the same ratio for the inter-BOTS comparison was also very high, particularly when DMRs were considered. Moreover, BOT.V600E tumors emerged as the group with the lowest number of differentially methylated CpGs and DMRs compared to all the remaining

groups. This suggests that extensive hypomethylation of the genome is what distinguishes BOT.V600E from BOT and, when methylome is considered, BOT.V600E tumors might be placed somewhere in-between BOT and OvCa.

Table 1. Numbers of differentially methylated CpGs and DMRs between the groups of tumors.

	CpGs					
DM CpGs	BOT vs. BOT V600E	BOT vs. lgOvCa	BOT vs. hgOvCa	BOT V600E vs. lgOvCa	BOT V600E vs. hgOvCa	lgOvCa vs. hgOvCa
Upmethylated	16,108	86,834	93,667	5438	12,170	136,293
Downmethylated	4035	88,467	30,227	11,665	7369	32,832
Sum of DM CpGs	20,143	175,301	123,894	17,103	19,539	169,125
NS	579,360	424,202	475,609	582,400	579,964	430,378
Up/Down ratio	3.99	0.98	3.1	0.47	1.65	4.15
	DMRs					
DMRs	BOT vs. BOT V600E	BOT vs. lgOvCa	BOT vs. hgOvCa	BOT V600E vs. lgOvCa	BOT V600E vs. hgOvCa	lgOvCa vs. hgOvCa
Upmethylated	1837	12,438	11,442	1062	2127	21,555
Downmethylated	25	7646	1979	869	1385	5759
Sum of DMRs	1862	20,084	13,421	1931	3512	27,314
Up/Down ratio	73.48	1.63	5.78	1.22	1.54	3.74

The up/down prefixes refer to the first element in each comparison. DM—differentially methylated; DMR—differentially methylated region; NS—non-significant.

3.3. CpG Sites with the Most Differentiated Methylation

Based on *p*-values obtained in the differential methylation analysis of individual CpGs, we identified the most differentiated CpG sites for all six inter-tumor-group comparisons. The upset plot demonstrating the numbers of differentially methylated (DM) CpGs in each inter-tumor-group comparison and the numbers of such CpGs for the specific intersection of tumor groups is shown in Figure 2A. In Figure 2B–G, the distribution of M-values for the most DM CpG site in each inter-tumor-group comparison is displayed. Additionally, Figure 2 is supplemented with Table 2, which shows the 10 most significantly differentiating CpGs (and the genes they are located in) for each inter-tumor-group comparison.

DM CpGs distinguishing BOT from BOT.V600E the most occurred in genes involved in cell adhesion (*MIP*, *ODAD3*, *PTPRF* and *ITGA7*), lipid metabolism (*LRP1*, *CBY1*), cell differentiation (*PTPRF*, *CBY1*), apoptosis (*SPRYD4*, *LRP1*), and ER (endoplasmic reticulum)-related processes (*PRKCSH*, *CYB5R4*). One CpG site, cg19623237, was located in an intergenic region.

The CpG differentiating BOT from lgOvCa the most was located in a pseudogene, *NBPF13P*, involved in nervous system development. Some other CpGs/genes differentiating these tumor groups were also engaged in neuronal processes (*ZIC2*, *GNB1L*). However, the biggest group of CpGs with divergent methylation patterns between BOT and lgOvCa lay in genes associated with transcriptional regulation, such as *ZNF585*, *ZNF341*, *ZIC2*, *RECQ25*, *SAP30BP*, and *ETV4*. CpGs in genes participating in mitochondrial processes (*RTL10*, *COX16*, *SYNJ2BP-CO16*) and cell differentiation (*ZIC2*, *ETV4*) were also identified as differentially methylated between BOT and lgOvCa. There was also one CpG, cg10479053, present on the opposite (minus) strand to the coding sequence of the *PSMD3* gene.

In the BOT vs. hgOvCa comparison, the most differentiating CpG, cg18813601, lay in an intergenic region on chromosome 10. Other DM CpGs occurred in genes involved in neuronal processes (*NBPF13P*, *ZIC2*, *SLC4A10*, *DLX6*, and *CSNK1G2*) and cell differentiation/development (*CTBP1*, *DLX6*, *CSNK1G2*). Additionally, some CpGs were found in genes regulating transcription (*ZIC2*, *CTBP1*, *HNRNPA1L2*), Golgi apparatus functioning (*GORASP2*, *CTBP1*), as well as in pseudogenes (*NBPF13P*, *MRPS31P4*).

Interestingly, in the BOT.V600E vs. lgOvCa comparison, we observed some different processes than when BOT were compared to lgOvCa. CpGs with the most divergent patterns were located in genes involved in cell differentiation and development (*FOXA1*, *PLEKHO1*, *TFDP1*, *ZIC2*). In addition, DM CpGs were found in genes related to cell

proliferation (*CAMK2N1*, *PVT1*), apoptosis (*FOXA1*, *PLEKHO1*, *PVT1*), adhesion (*PIP5K1C*, *PLEKHO1*, *TTC6*), cell cycle (*FOXA1*, *TFDP1*), lipid metabolism (*CAMK2N1*, *TFDP1*), neuronal processes (*ZIC2*, *CAMK2N1*), and transcription regulation (*FOXA1*, *TFDP1*, *ZIC2*). One CpG site was present in the gene of unknown function (*TMEM104*).
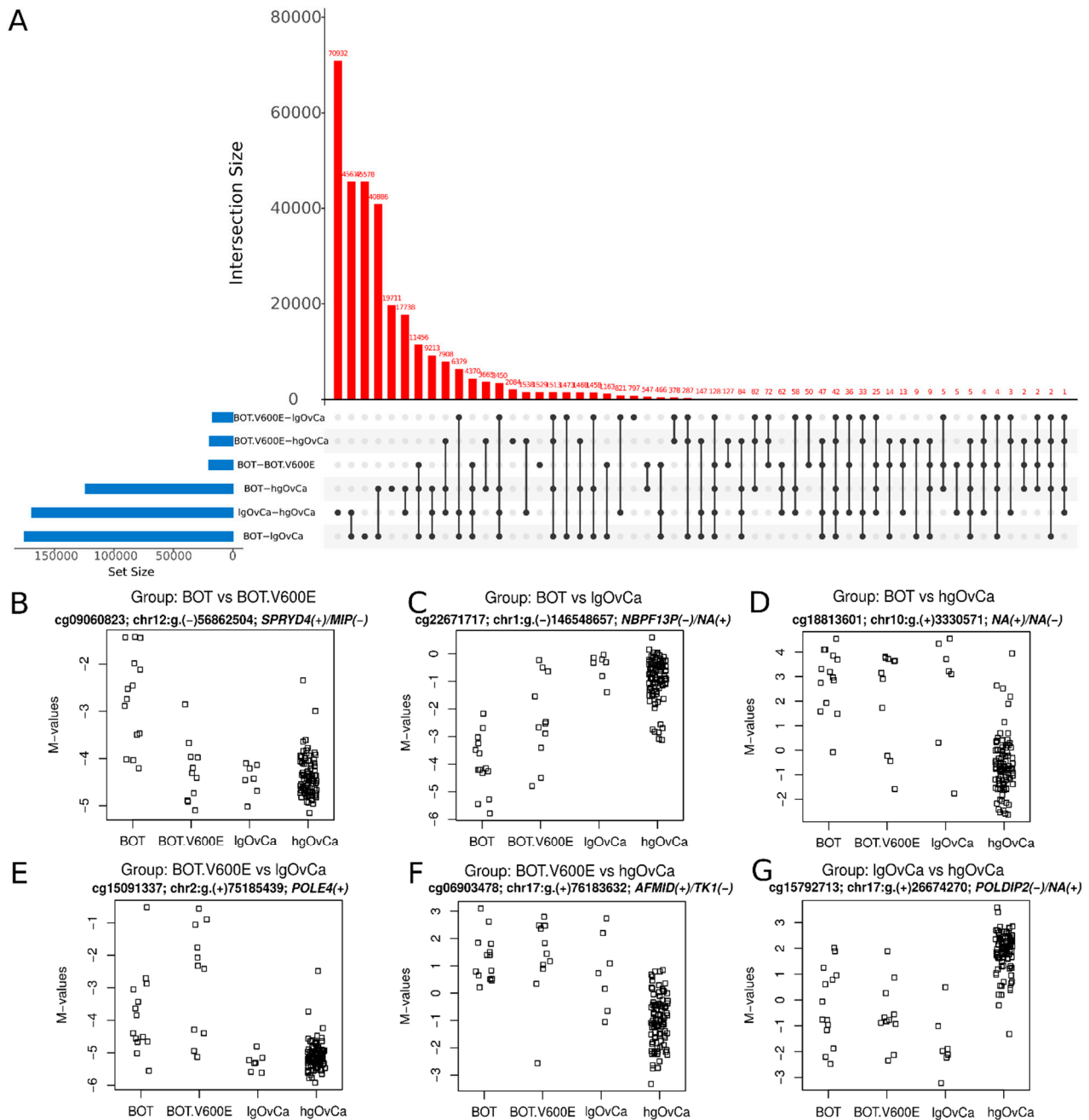

Figure 2. Differentially methylated CpGs. (**A**): the upset plot demonstrating the number of differentially methylated CpGs in each inter-tumor-group comparison (blue bars) and the number of such CpGs (red bars) for the specific intersection of tumor groups (all sets included in the given intersection are indicated with black dots, that are connected with a line if the intersection contains more than one set). (**B–G**): the distribution of M-values for the most differentiating CpGs for each inter-tumor-group comparison, followed by genomic locations and gene names with strand identificators shown in brackets. M-value is the log2 of the ratio between signal intensities for probes specific to methylated (numerator) and unmethylated (denominator) cytosines in the given CpG site. The higher the M-value, the higher the methylation level.

Table 2. CpG sites with the most differentiated methylation in all inter-tumor-group comparisons.

BOT vs. BOT.V600E	BOT vs. lgOvCa	BOT vs. hgOvCa
cg09060823; chr12:g.(−)56862504 *SPRYD4(+)/MIP(−)*	cg22671717; chr1:g.(−)146548657 *NBPF13P(−)/NA(+)*	cg18813601; chr10:g.(+)3330571 *NA(+)/NA(−)*
cg00598858; chr19:g.(−)11545966 *PRKCSH(+)/ODAD3 (CCDC151)(−)*	cg06869971; chr15:g.(−)69706519 *KIF23(+)/RP11-253M7.1 (KIF23-AS1)(−)*	cg25977528; chr13:g.(+)100633444 *ZIC2(+)*
cg24443198; chr6:g.(−)84569302 *CYB5R4(+)/NA(−)*	cg22011361; chr14:g.(−)70821355 *COX16(−)/SYNJ2BP-COX16(−)*	cg00614081; chr4:g.(−)1233439 *CTBP1(−)*
cg10664618; chr12:g.(+)57579466 *LRP1(+)*	cg25977528; chr13:g.(+)100633444 *ZIC2(+)*	cg06903478; chr17:g.(+)76183632 *AFMID(+)/TK1(−)*
cg15086746; chr1:g.(−)44084965 *PTPRF(+)/NA(−)*	cg03751813; chr19:g.(−)37701393 *ZNF585B(−)*	cg02608914; chr2:g.(−)171784720 *GORASP2(+)/NA(−)*
cg00500457; chr22:g.(−)39055589 *CBY1(+)/FAM227A(−)*	cg23639257; chr17:g.(−)73663270 *RECQL5(−)/SAP30BP(+)*	cg22671717; chr1:g.(−)146548657 *NBPF13P(−)/NA(+)*
cg08427970; chr10:g.(−)99122398 *RRP12(−)*	cg10479053; chr17:g.(−)38136919 *PSMD3(+)/NA(−)*	cg11704490; chr2:g.(−)162284894 *NA(−)/SLC4A10(+)/AC009487.5(+)*
cg02608656; chr12:g.(+)56090830 *ITGA7(−)/NA(+)*	cg17908846; chr20:g.(+)32320553 *ZNF341(+)*	cg10659805; chr7:g.(+)96631680 *DLX6(+)/DLX6-AS1(−)*
cg02901790; chr8:g.(+)144391601 *TOP1MT(−)/NA(+)*	cg22437020; chr17:g.(−)41623744 *ETV4(−)/RP11-392O1.4(+)*	cg02215357; chr13:g.(−)53191046 *NA(−)/HNRNPA1L2(+)/MRPS31P4(+)*
cg19623237; chr17:g.(+)77818582 *NA(+)/NA(−)*	cg00528793; chr22:g.(−)19842837 *GNB1L(−)/RTL10 (C22Orf29)(−)*	cg25899337; chr19:g.(−)1970441 *CSNK1G2(+)/NA(−)*
BOT.V600E vs. lgOvCa	**BOT.V600E vs. hgOvCa**	**lgOvCa vs. hgOvCa**
cg15091337; chr2:g.(+)75185439 *POLE4(+)*	cg06903478; chr17:g.(+)76183632 *AFMID(+)/TK1(−)*	cg15792713; chr17:g.(+)26674270 *POLDIP2(−)/NA(+)*
cg13518540; chr17:g.(+)72781248 *TMEM104(+)*	cg27641801; chr4:g.(−)4429265 *STX18(−)*	cg11610925; chr10:g.(−)134978049 *KNDC1(+)/NA(−)*
cg00376288; chr19:g.(+)3656580 *PIP5K1C(−)/NA(+)*	cg08271229; chr1:g.(+)2222674 *SKI(+)*	cg00454305; chr16:g.(−)1429905 *UNKL(−)*
cg10168722; chr14:g.(−)38068608 *FOXA1(−)/TTC6(+)*	cg18813601; chr10:g.(+)3330571 *NA(+)/NA(−)*	cg18468569; chr8:g.(+)125984720 *ZNF572(+)*
cg11199810; chr1:g.(−)150123146 *PLEKHO1(+)/NA(−)*	cg17026391; chr11:g.(+)61159442 *TMEM216(+)*	cg14636714; chr10:g.(−)135018298 *KNDC1(+)/NA(−)*
cg18656829; chr13:g.(−)100632250 *NA(−)/ZIC2(+)*	cg00614081; chr4:g.(−)1233439 *CTBP1(−)*	cg07570470; chr8:g.(+)142318841 *NA(+)/SLC45A4(−)*
cg02941008; chr1:g.(+)20810527 *CAMK2N1(−)/NA(+)*	cg00817355; chr2:g.(−)85073409 *TRABD2A(−)*	cg19823504; chr19:g.(+)4556982 *SEMA6B(−)/NA(+)*
cg27641801; chr4:g.(−)4429265 *STX18(−)*	cg15792713; chr17:g.(+)26674270 *POLDIP2(−)/NA(+)*	cg21633143; chr7:g.(−)154862021 *HTR5A(+)/HTR5A-AS1(−)*
cg07819108; chr8:g.(+)128921817 *PVT1(+)*	cg05222982; chr13:g.(+)28545214 *NA(+)/CDX2(−)*	cg05640731; chr10:g.(−)135018226 *KNDC1(+)/NA(−)*
cg17707487; chr13(+)114261869 *TFDP1(+)*	cg19875936; chr12:g.(−)7858848 *NA(−)/NA(+)*	cg19307500; chr19:g.(−)1083193 *HMHA1 (ARHGAP45)(+)/NA(−)*

Names of genes in which the given CpG sites are located including the coding DNA strand (+/−) are emboldened. Overlapping genes are separated with a slash (/). CpG sites' identifiers and their chromosomal locations, including the strand they lie on, are shown above the gene name and are not emboldened.

In the BOT.V600E vs. hgOvCa comparison, except for cg06903478 in *AFMID/TK1* and cg00614081 in *CTBP1*, we observed distinct DM CpGs/genes from those differentiating BOT from hgOvCa. Nonetheless, biological processes affected by these epigenetic changes were similar in both comparisons, since cell development/differentiation (genes: *SKI*, *CTBP1*, *TRABD2A*, *CDX2*), transcription (genes: *CDX2*, *CTBP1*), neuronal processes (genes:

TRABD2A, *SKI*), and Golgi-dependent processes (genes: *CTBP1*, *STX18*) were identified as terms enriched in genes with CpGs most significantly differentiating BOT.V600E from hgOvCa. Two other DM CpGs, cg18813601 and cg19875936, were located in intergenic regions.

The biggest group of DM CpGs between lgOvCa and hgOvCa lay in genes associated with neuronal processes (*KNDC1*, *SEMA6B*, *HTR5A*). Many such CpGs were present on the opposite strand as the coding sequence of known genes (cg15792713, cg11610925, cg14636714, cg07570470, cg19823504, cg05640731, and cg19307500). For detailed information on these and other CpGs described in the present paper, refer to Supplementary File Illumina_Infinium_methyl_EPIC_array_hg19_ext_attributes.xlsx.

In order to verify our microarray results and validate the entire bioinformatic workflow, three CpG sites characterized by diverse methylation patterns between the groups of tumors analyzed herein, cg13488570; chr1:g.(+)2222253 in the *SKI*(+) gene and two CpGs in the *DHDDS*(+) gene, cg26108329; chr1:g.(+)26797585 and cg05304531, chr1:g.(+)26797576, were further investigated by methylation-specific PCR and Sanger sequencing. Positive results of this validation are presented in Figure S4.

3.4. Ontological Analyses

By using the ShinyGO web app, we performed a detailed ontology analysis for DM CpGs, taking into account not only the DNA strand (+/−) on which each CpG site is located, but also the direction of a methylation change (up- vs. downmethylated CpGs/genes). The results of our gene ontology (GO)-enrichment analysis (categories: biological process (BP), molecular function (MF), cellular compartment (CC)), as well as Molecular Signature Database analysis (MSigDB, Hallmark gene sets) for all inter-tumor-group comparisons, are presented in Figures S5–S8.

In the BP analyses, we observed downmethylation of genes involved in the regulation of cytoskeleton/cell adhesion in BOTS compared to carcinomas (Figures S5–S7). Such processes were also more frequently downmethylated in BOT than in BOT.V600E. By contrast, genes involved in the cell cycle progression and RNA metabolism were upmethylated in BOT compared to BOT.V600E and lgOvCa (Figure S5A,C). Of note, when comparing BOT to hgOvCa, only genes associated with the cell cycle progression were upmethylated in the former group (Figure S5E), while the genes involved in RNA metabolism were deregulated in both directions (Figure S5E,F). Altered DNA methylation was also observed in genes encoding proteins regulating the cell cycle when BOT.V600E were compared to lgOvCa, with hypermethylation in the BOT.V600E group (Figure S5G). Interestingly, genes linked to RNA processing/metabolism were deregulated in both directions in the BOT.V600E vs. lgOvCa comparison (Figure S5G,H) but only downmethylated in BOT.V600E compared to hgOvCa (Figure S5J). In the lgOvCa vs. hgOvCa comparison, only a few cell adhesion-related terms were enriched, and the genes involved in those processes were deregulated in both directions (Figure S5K,L). As for the genes participating in RNA metabolism/processing and the cell cycle regulation, we observed downmethylation in lgOvCa compared to hgOvCa (Figure S5K,L).

As to the genes involved in cell differentiation, development, and morphogenesis, no differences in methylation patterns were found between BOT and BOT.V600E (Figure S5A,B). Simultaneously, genes involved in the aforementioned terms were mainly downmethylated in BOTS compared to carcinomas (Figure S5D,F,H,J). Still, in the BOT.V600E vs. hgOvCa comparison, up- and downmethylation were detected at the same time (Figure S5I,J). By contrast, when lgOvCa and hgOVCa were compared to each other, genes associated with differentiation, development, and morphogenesis turned out to be upmethylated in less aggressive tumors (Figure S5K). Consistently, the genes responsible for neuronal processes were also upmethylated in lgOvCa compared to aggressive carcinomas (Figure S5K). However, when this group of genes was investigated in BOTS, their methylation changes did not differentiate BOT from BOT.V600E (Figure S5A,B). The neuronal processes-related GO terms were, however, deregulated in both ways when BOTS were confronted with hgOvCa

(Figure S5E,F,I,J). Finally, when compared to lgOvCa, genes related to neuronal processes were downmethylated in BOT and upmethylated in BOT.V600E (Figure S5D,G, respectively).

Methylation alterations in genes associated with intracellular transport were identified when the BOT group was compared to carcinomas with hypomethylation found in more aggressive tumors (Figure S5C,E). Similar regularity was observed in the lgOvCa vs. hgOvCa comparison, where the transport-related terms were enriched in upmethylated genes in lgOvCa (Figure S5K). Interestingly, no such GO terms were enriched when BOT.V600E were compared to carcinomas (Figure S5G–J). Notably, our results of the GO analysis for the MF and CC categories were consistent with those for BP, presented above (Figures S6 and S7).

In the MSigDB analysis, we observed the upmethylation of genes linked to the TP53 pathway, mTORC1 complex, oxidative phosphorylation, and unfolded protein response when BOT (but not BOT.V600E) were compared to other tumor groups (Figure S8A,C,E). By contrast, the same terms were also enriched in genes downmethylated in lgOvCa compared to hgOvCa (Figure S8L). Genes involved in fatty acid metabolism and adipogenesis were hypermethylated in BOT compared to the other groups. Another process worth mentioning, glycolysis, differentiated BOT from BOT.V600E, and the related genes were hypermethylated in the former group (Figure S8A). Genes involved in glycolysis were also upmethylated in BOT compared to lgOvCa (Figure S8C) and deregulated in both directions when BOT were compared to hgOvCa (Figure S8E,F). As for the molecular signatures distinguishing BOT.V600E from lgOvCa, we observed upmethylation of genes involved in the heme metabolism in the former group (Figure S8G). Remarkably, the same term was significantly enriched in the BOT vs. BOT.V600E comparison as well, though the changes in methylation patterns were bidirectional (Figure S8A,B). Another interesting observation refers to angiogenesis, as genes associated with this process were downmethylated in both BOTS groups but only compared to hgOvCa (Figure S8F,J). Lastly, the hypermethylation of genes upregulated by KRAS as well as genes related to epithelial-mesenchymal transition distinguished lgOvCa from hgOvCa only (Figure S8K) and did not differentiate BOT from BOT.V600E or BOTS from OvCa (Figure S8A–J).

3.5. The Most Statistically Significant DMRs

Based on *p*-values, we identified the 10 most significant DMRs for each inter-tumor-group comparison (Table 3). In Figure 3, the best DMR for every comparison is shown, being additionally supplemented with the visualization of DNase I hypersensitive sites (DHSS) as well as transcription factor binding sites (TFBS) to evaluate whether the given DMR is transcriptionally active.

DMRs distinguishing BOT from BOT.V600E the most occurred mainly in genes involved in lipid/steroid/ester metabolism (*NR1H3*, *ACP2*, *ACSS2*, *AKR1D1*) and the cell cycle (*KIF23*, *WEE1*).

Interestingly, all the most significant DMRs discriminating BOT from lgOvCa overlapped the MHC region on chromosome 6 (about 3.5 million bp in length). These DMRs were located in genes linked to the immune response (*HLA-DMA*, *GPANK1*, *LY6G5B*, *TAPBP*, *GNL1*) but also to transcription regulation (*BRD2*, *GTF2H4*, *EHMT2*, *ZBTB22*, *DAXX*, *PHF1*), development and differentiation (*BRD2*, *CSNK2B*, *PPP1R18*, *PHF1*), DNA repair (*MDC1*, *GTF2H4*, *PHF1*), apoptosis (*CSNK2B*, *DAXX*, *NRM*), and neuronal functions (*SLC44A4*, *SYNGAP1*, *CUTA*). Some genes were also associated with cytoskeleton (*TUBB*, *PPP1R18*).

In the BOT vs. hgOvCa comparison, the most significant DMRs occurred mainly in genes participating in transcriptional regulation (*EMX2OS*, *CTBP1*, *PRAME*, *MEIS2*, *ATF6B*, *PITX1*), differentiation and development (*EMX2OS*, *CTBP1*, *MEIS2 PITX1*), and protein folding (*ATF6B*, *FKBPL*, *GORASP2*). A few genes were also involved in the regulation of cytoskeleton (*EHBP1*, *TUBB*) and Golgi apparatus (*CTBP1*, *GORSAP2*), cell cycle (*MDC1*, *FKBPL*), and lipid metabolism (*CPT1B*, *CHKB*).

Table 3. The most significant differentially methylated regions (DMRs) in all inter-tumor-group comparisons.

BOT vs. BOT.V600E	BOT vs. lgOvCa	BOT vs. hgOvCa
chr11:g.both 47269539–47270908; *NR1H3(+)/ACP2(−)*	chr6:g.both 32935236–32943025; *BRD2(+)/BRD2-IT1(+)/XXbac-BPG181M17.6(−)/HLA-DMA(−)*	chr2:g.both 63275602–63285097; *EHBP1-AS1(AC009501.4)(−)/OTX1(+)*
chr6:g.both 31762409–31763873; *VARS1(−)/NA(+)*	chr6:g.both 30684340–30690844; *TUBB(+)/MDC1(−)*	chr6:g.both 30683787–30690844; *TUBB(+)/MDC1(−)*
chr15:g.(−)69706375–69707291; *KIF23(+)/RP11-253M7.1(KIF23-AS1)(−)*	chr6:g.both 31626915–31634890; *C6orf47(−)/C6orf47-AS1(+)/CSNK2B(+)/GPANK1(−)/LY6G5B(+)*	chr10:g.both 119291766–119296942; *EMX2OS(−)/NA(+)*
chr6:g.(−)31762409–31763873; *VARS1(−)/NA(+)*	chr6:g.both 30874989–30886161; *GTF2H4(+)/VARS2(+)/NA(−)*	chr4:g.both 1232112–1236678; *CTBP1(−)/NA(+)*
chr20:g.both 33459881–33461321; *ACSS2(+)/GGT7(−)*	chr6:g.(+)32935236–32943025; *BRD2(+)/BRD2-IT1(+)/XXbac-BPG181M17.6(−)/HLA-DMA(−)*	chr22:g.both 22899991–22902665; *IGL locus (+): LL22NC03-63E9.3(+)/PRAME(−)*
chr12:g.both 7282081–7283890; *CLSTN3(+)/RBP5(−)/RP11-273B20.1(−)*	chr6:g.both 31850189–31857100; *SLC44A4(−)/EHMT2(−)/EHMT2-AS1(+)*	chr15:g.both 37391121–37395115; *MEIS2(−)/RP11-128A17.1(+)*
chr7:g.both 137686266–137687260; *AKR1D1(+)/CREB3L2(−)*	chr6:g.both 33279563–33287809; *TAPBP(−)/ZBTB22(−)/DAXX(−)/ NA(+)*	chr6:g.both 32094845–32098253; *ATF6B(−)/FKBPL(−)/NA(+)*
chr6:g.both 32861863–32862953; *LOC100294145(+)/HLA-Z(+)NA(−)*	chr6:g.both 30519312–30525976; *GNL1(−)/PRR3(+)*	chr22:g.both 51016386–51017723; *CPT1B(−)/CHKB-CPT1B(−)/CHKB-DT(+)/CHKB(−)*
chr11:g.both 9595191–9596475; *WEE1(+)/NA(−)*	chr6:g.both 30651511–30659692; *PPP1R18(−)/NRM(−)/NA(+)*	chr2:g.both 171784610–171786316; *GORASP2(+)/NA(−)*
chr11:g.(+)47269539–47270669; *NR1H3(+)/ACP2(−)*	chr6:g.both 33381680–33387205; *PHF1(+)/SYNGAP1(+)/CUTA(−)*	chr5:g.both 134362967–134369605; *PITX1(−)/PITX1-AS1(+)*
BOT.V600E vs. lgOvCa	**BOT.V600E vs. hgOvCa**	**lgOvCa vs. hgOvCa**
chr6:g.both 30651511–30654559; *PPP1R18(−)/NA(+)*	chr1:g.both 2221807–2222674; *SKI(+)/NA(−)*	chr10:g.both 134977981–134981930; *KNDC1(+)/NA(−)*
chr6:g.both 31733434–31734580; *VWA7(−)/SAPCD1-AS1(−)/NA(+)*	chr19:g.both 58220080–58220818; *ZNF551(+)/AC003006.7(+)/ZNF154(−)*	chr6:g.both 32044869–32057846; *TNXB(−)/RNA5SP206(−)/NA(+)*
chr1:g.both 19664276–19665757; *CAPZB(−)/NA(+)*	chr1:g.both 1102276–1106175; *MIR200B(+)/MIR200A(+)/MIR429(+)/TTLL10(+)/RP11-465B22.8(+)/NA(−)*	chr6:g.both 30127760–30132715; *TRIM15(+)/TRIM10(−)*
chr6:g.both 152127812–152129791; *ESR1(+)/ NA(−)*	chr17:g.both 78865087–78866579; *RPTOR(+)/NA(−)*	chr19:g.both 405795–409510; *C2CD4C(−)/NA(+)*
chr7:g.both 964629–967277; *ADAP1(−)/NA(+)*	chr22:g.both 51016386–51017723; *CPT1B(−)/CHKB-CPT1B(−)/CHKB-DT(+)/CHKB(−)*	chr10:g.both 119291766–119297716; *EMX2OS(−)/EMX2(+)*
chr11:g.61521905–61523045; *MYRF(+)/MYRF-AS1(−)/RP11-467L20.10(−)*	chr16:g.2082689–2083393; *NHERF2(SLC9A3R2)(+)/NA(−)*	chr12:g.both 132686912–132689907; *GALNT9(−)/NA(+)*
chr3:g.both 129692836–129694665; *TRH(+)/NA(−)*	chr19:g.(+)58220080–58220818; *ZNF551(+)/AC003006.7(+)/ZNF154(−)*	chr12:g.both 132847907–132856142; *LOC100130238(+)/GALNT9(−)/RP13-895J2.3(+)*
chr12:g.both 6483708–6487080; *LTBR(+)/SCNN1A(−)*	chr3:g.both 185911208–185912486; *DGKG(−)/NA(+)*	chr4:g.both 100571622–100574653; *NA(+)/C4orf54(−)*
chr3:g.both 188664632–188666540; *TPRG1(+)/TPRG1-AS1(−)*	chr16:g.(−)2082745–2083178; *NHERF2(SLC9A3R2)(+)/NA(−)*	chr16:g.both 1127792–1132709; *SSTR5(+)/SSTR5-AS1(−)*
chr3:g.(+)129692836–129694665; *TRH(+)/NA(−)*	chr1:g.(+)1102276–1106175; *MIR200B(+)/MIR200A(+)/MIR429(+)/TTLL10(+)/RP11-465B22.8(+)/NA(−)*	chr16:g.both 1428639–1430367; *UNKL(−)/NA(+)*

Names of genes encompassed by the given DMR, including the DNA strand (+/−) on which the coding sequence of the gene is located, are emboldened. Overlapping genes are separated with a slash (/). A chromosomal localization for each DMR, along with the information whether the DMR was calculated for the plus (+), minus (−) or both DNA strands, is shown above gene name(s).
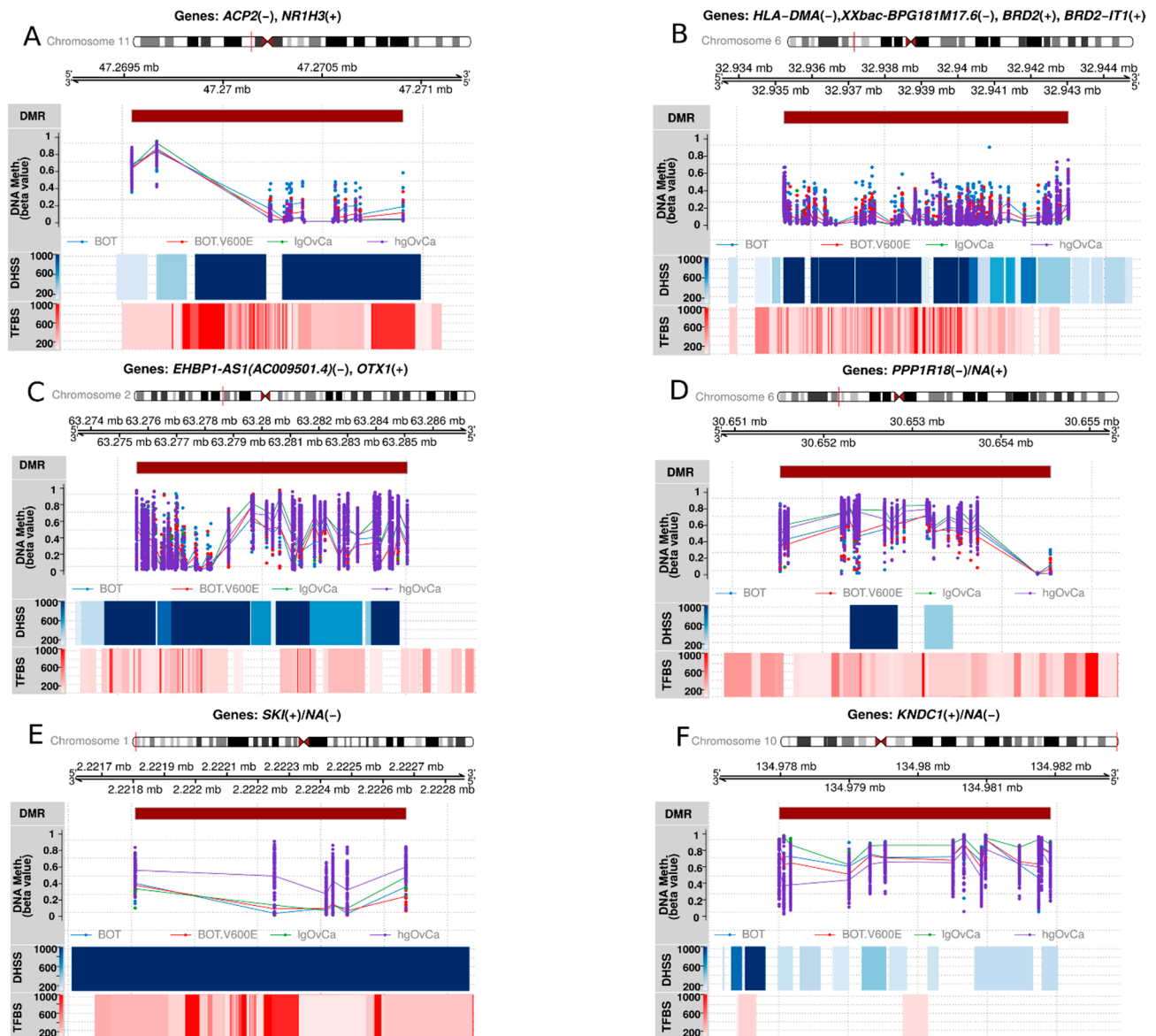
Figure 3. Context plots depicting the most significant DMR for each inter-tumor-group comparison. Each plot title contains encompassed gene name(s) with the DNA strand identifier (+/−), on which the coding sequence of each gene is located. Below, a chromosome ideogram, graphical representation of the genomic range, and DMR location within the genome are shown. These are followed by a line + dot plot demonstrating the distribution of beta values for each CpG and sample (dot) along with mean values for each CpG (line). The visualization of Dnase I hypersensitive sites (DHSS) and transcription factor binding sites (TFBS) is also provided for the assessment of transcriptional activity in each DMR. (**A**): BOT vs. BOT.V600E (chr11:g.both 47269539–47270908); (**B**): BOT vs. lgOvCa (chr6:g.both 32935236–32943025); (**C**): BOT vs. hgOvCa (chr2:g.both 63275602–63285097); (**D**): BOT.V600E vs. lgOvCa (chr6:g.both 30651511–30654559); (**E**): BOT.V600E vs. hgOvCa (chr1:g. 2221807–2222674); (**F**): lgOvCa vs. hgOvCa (chr10:g.both 134977981–134981930).

When comparing BOT.V600E to lgOvCa, we observed some similar processes as for the BOT vs. lgOvCa comparison. Genes linked to immune processes (*ADAP1, LTBR, TPRG1*) were also identified as differentially methylated, but they were not so abundant. The most significant DMRs were associated with neurological processes (*ADAP1, MYRF, SCNN1A*), adhesion (*PPP1R18, CAP2B, SCNN1A*), and lipid metabolism (*ESR1, LTBR*), too.

If BOT.V600E were confronted with hgOvCa, the biggest differences in methylation patterns were found in genes involved in lipid metabolism (*CPT1B, CHKB, DGKG*), cytoskeletal

regulation (*TTLL10*, *NHERF2*), neurological processes (*SKI*, *RPTOR*), differentiation and development (*RPTOR*, *SKI*), and the regulation of transcription (*ZNF551*, *ZNF154*).

Finally, the biggest methylation alterations between lgOvCa and hgOvCa were revealed in genes participating in neuronal processes (*KNDC1*, *EMX2*, *SSTR5*), ubiquitination (*TRIM15*, *TRIM10*, *UNKL*), cytoskeletal regulation/adhesion (*TNXB*, *TRIM15*), differentiation/development (*EMX2*, *TRIM10*), and immune response (*TRIM15*, *TRIM10*).

3.6. Cox and Logistic Regression Analyses for DMRs in BOTS and hgOvCa

Each DMR had to be differentially methylated in at least one of six inter-tumor-group comparisons to be subjected to the regression testing, which gave the total number of 128,168 tested DMRs. Uni- and multivariable regression analyses were carried out for all BOTS and hgOvCa available in our sample set. Remarkably, due to the small number of specimens making the multivariable statistical testing impossible, the lgOvCa group was excluded from the regression analysis herein.

To decrease the risk of false-positive hits, we decided to change the statistical significance level (alpha) of our Cox regression models and logistic regression models (lrm) in hgOvCa to 0.0005 and 0.005, respectively. Considering the relatively small size of the BOTS series, the default alpha value of 0.05 was kept in all regression models performed in this series of tumors. To further decrease the risk of obtaining false-positive hits, we focused on those DMRs only for which the results of univariable and multivariable regression tests matched. The models were considered matching when the analyzed DMRs and groups of tumors were the same, both *p*-values < alpha value, both HR/OR values either higher or lower than 1, and concomitantly the discriminative capabilities of all models, uni- and multivariable, before and after a bootstrap-based cross-validation were good enough (all AUC values > 0.7). This approach let us identify 112 and 168 unique matching DMRs in Cox and lrm analyses in hgOvCa, respectively. For BOTS, we obtained 143 matching DMRs, all in the lrm analysis. The detailed results of our regression analyses are provided in Supplementary Files: Reg.analyses.Cox.hgOvCa.p.val.0.0005.xlsx, Reg.analyses.lrm.hgOvCa.p.val.0.005.xlsx, and Reg.analyses.lrm.BOTS.p.val.0.05.xlsx, collectively abbreviated as Reg.anal.suppl.results. We also performed the GO analysis for all the genes identified in our regression tests as good discriminators in hgOvCa and BOTS. The enriched GO terms along with the genes assigned to each term are provided in Tables S5 and S6, respectively. Next, we nominated five DMRs with the lowest *p*-values from each of the three xlsx files as the most promising potential biomarkers in BOTS and hgOvCa. The regression analyses' results for these DMRs are described below and presented in Table 4, and in Figures 4 and 5. For detailed information on the DMRs listed in this table, including the CpG sites forming each DMR, refer to Supplementary Table S7.

In hgOvCa, we managed to identify DMRs predictive of both cancer prognosis and response to chemotherapy. In the former group, all the DMRs were located on chromosome 22, two of them, chr22:g.(−)35776686–35777032 and chr22:g.(−)35775959–35777032, overlapped the *HMOX1* gene, whereas the remaining three, chr22:g.(−)31002067–31003655, chr22:g.both 31002067–31003655, and chr22:g.both 31002362–31004367, encompassed the *TCN2*, *PES1*, and *RP1-56J10.8* genes. Hypermethylation of *HMOX1*-containing DMRs improved the overall survival of hgOvCa patients treated with taxane/platinum (TP), whose tumors exhibited accumulation of the TP53 protein. This favorable factor turned out to be independent of a large residual tumor size, being the marker of poor prognosis. Similarly to the *HMOX1*-overlapping DMRs, those encompassing the *TCN2*, *PES1*, and *RP1-56J10.8* genes, if hypermethylated, were also predictors of good prognosis, and their clinical importance was revealed in the TP-treated patients and/or those with tumors harboring the accumulation of the TP53 protein.

Table 4. The selected results of multivariable Cox and logistic regression analyses for DMRs with the best discriminative capabilities in hgOvCa and BOTS.

hgOvCa						
Cox Regression (alpha = 0.0005)			**Mean beta Value (%) for DMR**			
OS in the TP53 Accumulation = Yes Subgroup	**HR [95% Cl]**	*p*-Value	**BOT**	**BOT V600E**	**lgOvCa**	**hgOvCa**
HMOX1(+)/NA(−): chr22:g.(−)35776686–35777032 [a]	8.4×10^{-5} [0–0.005]	4.11×10^{-6}	51.05	54.64	49.59	45.18
Residual tumor > 2 cm vs. 0 cm	6.24 [2.315–16.823]	0.0003				
OS in the TP therapy and TP53 accumulation = yes subgroup						
HMOX1(+)/NA(−): chr22:g.(−)35775959–35777032 [b]	3.71×10^{-6} [0–0.001]	4.33×10^{-6}	63.24	66.81	65.14	60.05
Residual tumor > 2 cm vs. 0 cm	8.3 [2.525–27.269]	0.0005				
TCN2(+)/PES1(−)/RP1-56J10.8(+): chr22:g.(−)31002067–31003655 [c]	1.13×10^{-7} [0–0]	5.26×10^{-6}	36.66	32.48	31.57	26.55
TCN2(+)/PES1(−)/RP1-56J10.8(+): chr22:g.both 31002067–31003655 [c]	4.06×10^{-11} [0–0]	6.35×10^{-6}	27.65	23.92	22.3	18.88
TCN2(+)/PES1(−)/RP1-56J10.8(+): chr22:g.both 31002362–31004367 [c]	1.15×10^{-9} [0–0]	7.31×10^{-6}	31.29	27.29	25.84	22.48
Logistic regression (alpha = 0.005)			**Mean beta value (%) for DMR**			
CR in the TP therapy subgroup	**OR [95% Cl]**	*p*-value	**BOT**	**BOT V600E**	**lgOvCa**	**hgOvCa**
NA(−)/NA(+): chr16:g.(−)880831–880831	5.14 [2.207–11.957]	0.00015	83.21	85.29	92.53	77.47
CR in the whole group (full table)						
ABR(−)/NA(+): chr17:g.(−)1131424–1131781 [d]	7.86 [2.566–24.063]	0.00031	31.71	26.14	38	21.59
NA(−)/NA(+): chr16:g.(−)880831–880831	3.4 [1.72–6.707]	0.00043	83.21	85.29	92.53	77.47
NCAM1(+)/RP11-629G13.1(−): chr11:g.(−)112831728–112832249 [c]	4.77 [1.975–11.535]	0.00052	28.82	19.77	17.35	13.42
AC006372.4 (+)/NA(−): chr7:g.(−)157258854–157259343 [c]	5.54 [2.104–14.596]	0.00053	57.89	60.4	65.37	42.17
PS in the whole group (full table)						
NPTXR(−)/NA(+): chr.22:g.(+)39240094–39240424	4.04 [1.81–9.03]	0.00066	13.97	8.24	3.42	3.86
Residual tumor > 2 cm vs. 0 cm	0.042 [0.006–0.294]	0.0014				
BOTS						
Logistic regression (alpha = 0.05)			**Mean beta value (%) for DMR**			
The presence of microinvasion and/or non-invasive implants in the whole group (full table)	**OR [95% Cl]**	*p*-value	**BOT**	**BOT V600E**	**lgOvCa**	**hgOvCa**
BAIAP3(+)/NA(−): chr.16:g.(−)1389301–1389301	49.04 [1.863–1290.778]	0.02	45.4	52.22	63.23	38.27
IL34(+)/NA(−): chr16:g.both 70613332–70613944	0.168 [0.037–0.769]	0.022	52.68	49.89	42.6	47.9
FIGO II/III vs FIGO IA/IB	185.5 [2.166–15883.94]	0.021				
IL34(+)/NA(−): chr16:g.(−)70613332–70613944	0.139 [0.025–0.759]	0.023	54.96	51.69	47.07	50.71
FIGO II/III vs. FIGO IA/IB	117.39 [1.936–7116.43]	0.023				
WNT10A(+)/NA(−): chr2:g.(+)219748780–219748780	0.14 [0.025–0.762]	0.023	41.98	36.23	44.2	30.48
FIGO II/III vs. FIGO IA/IB	157.11 [1.691–14593.4]	0.029				
NEU1(−)/SLC44A4(−)/NA(+): chr.6:g.(+)31827414–31834178	0.022 [0.001–0.601]	0.024	53.63	53.38	53.2	53.14
FIGO II/III vs. FIGO IA/IB	569.6 [1.093–296737.5]	0.047				

OS—overall survival; HR—hazard ratio; OR—odds ratio; CR—complete remission; PS—platinum sensitivity; TP—taxane/platinum chemotherapy; [a]—the same regularity was found in the subgroup: TP therapy and TP53 accumulation = yes; [b]—the same regularity was found in the subgroup: TP53 accumulation = yes; [c]—the same regularity was found in the TP-treated subgroup; [d]—the same regularity was found for CR in the TP-treated subgroup and for PS in both the whole group and the TP-treated subgroup. The missing models can be found in Reg.anal.suppl.results.
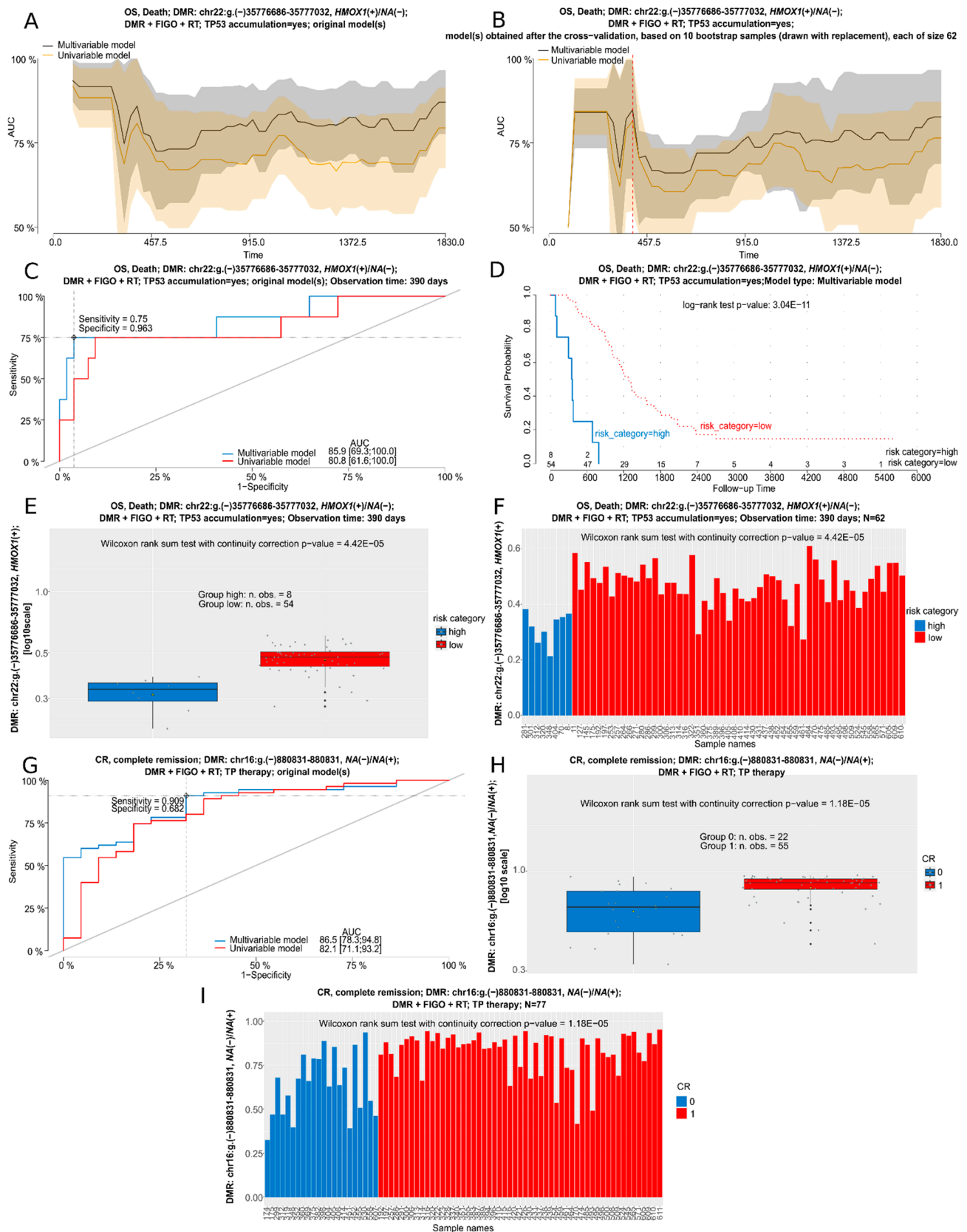
Figure 4. Nominated regression analyses for selected DMRs in hgOvCa. (**A**–**F**): Cox regression analysis (OS) in the subgroup of tumors with TP53 accumulation for the *HMOX1(+)/NA(−)* genes. (**A**,**B**): AUC plot for uni- and multivariable models obtained before (**A**) and after (**B**) a bootstrap-based cross-validation of the original data set. A red dashed line in B indicates the same time point which

was used to draw the time-dependent ROC curve (**C**). An optimal cutoff point for this ROC curve, was calculated based on the multivariable model using the Youden index. Discrimination sensitivity and specificity values for this cutoff point are also provided. (**D**): Kaplan-Meier survival curves obtained for the patients divided into two categories (risk higher (high) or lower (low) than for the ROC curve (**C**)-estimated cutoff point) based on the risk of death, calculated using the multivariable model. The Kaplan-Meier curves are supplemented with the result of the log-rank test, as well. Box (**E**) and bar (**F**) plots depicting mean methylation beta values within the DMR in patients with the high or low risk of death. (**G–I**): logistic regression analysis (CR) for a DMR in unknown gene(s), in the subgroup of patients treated with the TP regimen. (**G**): ROC curves for uni- and multivariable logistic regression models. Box (**H**) and bar (**I**) plots depicting mean methylation beta values within the DMR in patients with (1) and without (0) CR. RT: residual tumor; TP: taxane/platinum chemotherapy; CR: complete remission. Low p-values are displayed in exponential notation (e−n), in which e (exponent) multiplies the preceding number by 10 to the minus nth power.
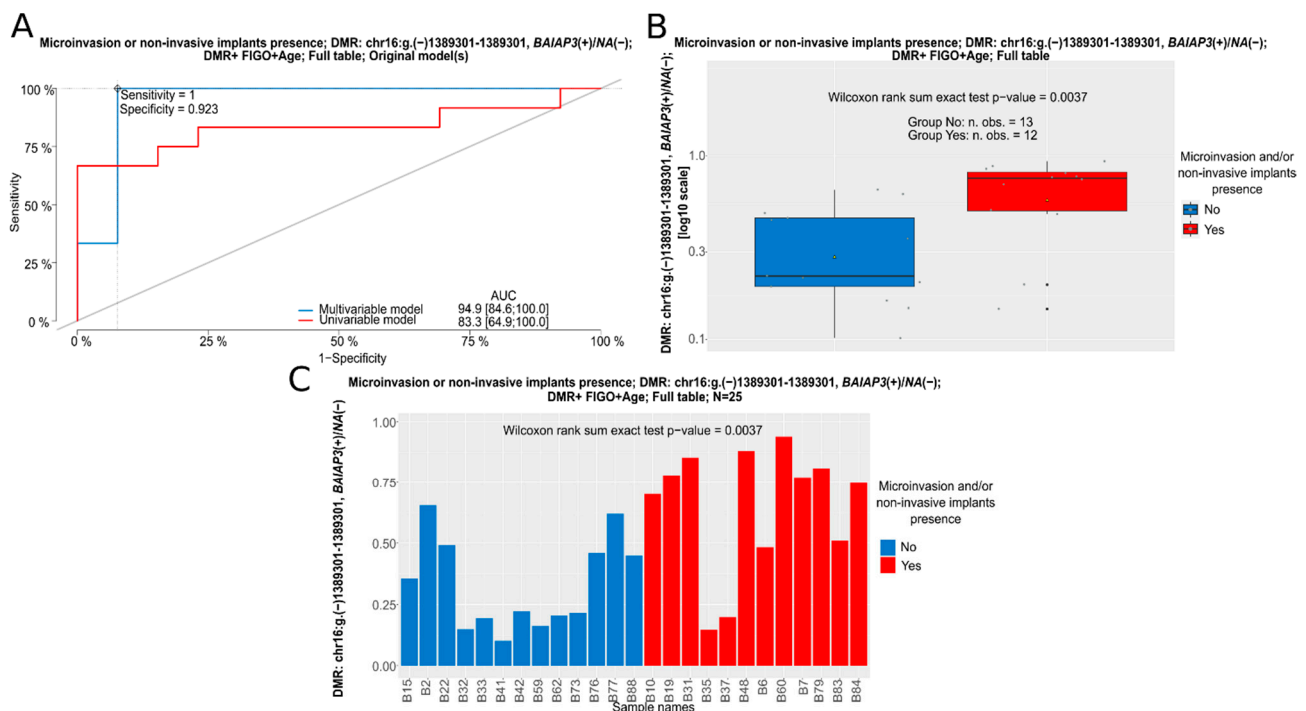
Figure 5. A nominated logistic regression analysis for a DMR in the *BAIAP3(+)/NA(−)* gene in the whole group of BOTS patients (Full table). (**A**): ROC curves for uni- and multivariable logistic regression models; Box (**B**) and bar (**C**) plots depicting mean methylation beta values within the DMR in tumors with (Yes) and without (No) microinvasion/non-invasive implants.

As to the response to chemotherapy, the strongest predictor was a single CpG site, cg10273669, located on the minus strand of chromosome 16, chr16:g.(−)880831–880831. Its hypermethylation increased the chance of tumor complete remission (CR), and this regularity was found in the entire cohort of hgOvCa patients and also in those who underwent the TP treatment. In addition, we identified two other DMRs, *NCAM1(+)/RP11-629G13.1(−)*:chr11:g.(−)112831728–112832249 and *AC006372.4(+)/NA(−)*:chr7:g.(−)157258854–157259343, that could potentially be used to predict the treatment outcome. Hypermethylation in both these regions was recognized herein as the favorable factor increasing the probability of cancer remission. This association was found in the entire cohort of patients and the subgroup treated with TP, as well. When the impact on platinum sensitivity (PS) was considered, two promising potential biomarkers were discovered in our study. The first DMR, *NPTXR(−)/NA(+)*:chr.22:g.(+)39240094–39240424, was located on chromosome 22 and encompassed the *NPTXR* gene. The elevated methylation of CpGs forming this DMR emerged as an advantageous predictive marker, increasing the sensitiv-

ity of the tumors to chemotherapy. Its clinical meaning turned out to be independent of the large residual disease, being the factor that significantly worsened cancer prediction. The last DMR, ABR(−)/NA(+):chr17:g.(−)1131424–1131781, being located on chromosome 17 and overlapping the *ABR* gene, was found herein to affect CR and PS alike, and, similarly to other DMRs described in this section, its hyperpermethylation made the hgOvCa tumors more sensitive to chemical treatment in both the entire cohort of patients and also those treated with TP.

In BOTS, no prognostic factors (determining relapse-free surivival (RFS)) were found, but still we managed to identify DMRs potentially suitable as biomarkers predictive of the occurrence of microinvasion and/or non-invasive implants. All these DMRs were discovered in the entire cohort of BOTS patients, irrespective of the presence of the *BRAF* V600E mutation in tumors. The DMR on chromosome 16, *BAIAP3(+)/NA(−)*:chr.16:g.(−)1389301–1389301, containing a single CpG site in the *BAIAP3* gene, cg01881308, may be considered the most promising biomarker in BOTS given the lowest *p*-value of all analyzed DMRs. Remarkably, out of all DMRs presented in this section, this was the only one the hypermethylation of which was a negative predictive factor, elevating the risk that microinvasion or non-invasive implants occur. Methylation changes in all the remaining DMRs in BOTS, listed in Table 4, exhibited a similar clinical effect, as hypermethylation of each of the following regions, *IL34(+)/NA(−)*:chr16:g.both 70613332–70613944; *IL34(+)/NA(−)*:chr16:g.(−)70613332–70613944; *WNT10A(+)/NA(−)*:chr2:g.(+)219748780–219748780; and *NEU1(−)/SLC44A4(−)/NA(+)*:chr.6:g.(+)31827414–31834178, was identified herein as a favorable clinical factor, decreasing the risk of microinvasion and/or non-invasive implants in BOTS. All these four DMRs were found to be potential biomarkers independent of the high FIGO stage, being a strong, negative predictive factor.

4. Discussion

In this study, the global genome-wide hypomethylation positively correlated with the increasing aggressiveness of ovarian tumors, being the strongest in hgOvCa. As expected, the *TP53* tumor suppressor gene was hypermethylated in carcinomas compared to BOTS. The methylation was especially high in *TP53* exons in lgOvCa, where no missense mutations were found. Remarkably, all the ten most significant DMRs, discriminating BOT from lgOvCa, encompassed the MHC region on chromosome 6, where genes linked to the immune response are located. Of note, the biggest number of unique DM CpGs and DMRs was found between lgOvCa and hgOvCa, thus corroborating vast methylation differences between these two cancer types reported by others [11]. By contrast, the BOT.V600E tumors had the lowest number of DM CpGs and DMRs compared to all other groups and, in relation to BOT, their genome was strongly downmethylated. This suggests that extensive hypomethylation is what distinguishes BOT.V600E from BOT and, when methylome is considered, BOT.V600E tumors might be placed somewhere in-between BOT and OvCa. By assessing differentially methylated CpGs, we revealed downmethylation of genes involved in the regulation of cytoskeleton/cell adhesion in BOTS compared to carcinomas. Such processes were also more frequently downmethylated in BOT than in BOT.V600E. By contrast, genes involved in cell cycle progression and RNA metabolism were upmethylated in BOT compared to BOT.V600E and lgOvCa. When comparing BOT to hgOvCa, only genes associated with cell cycle progression were upmethylated in the former group. As to the genes involved in cell differentiation, development, and morphogenesis, they were mainly downmethylated in BOTS compared to carcinomas. By contrast, when lgOvCa and hgOvCa were compared, such genes turned out to be upmethylated in less aggressive tumors, suggesting that in highly undifferentiated cancers, likely in the subpopulation of cancer stem cells (CSC), the pathological differentiation to various cell lineages might be advantageous for hgOvCa cells, enabling their epithelial-mesenchymal plasticity [28]. Lastly, in lgOvCa compared to hgOvCa, we detected the hypermethylation of genes upregulated by KRAS as well as genes related to epithelial-mesenchymal transition. These terms did not differentiate either BOT from BOT.V600E or BOTS from OvCa. We also identified

hundreds of DMRs in the genome, being of potential use as predictive biomarkers in BOTS and hgOvCa. DMRs with the best discriminative capabilities overlapped the following genes: *BAIAP3*, *IL34*, *WNT10A*, *NEU1*, *SLC44A4*, and *HMOX1*, *TCN2*, *PES1*, *RP1-56J10.8*, *ABR*, *NCAM1*, *RP11-629G13.1*, *AC006372.4*, *NPTXR* in BOTS and hgOvCa, respectively.

Methylation changes are often associated with the initial phase of tumorigenesis and can serve as valuable prognostic and predictive markers [2,29]. Notably, our methylome analyses were performed not only collectively in both DNA strands but also independently in separate strands (either plus or minus) to enhance the precision of the entire workflow. To date, in the literature, there were practically no scientific reports utilizing a similar approach, except for a study demonstrating that CpG methylation solely on the sense DNA strand of the APC gene was specific to hepatocellular carcinoma [30]. Another noteworthy feature of our workflow is its capability to determine methylation alterations in functionally annotated gene regions, including not only coding sequences, but also intron/exon boundaries, introns, UTRs, and proximal and distal promoters. So far, for ovarian tumors, no scientific reports employing such a comprehensive and detailed analytical workflow have been published, which makes our study unique and exceptionally thorough. Alterations in promoter methylation and their influence on gene expression are quite well known in ovarian cancer [27,31]. However, intragenic methylation changes have also been shown to affect transcription. Singer et al. [32] demonstrated two opposite phenomena. Firstly, they observed that some exons are more highly methylated than adjacent introns. Yet, they also identified a subset of mostly hypomethylated exons, which was associated with loose chromatin and thus higher transcriptional activity. Other studies showed that the methylation of first exons [26] and first introns [33] was negatively correlated with transcription, too. Aberrant methylation within the 3′UTRs possibly also affects gene expression, as it was shown that high methylation level of 3′UTRs may stimulate transcription [34]. This outcome, seemingly antithetical with those observed for promoter regions, suggests that the interplay between gene methylation and expression is far more complex and conceivably involves other regulatory processes. In fact, two possible mechanisms might link DNA methylation to gene expression. The first one involves proteins with domains binding to methylated DNA, acting as anchors for other proteins, being gene activity regulators. The second mechanism may rely on changes in DNA properties, such as its affinity to transcription factors and the 3-dimensional structure of chromatin [35]. Furthermore, it needs to be emphasized that gene expression depends not only on DNA methylation alterations but also on other phenomena, e.g., the miRNA-guided transcriptional control [36].

Of note, the results of our methylation analysis within gene regions, for the genes discussed below but not described in the Results section, are available in the Supplementary File: GeneRegions.pdf (GR file).

Cancer methylome changes cannot be simply put as either hypo- or hypermethylation of the genome. In fact, both these events occur in malignant cells to some extent, with a tendency towards global, genome-wide hypomethylation in advanced carcinomas. However, hypermethylation of CpG islands associated with, e.g., tumor suppressor genes and developmental regulators is also the hallmark of cancer cells. Additionally, methylation patterns can change dynamically at different stages of tumorigenesis [27,37]. The results shown herein are consistent with those presented in the papers cited above, since we found both hyper- and hypomethylated CpGs and DMRs in our series of cancers, especially in the hgOvCa group, compared to BOTS.

In the results section, we first concentrated on methylation changes within the *MDM2/TP53/CDKN1A* axis, involved in the control of genomic stability [25], as this aspect is still relatively poorly investigated. Despite the fact that we did not find either missense mutations or TP53 protein accumulation in our lgOvCa tumors, we discovered strong hypermethylation of the *TP53* gene in this tumor group compared to all the others. This implies that, in lgOvCa, the activity of the TP53 tumor suppressor may be mainly decreased by epigenetic changes and not mutations. So far, this phenomenon has not been reported by other researchers. Decreased methylation of *MDM2* in hgOvCa probably results in

the overexpression of this oncogene, which further impairs the anticancer role of TP53, as MDM2 catalyzes TP53 polyubiquitination, thus causing its degradation in proteasomes [38]. As for another tumor suppressor gene, *CDKN1A*, we expected it to be hypermethylated in OvCa compared to BOTS, as the high *CDKN1A* promoter methylation, leading to its low expression, can help cancer cells evade the cell cycle arrest by diminishing the amount of the p21 tumor suppressor, being a product of this gene [39]. In line with this assumption, the *CDKN1A* promoter hypermethylation was found in various cancers, such as lung, prostate, breast and pancreatic cancer, and leukemia. However, depending on the molecular context, p21 may play either an oncogenic or a tumor-suppressor role [39]. In ovarian cancer cells, especially those harboring the TP53 mutations, the mechanism of *CDKN1A* action may be different, given that the p21 activity depends on TP53 [40]. As shown in our previous study [21], over 60% of hgOvCa samples harbored missense *TP53* mutations, leading mainly to TP53 protein accumulation. By contrast, in lgOvCa, lacking genetic alterations in *TP53*, exceptionally strong hypermethylation of *TP53* was detected herein, as mentioned above. Thus, in both carcinoma groups investigated in this paper, the activity of TP53 seemed substantially impaired which arguably affected its interactions with p21, too. Considering that some genetic alterations in TP53 have previously been reported as gain-of-function, oncogenic mutations [41], it is probable that the role of *CDKN1A* and p21 may also change from anticancer to cancer-promoting when the TP53-dependent molecular context is aberrated. Such a functional shift would explain the negative correlation between *CDNK1A* methylation and tumor aggressiveness revealed in the present study.

Our ontological analyses showed that the processes mainly deregulated in our tumor groups were development/differentiation, adhesion, nervous system, cell cycle, and processes affecting RNA metabolism. Cell differentiation and development are predominantly controlled by transcription co-regulators belonging to the Polycomb group (PcG), including Polycomb Repressive Complex 1 (PRC1) and 2 (PRC2) [42], as well as their targets. One of the PRC targets, the HOXA5 gene, seems to play a significant role in ovarian biology and may be involved in ovarian cancer predisposition, since the loss of *HOXA5* function leads to the formation of ovarian epithelial cysts in older females [43,44]. Moreover, the promoter region of this gene was shown to be hypermethylated in breast cancer [45]. Consistently, in our study, we found high methylation in the coding sequence (cds), distal promoter, and exonic regions of *HOXA5*, especially in hgOvCa but also in BOT.V600E compared to BOT (GR file). In contrast to hypermethylation of Polycomb target genes, in OvCa, we observed hypomethylation of Polycomb genes, as well. In the *EZH2* gene (encoding a protein being a member of the PRC2 complex), especially in hgOvCa compared to BOTS, we detected strong hypomethylation in many regions, including the first exon/5′UTR, exons, and both promoters (GR file). The *BMI1* gene (the protein product of which is a part of the PRC1 complex) was also hypomethylated in many regions not only in hgOvCa (exons, 3′UTR and distal promoter) but in both carcinoma groups (proximal promoter and the first exon), which implies its high expression in OvCa (GR file). Remarkably, one study supports our results, proving that overexpression of *BMI1* in ovarian cancer promotes metastasis, decelerates apoptosis, and desensitizes tumor cells to platinum treatment [46]. Of note, in the present study, the genes involved in cell differentiation, development, and morphogenesis were downmethylated in BOTS compared to carcinomas. By contrast, when lgOvCa and hgOvCa were confronted with each other, such genes turned out to be upmethylated in less aggressive tumors, suggesting that in highly undifferentiated cancers, likely in the subpopulation of CSC, the pathological differentiation to various cell lineages might be advantageous for hgOvCa cells, enabling their epithelial–mesenchymal plasticity [28,47].

Adhesion and cytoskeletal processes were enriched in genes mainly downmethylated in BOTS compared to carcinomas and also when BOT were confronted with BOT.V600E. Two studies employing gene expression microarrays, performed on a small group of cystadenomas, BOTS, and OvCa, all of a serous type, seem to support our results. One of the reports unraveled that the malignant subtype of BOTS exhibited a cell adhesion signature [48], whereas in the other, genes implicated in adhesion, cell cycle, and motility

were shown to account for phenotypic differences between borderline tumors and high-grade cancers [49].

GO terms associated with the nervous system were also significantly enriched in differentially methylated genes herein. The literature data are mostly consistent with our results, demonstrating that the pathway enrichment analysis for transcriptomic data revealed neural activities (axon guidance, neurogenesis) as promoters of ovarian cancer progression and indicators of poor prognosis. Moreover, four neural genes (*NTN1*, *UNC5B*, *EFNB2*, and *EFNA5*) were nominated as promising biomarkers and therapeutic targets in ovarian cancer patients [50]. Notably, in our regression analyses for DMRs in hgOvCa, predictive capabilities were not confirmed for any of those genes when methylation changes were considered. Another study unveiled the correlation between the elevated expression of neuronal transcription factor Brn-3a (POU4F1) and the decreased rate of apoptosis in ovarian cancer cells [51]. Consistently, we observed significant hypomethylation in the proximal promoter of *POU4F1* in carcinomas compared to BOTS, as well as in the first exon in hgOvCa in comparison with the remaining groups (GR file). A putative tumor suppressor, *ZIC1*, involved in neurogenesis, dorsal spinal cord development, and maturation of the cerebellum [40] was shown to be hypermethylated and silenced in OvCa. This was correlated with increased proliferation, migration, and invasiveness of tumor cells [52]. Our results align with these findings, as we revealed strong hypermethylation of *ZIC1* in carcinomas compared to BOTS in most regions of the gene (GR file).

As to the cell cycle, hypermethylation of genes coding for cell cycle inhibitors, like p16INK4a (CDKN2A) and p15INK4b (CDKN2B), is a well-known phenomenon, *reported for various tumors [53]*. Conversely, in the present study, we observed hypo- rather than hypermethylation of these two genes in carcinomas compared to BOTS. This seemingly antithetical outcome may be attributed to missense mutations in the *TP53* gene, occurring in hgOvCa. As we demonstrated in our previous research [15,16], the TP53 status can determine the clinical significance of other molecular biomarkers. However, this theory does not explain hypomethylation of those genes in lgOvCa, where neither *TP53* missense variants were found [21] nor TP53 protein accumulation was detected [15]. Nevertheless, as discussed above, the *TP53* methylation was exceptionally high in our lgOvCa series, which suggests that the level of TP53 protein in these tumors was conceivably too low to maintain its tumor suppressor activity.

When comparing BOTS to OvCa, genes involved in RNA transcription, metabolism, and processing were deregulated bidirectionally in our study. As to the transcription-related genes (coding for polymerase II subunits), the *POLR2D* gene was significantly hypomethylated not only in carcinomas (across almost all gene regions, except for 3′UTRs), but also in BOT.V600E (proximal promoter) compared to BOT (GR file). By contrast, some other genes encoding the polymerase II subunits were characterized by higher methylation in carcinomas than in BOTS (e.g., promoters and/or first exons of *POLR2G* and *POLR2L*, as well as the distal promoter of *POLR2C*, and the cds of *POLR2E*, GR file). These findings are supported by the study by Bhandari et al. [54], who revealed overexpression of *POLR2D* in multiple cancers, and also showed the *POLR2L* gene to be hypermethylated in a non-small-cell lung cancer cell line.

RNA metabolism and processing relies mainly on RNA binding proteins (RBPs). The role of genes encoding such proteins, *LUC7L2*, *MRPL46*, *MRPL14*, *PARP4*, *STRAP*, and *PAPOLA*, in ovarian tumor development has already been investigated in the literature [55]. In our study, those genes (except for *PARP4*) were predominantly hypomethylated in carcinomas compared to the BOT groups (GR file). Another RBP-coding gene, *CELF2*, was also downmethylated, in the hgOvCa series tested here and in the majority of OvCa cell lines assessed by Piqué et al. [56]. Nonetheless, in contradiction to these findings, the expression of *CELF2* was shown to positively correlate with better prognosis in ovarian cancer patients [57].

Interestingly, in our ontological analyses, some terms prevailed if a particular tumor group was compared to others, e.g., in the BOT group, fatty acid metabolism and adipogen-

esis were significantly enriched in hypermethylated genes in all three possible comparisons. This outcome is consistent with the literature, since upregulated lipid metabolic pathways were found to increase lipogenesis and lipolysis via exogenous and endogenous uptakes, thus allowing cancer cells to enhance membrane biogenesis and ATP production, and finally to evade apoptosis. In line with this notion, the researchers showed a high level of lipoproteins in serous hgOvCa and concomitantly increased transfer of cholesterol, phospholipids, and triglycerides to such tumors compared to serous BOTS [58]. Furthermore, the increased rate of fatty acid beta-oxidation leads to higher ATP production and faster cellular lamellipodia formation, which facilitates tumor cell migration and invasion [59].

Notably, two other ontological terms were enriched in our study only if two OvCa groups were compared to each other. One of these terms involved genes upregulated by KRAS, while the other was related to epithelial–mesenchymal transition (EMT). Both these terms were enriched in genes hypermethylated in lgOvCa. Given that there were no KRAS-activating mutations in our hgOvCa [21], hypomethylation of KRAS-dependent genes may be the way for these tumors to induce cell proliferation in the presence of a normal *KRAS* protooncogene. As to the EMT-related genes, their downmethylation in hgOvCa was expected, as it probably increased the aggressiveness, chemoresistance, and potential for metastasis of such cancers, e.g., by the overexpression of Snail transcription factors [47]. Accordingly, when we examined differences of methylation patterns in various regions of the *SNAI2* gene, its distal promoter and the 3′UTR were both hypomethylated in hgOvCa compared to lgOvCa (GR file).

As to the DMRs identified in the present study, all the ten most significant ones, discriminating BOT from lgOvCa, encompassed the MHC region on chromosome 6. The concentration of DMRs within a relatively short fragment of the same chromosome may imply that all these DMRs are located within a single chromatin domain. Such domains were previously shown to be regulated in a coordinated manner in the process of carcinogenesis [60]. The aforementioned region on chromosome 6, comprising approximately 3.5 million bp, is densely packed with immunologically important genes [61]. To date, no studies on this region are available in the literature for BOTS and lgOvCa alike. Still, based on our results, we may assume that the immune system, and possibly also other components of tumor microenvironment, may play a pivotal role in the transition from BOTS to lgOvCa. Yet, to shed more light on this complex process, further in-depth research is necessary.

In BOTS, one of the genes overlapped by DMRs with good discriminative capacities was *BAIAP3*. This TP53-dependent gene encodes a brain-specific angiogenesis inhibitor, involved in the endosome to Golgi retrograde transport [40]. Although there are no data on its role in ovarian tumors, its oncogenic meaning was demonstrated in desmoplastic small-round-cell tumor, an aggressive and rare cancer, in which the ectopic expression of *BAIAP3* dramatically enhanced growth and colony formation in vitro [62]. Our results seem to support that outcome, as we observed hypomethylation of the *BAIAP3* distal promoter and 5′UTR/first exon in hgOvCa compared to BOT and BOT.V600E alike (GR file). Still, if only borderline tumors were considered, high methylation of a one-CpG DMR, located in a *BAIAP3* intron, increased the risk of microinvasion/non-invasive implants in our regression analyses.

By contrast, hypermethylation of two DMRs encompassing the *IL34* gene turned out to be a favorable predictor, herein, decreasing the risk of microinvasion/non-invasive implants, which implies an oncogenic role of IL34 in BOTS. In accordance, the literature portrays IL34 as a cancer-promoting interleukin in OvCa, inducing the formation of tumor-associated macrophages (TAM), being the important part of a tumor microenvironment [63].

As for DMRs of potential use as predictors in hgOvCa, one of them encompassed the *HMOX1* (HO-1) gene. This gene encodes an essential enzyme in heme catabolism [40] and is considered an oncogene, highly expressed in gynecological malignancies, including ovarian, cervical, and endometrial cancers. HO-1 is involved in cell proliferation, metastasis, immune regulation and angiogenesis [64]. Consistently, our regression analyses also

contribute to the oncogenic role of *HMOX1*, showing that the elevated methylation level within the discussed DMR was associated with the lower risk of death in patients with tumors harboring the TP53 protein accumulation.

Two other genes, *TCN2*, and *PES1*, were overlapped by three DMRs discovered in the present study. If hypermethylated, all these DMRs emerged as markers of good prognosis in patients suffering from hgOvCa with TP53 accumulation who underwent the TP therapy. Thus, based on our results, *TCN2* and *PES1* might both be regarded as oncogenes. Considering the literature data, the elevated level of *TCN2*, a co-factor taking part in the kobalamin (vitamin B12) transport [40], was associated with the increased risk of thyroid cancer development [65], which supports the outcome obtained in the present study. Similarly, the high expression of the *PES1* gene, encoding a nucleolar protein involved in ribosome biogenesis and DNA replication, was shown to be related to tumor cell proliferation, invasion, and metastasis in multiple types of cancer, including ovarian cancer [66,67], which is concordant with our results, too.

The last gene to be discussed, *ABR*, coding for the protein having the GTPase-activating and the guanine exchange factor (GEF) domains [40], is overlapped by a DMR, hypermethylation of which was demonstrated here as a favorable factor increasing the chance of CR in the entire set of hgOvCa specimens. Thus, the gene in questions appears to be an oncogene in ovarian carcinomas. Our analysis of methylation changes in various functionally annotated gene regions (GR file) constitutes another confirmation of the likely pathogenic role of *ABR* in ovarian tumors, unveiling its hypomethylation in hgOvCa compared to less aggressive tumors in all regions except for 3′UTRs. Conversely, other researchers reported the putative tumor suppressive role of *ABR* in both solid tumors, such as medulloblastoma, astrocytoma, and breast cancer, and in acute myeloid leukemia, too [68]. Remarkably, none of those research were carried out on OvCa, which may explain why their results are inconsistent with ours.

5. Limitations of the Study

One of the limitations of our study originates from the fact that we analyzed bulk tumor samples being just a part of the entire tumor microenvironment, the complexity and heterogeneity of which might not have been fully captured due to the constraints of the experimental setup applied herein. Secondly, our research was performed on the retrospective (not prospective) cohort of patients, collected for 20 years, meticulously followed up, and carefully checked for compatibility of all clinicopathological parameters. This approach, though widely used, could introduce some hardly definable biases and limit the ability to control for potential confounding factors. Finally, due to the relatively poor quality of DNA isolated from formalin-fixed, paraffin-embedded (FFPE) blocks, we were forced to discard some hybridization probes (and also the corresponding CpG sites) to guarantee the reliability of the methylome profiling results. Approximately 69% of the probes passed all the filtering steps described in the Methods section. Thus, some potentially important methylation differences may have been missed in the present study.

6. Conclusions

Herein, the global genome-wide hypomethylation positively correlated with the increasing aggressiveness of ovarian tumors, being the strongest in hgOvCa. Based on our results, we may also assume that the immune system, and likely other components of tumor microenvironment too, possibly play a pivotal role in the transition from BOTS to lgOvCa. Interestingly, the BOT.V600E tumors had the lowest number of differentially methylated CpGs and DMRs compared to all other groups. Thus, when methylome is considered, such tumors might be placed in-between BOT and OvCa. Moreover, we identified hundreds of DMRs in the genome, being of potential use as predictive biomarkers in BOTS and hgOvCa. Therefore, our research not only forms a groundwork for future studies on ovarian tumor methylome but also, by identifying potential biomarkers, might facilitate the fight against this group of diseases and conceivably improve their outcome.

References

1. Heery, R.; Schaefer, M.H. DNA Methylation Variation along the Cancer Epigenome and the Identification of Novel Epigenetic Driver Events. *Nucleic Acids Res.* **2021**, *49*, 12692–12705. [CrossRef] [PubMed]
2. Hanson, H.E.; Liebl, A.L. The Mutagenic Consequences of DNA Methylation within and across Generations. *Epigenomes* **2022**, *6*, 33. [CrossRef] [PubMed]
3. Bourdel, N.; Huchon, C.; Abdel Wahab, C.; Azaïs, H.; Bendifallah, S.; Bolze, P.-A.; Brun, J.-L.; Canlorbe, G.; Chauvet, P.; Chereau, E.; et al. Borderline Ovarian Tumors: French Guidelines from the CNGOF. Part 2. Surgical Management, Follow-up, Hormone Replacement Therapy, Fertility Management and Preservation. *J. Gynecol. Obstet. Hum. Reprod.* **2021**, *50*, 101966. [CrossRef] [PubMed]
4. Timor-Tritsch, I.E.; Foley, C.E.; Brandon, C.; Yoon, E.; Ciaffarrano, J.; Monteagudo, A.; Mittal, K.; Boyd, L. New Sonographic Marker of Borderline Ovarian Tumor: Microcystic Pattern of Papillae and Solid Components. *Ultrasound Obstet. Gynecol. Off. J. Int. Soc. Ultrasound Obstet. Gynecol.* **2019**, *54*, 395–402. [CrossRef] [PubMed]
5. Niu, L.; Tian, H.; Xu, Y.; Cao, J.; Zhang, X.; Zhang, J.; Hou, J.; Lv, W.; Wang, J.; Xin, L.; et al. Recurrence Characteristics and Clinicopathological Results of Borderline Ovarian Tumors. *BMC Womens Health* **2021**, *21*, 134. [CrossRef]
6. Shih, K.; Zhou, Q.; Huh, J.; Morgan, J.; Iasonos, A.; Aghajanian, C.; Chi, D.; Barakat, R.; Abu-Rustum, N. Risk Factors for Recurrence of Ovarian Borderline Tumors. *Gynecol. Oncol.* **2011**, *120*, 480–484. [CrossRef]

7. Hauptmann, S.; Friedrich, K.; Redline, R.; Avril, S. Ovarian Borderline Tumors in the 2014 WHO Classification: Evolving Concepts and Diagnostic Criteria. *Virchows Arch.* **2017**, *470*, 125–142. [CrossRef]

8. Gershenson, D.M.; Silva, E.G.; Levy, L.; Burke, T.W.; Wolf, J.K.; Tornos, C. Ovarian Serous Borderline Tumors with Invasive Peritoneal Implants. *Cancer* **1998**, *82*, 1096–1103. [CrossRef]

9. Vang, R.; Hannibal, C.G.; Junge, J.; Frederiksen, K.; Kjaer, S.K.; Kurman, R.J. Long-Term Behavior of Serous Borderline Tumors Subdivided Into Atypical Proliferative Tumors and Noninvasive Low-Grade Carcinomas: A Population-Based Clinicopathologic Study of 942 Cases. *Am. J. Surg. Pathol.* **2017**, *41*, 725–737. [CrossRef]

10. Moujaber, T.; Balleine, R.L.; Gao, B.; Madsen, I.; Harnett, P.R.; DeFazio, A. New Therapeutic Opportunities for Women with Low-Grade Serous Ovarian Cancer. *Endocr. Relat. Cancer* **2022**, *29*, R1–R16. [CrossRef]

11. Shih, I.-M.; Chen, L.; Wang, C.; Gu, J.; Davidson, B.; Cope, L.; Kurman, R.J.; Xuan, J.; Wang, T.-L. Distinct DNA Methylation Profiles in Ovarian Serous Neoplasms and Their Implications in Ovarian Carcinogenesis. *Am. J. Obstet. Gynecol.* **2010**, *203*, 584.e1–584.e22. [CrossRef] [PubMed]

12. Zeller, C.; Dai, W.; Curry, E.; Siddiq, A.; Walley, A.; Masrour, N.; Kitsou-Mylona, I.; Anderson, G.; Ghaem-Maghami, S.; Brown, R.; et al. The DNA Methylomes of Serous Borderline Tumors Reveal Subgroups with Malignant- or Benign-like Profiles. *Am. J. Pathol.* **2013**, *182*, 668–677. [CrossRef] [PubMed]

13. Reyes, H.D.; Devor, E.J.; Warrier, A.; Newtson, A.M.; Mattson, J.; Wagner, V.; Duncan, G.N.; Leslie, K.K.; Gonzalez-Bosquet, J. Differential DNA Methylation in High-Grade Serous Ovarian Cancer (HGSOC) Is Associated with Tumor Behavior. *Sci. Rep.* **2019**, *9*, 17996. [CrossRef] [PubMed]

14. Ferris, J.S.; Wang, T.; Wang, S.; Hibshoosh, H.; Su, T.; Wang, X.; Chen, X.; Yu, A.; Santella, R.M.; Wright, J.D.; et al. Identifying DNA Methylation Signatures in High-Grade Serous Ovarian Cancer: Results Vary by Control Tissue Type. *J. Clin. Oncol.* **2022**, *40*, e17559. [CrossRef]

15. Kupryjańczyk, J.; Szymańska, T.; Madry, R.; Timorek, A.; Stelmachów, J.; Karpińska, G.; Rembiszewska, A.; Ziółkowska, I.; Kraszewska, E.; Debniak, J.; et al. Evaluation of Clinical Significance of TP53, BCL-2, BAX and MEK1 Expression in 229 Ovarian Carcinomas Treated with Platinum-Based Regimen. *Br. J. Cancer* **2003**, *88*, 848–854. [CrossRef]

16. Kupryjańczyk, J.; Madry, R.; Plisiecka-Hałasa, J.; Bar, J.; Kraszewska, E.; Ziółkowska, I.; Timorek, A.; Stelmachów, J.; Emerich, J.; Jedryka, M.; et al. TP53 Status Determines Clinical Significance of ERBB2 Expression in Ovarian Cancer. *Br. J. Cancer* **2004**, *91*, 1916–1923. [CrossRef]

17. Mayr, D.; Hirschmann, A.; Löhrs, U.; Diebold, J. KRAS and BRAF Mutations in Ovarian Tumors: A Comprehensive Study of Invasive Carcinomas, Borderline Tumors and Extraovarian Implants. *Gynecol. Oncol.* **2006**, *103*, 883–887. [CrossRef]

18. Wong, K.-K.; Tsai, C.-C.; Gershenson, D.M. BRAF Mutational Analysis in Ovarian Tumors: Recent Perspectives. *Pathol. Lab. Med. Int.* **2015**, *7*, 75–82. [CrossRef]

19. Szafron, L.A.; Iwanicka-Nowicka, R.; Podgorska, A.; Bonna, A.M.; Sobiczewski, P.; Kupryjanczyk, J.; Szafron, L.M. The Clinical Significance of CRNDE Gene Methylation, Polymorphisms, and CRNDEP Micropeptide Expression in Ovarian Tumors. *Int. J. Mol. Sci.* **2024**, *25*, 7531. [CrossRef]

20. Mehra, P.; Aditi, S.; Prasad, K.M.; Bariar, N. k Histomorphological Analysis of Ovarian Neoplasms According to the 2020 WHO Classification of Ovarian Tumors: A Distribution Pattern in a Tertiary Care Center. *Cureus* **2023**, *15*, e38273. [CrossRef]

21. Szafron, L.A.; Sobiczewski, P.; Dansonka-Mieszkowska, A.; Kupryjanczyk, J.; Szafron, L.M. An Analysis of Genetic Polymorphisms in 76 Genes Related to the Development of Ovarian Tumors of Different Aggressiveness. *International Journal of Molecular Sciences* **2024**, *25*, 10876. [CrossRef]

22. Woroniecka, R.; Rymkiewicz, G.; Szafron, L.M.; Blachnio, K.; Szafron, L.A.; Bystydzienski, Z.; Pienkowska-Grela, B.; Borkowska, K.; Rygier, J.; Kotyl, A.; et al. Cryptic MYC Insertions in Burkitt Lymphoma: New Data and a Review of the Literature. *PLoS ONE* **2022**, *17*, e0263980. [CrossRef] [PubMed]

23. Maksimovic, J.; Phipson, B.; Oshlack, A. A Cross-Package Bioconductor Workflow for Analysing Methylation Array Data. *F1000Research* **2016**, *5*, 1281. [CrossRef] [PubMed]

24. Gerds, T.A.; Cai, T.; Schumacher, M. The Performance of Risk Prediction Models. *Biom. J.* **2008**, *50*, 457–479. [CrossRef]

25. Lotfi Garavand, A.; Mohammadi, M.; Mohammadzadeh, S. Evaluation of TP53 Codon 72, P21 Codon 31, and MDM2 SNP309 Polymorphisms in Iranian Patients with Acute Lymphocytic Leukemia. *Rep. Biochem. Mol. Biol.* **2020**, *9*, 26–32. [CrossRef]

26. Li, S.; Zhang, J.; Huang, S.; He, X. Genome-Wide Analysis Reveals That Exon Methylation Facilitates Its Selective Usage in the Human Transcriptome. *Brief. Bioinform.* **2018**, *19*, 754–764. [CrossRef]

27. Lakshminarasimhan, R.; Liang, G. The Role of DNA Methylation in Cancer. *Adv. Exp. Med. Biol.* **2016**, *945*, 151–172. [CrossRef]

28. Haerinck, J.; Goossens, S.; Berx, G. The Epithelial–Mesenchymal Plasticity Landscape: Principles of Design and Mechanisms of Regulation. *Nat. Rev. Genet.* **2023**, *24*, 590–609. [CrossRef]

29. Hentze, J.L.; Høgdall, C.K.; Høgdall, E.V. Methylation and Ovarian Cancer: Can DNA Methylation Be of Diagnostic Use? *Mol. Clin. Oncol.* **2019**, *10*, 323–330. [CrossRef]

30. Jain, S.; Chang, T.-T.; Hamilton, J.P.; Lin, S.Y.; Lin, Y.-J.; Evans, A.A.; Selaru, F.M.; Lin, P.-W.; Chen, S.-H.; Block, T.M.; et al. Methylation of the CpG Sites Only on the Sense Strand of the APC Gene Is Specific for Hepatocellular Carcinoma. *PLoS ONE* **2011**, *6*, e26799. [CrossRef]

31. Chmelarova, M.; Krepinska, E.; Spacek, J.; Laco, J.; Beranek, M.; Palicka, V. Methylation in the P53 Promoter in Epithelial Ovarian Cancer. *Clin. Transl. Oncol. Off. Publ. Fed. Span. Oncol. Soc. Natl. Cancer Inst. Mex.* **2013**, *15*, 160–163. [CrossRef] [PubMed]

32. Singer, M.; Kosti, I.; Pachter, L.; Mandel-Gutfreund, Y. A Diverse Epigenetic Landscape at Human Exons with Implication for Expression. *Nucleic Acids Res.* **2015**, *43*, 3498–3508. [CrossRef] [PubMed]

33. Anastasiadi, D.; Esteve-Codina, A.; Piferrer, F. Consistent Inverse Correlation between DNA Methylation of the First Intron and Gene Expression across Tissues and Species. *Epigenetics Chromatin* **2018**, *11*, 37. [CrossRef] [PubMed]

34. McGuire, M.H.; Herbrich, S.M.; Dasari, S.K.; Wu, S.Y.; Wang, Y.; Rupaimoole, R.; Lopez-Berestein, G.; Baggerly, K.A.; Sood, A.K. Pan-Cancer Genomic Analysis Links 3′UTR DNA Methylation with Increased Gene Expression in T Cells. *EBioMedicine* **2019**, *43*, 127–137. [CrossRef]

35. Buitrago, D.; Labrador, M.; Arcon, J.P.; Lema, R.; Flores, O.; Esteve-Codina, A.; Blanc, J.; Villegas, N.; Bellido, D.; Gut, M.; et al. Impact of DNA Methylation on 3D Genome Structure. *Nat. Commun.* **2021**, *12*, 3243. [CrossRef]

36. Catalanotto, C.; Cogoni, C.; Zardo, G. MicroRNA in Control of Gene Expression: An Overview of Nuclear Functions. *Int. J. Mol. Sci.* **2016**, *17*, 1712. [CrossRef]

37. Kulis, M.; Esteller, M. 2—DNA Methylation and Cancer. In *Advances in Genetics*; Herceg, Z., Ushijima, T., Eds.; Epigenetics and Cancer, Part A; Academic Press: Cambridge, MA, USA, 2010; Volume 70, pp. 27–56.

38. Shi, D.; Gu, W. Dual Roles of MDM2 in the Regulation of P53. *Genes Cancer* **2012**, *3*, 240–248. [CrossRef]

39. Manousakis, E.; Miralles, C.M.; Esquerda, M.G.; Wright, R.H.G. CDKN1A/P21 in Breast Cancer: Part of the Problem, or Part of the Solution? *Int. J. Mol. Sci.* **2023**, *24*, 17488. [CrossRef]

40. Stelzer, G.; Rosen, N.; Plaschkes, I.; Zimmerman, S.; Twik, M.; Fishilevich, S.; Stein, T.I.; Nudel, R.; Lieder, I.; Mazor, Y.; et al. The GeneCards Suite: From Gene Data Mining to Disease Genome Sequence Analyses. *Curr. Protoc. Bioinform.* **2016**, *54*, 1–30. [CrossRef]

41. Roszkowska, K.A.; Piecuch, A.; Sady, M.; Gajewski, Z.; Flis, S. Gain of Function (GOF) Mutant P53 in Cancer-Current Therapeutic Approaches. *Int. J. Mol. Sci.* **2022**, *23*, 13287. [CrossRef]

42. Parreno, V.; Martinez, A.-M.; Cavalli, G. Mechanisms of Polycomb Group Protein Function in Cancer. *Cell Res.* **2022**, *32*, 231–253. [CrossRef] [PubMed]

43. Gendronneau, G.; Boucherat, O.; Aubin, J.; Lemieux, M.; Jeannotte, L. The Loss of Hoxa5 Function Causes Estrous Acyclicity and Ovarian Epithelial Inclusion Cysts. *Endocrinology* **2012**, *153*, 1484–1497. [CrossRef] [PubMed]

44. Jeannotte, L.; Gotti, F.; Landry-Truchon, K. Hoxa5: A Key Player in Development and Disease. *J. Dev. Biol.* **2016**, *4*, 13. [CrossRef] [PubMed]

45. Bracken, A.P.; Dietrich, N.; Pasini, D.; Hansen, K.H.; Helin, K. Genome-Wide Mapping of Polycomb Target Genes Unravels Their Roles in Cell Fate Transitions. *Genes Dev.* **2006**, *20*, 1123–1136. [CrossRef] [PubMed]

46. Zhao, Q.; Qian, Q.; Cao, D.; Yang, J.; Gui, T.; Shen, K. Role of BMI1 in Epithelial Ovarian Cancer: Investigated via the CRISPR/Cas9 System and RNA Sequencing. *J. Ovarian Res.* **2018**, *11*, 31. [CrossRef]

47. Kielbik, M.; Przygodzka, P.; Szulc-Kielbik, I.; Klink, M. Snail Transcription Factors as Key Regulators of Chemoresistance, Stemness and Metastasis of Ovarian Cancer Cells. *Biochim. Biophys. Acta Rev. Cancer* **2023**, *1878*, 189003. [CrossRef]

48. Curry, E.W.; Stronach, E.A.; Rama, N.R.; Wang, Y.Y.; Gabra, H.; El-Bahrawy, M.A. Molecular Subtypes of Serous Borderline Ovarian Tumor Show Distinct Expression Patterns of Benign Tumor and Malignant Tumor-Associated Signatures. *Mod. Pathol.* **2014**, *27*, 433–442. [CrossRef]

49. Donninger, H.; Bonome, T.; Li, J.-Y.; Park, D.-C.; Radonovich, M.; Pise-Masison, C.; Brady, J.; Barrett, J.C.; Mok, S.C.; Birrer, M.J. Expression Profiling of Microdissected Papillary Serous Ovarian Epithelial Cancers Identifies Genes Describing the Unique Phenotypes of Borderline and Malignant Tumors. *J. Clin. Oncol.* **2005**, *23*, 5029. [CrossRef]

50. Yang, L.; Bie, L.; Sun, L.; Yue, Y. Neural Activities Are Unfavorable for the Prognosis of Ovarian Cancer through mRNA Expression Analysis. *Biomark. Med.* **2019**, *13*, 663–673. [CrossRef]

51. Ahmed, N.; Latifi, A.; Riley, C.B.; Findlay, J.K.; Quinn, M.A. Neuronal Transcription Factor Brn-3a(l) Is over Expressed in High-Grade Ovarian Carcinomas and Tumor Cells from Ascites of Patients with Advanced-Stage Ovarian Cancer. *J. Ovarian Res.* **2010**, *3*, 17. [CrossRef]

52. Huang, R.-L.; Gu, F.; Kirma, N.B.; Ruan, J.; Chen, C.-L.; Wang, H.-C.; Liao, Y.-P.; Chang, C.-C.; Yu, M.-H.; Pilrose, J.M.; et al. Comprehensive Methylome Analysis of Ovarian Tumors Reveals Hedgehog Signaling Pathway Regulators as Prognostic DNA Methylation Biomarkers. *Epigenetics* **2013**, *8*, 624–634. [CrossRef] [PubMed]

53. Esteller, M.; Corn, P.G.; Baylin, S.B.; Herman, J.G. A Gene Hypermethylation Profile of Human Cancer. *Cancer Res.* **2001**, *61*, 3225–3229. [PubMed]

54. Bhandari, N.; Acharya, D.; Chatterjee, A.; Mandve, L.; Kumar, P.; Pratap, S.; Malakar, P.; Shukla, S.K. Pan-Cancer Integrated Bioinformatic Analysis of RNA Polymerase Subunits Reveal RNA Pol I Member CD3EAP Regulates Cell Growth by Modulating Autophagy. *Cell Cycle* **2023**, *22*, 1986–2002. [CrossRef] [PubMed]

55. Wu, J.; Wu, Y.; Guo, Q.; Wang, S.; Wu, X. RNA-Binding Proteins in Ovarian Cancer: A Novel Avenue of Their Roles in Diagnosis and Treatment. *J. Transl. Med.* **2022**, *20*, 37. [CrossRef] [PubMed]

56. Piqué, L.; Martinez de Paz, A.; Piñeyro, D.; Martínez-Cardús, A.; Castro de Moura, M.; Llinàs-Arias, P.; Setien, F.; Gomez-Miragaya, J.; Gonzalez-Suarez, E.; Sigurdsson, S.; et al. Epigenetic Inactivation of the Splicing RNA-Binding Protein CELF2 in Human Breast Cancer. *Oncogene* **2019**, *38*, 7106–7112. [CrossRef]

57. Guo, Q.; Wu, Y.; Guo, X.; Cao, L.; Xu, F.; Zhao, H.; Zhu, J.; Wen, H.; Ju, X.; Wu, X. The RNA-Binding Protein CELF2 Inhibits Ovarian Cancer Progression by Stabilizing FAM198B. *Mol. Ther. Nucleic Acids* **2021**, *23*, 169–184. [CrossRef]

58. Bae, G.; Berezhnoy, G.; Koch, A.; Cannet, C.; Schäfer, H.; Kommoss, S.; Brucker, S.; Beziere, N.; Trautwein, C. Stratification of Ovarian Cancer Borderline from High-Grade Serous Carcinoma Patients by Quantitative Serum NMR Spectroscopy of Metabolites, Lipoproteins, and Inflammatory Markers. *Front. Mol. Biosci.* **2023**, *10*, 1158330. [CrossRef]
59. Huang, Y.; Du, Y.; Zheng, Y.; Wen, C.; Zou, H.; Huang, J.; Zhou, H.; Zhao, H.; Wu, L. Ct-OATP1B3 Promotes High-Grade Serous Ovarian Cancer Metastasis by Regulation of Fatty Acid Beta-Oxidation and Oxidative Phosphorylation. *Cell Death Dis.* **2022**, *13*, 556. [CrossRef]
60. Xue, Y.; Yang, Y.; Tian, H.; Quan, H.; Liu, S.; Zhang, L.; Yang, L.; Zhu, H.; Wu, H.; Gao, Y.Q. Computational Characterization of Domain-Segregated 3D Chromatin Structure and Segmented DNA Methylation Status in Carcinogenesis. *Mol. Oncol.* **2022**, *16*, 699–716. [CrossRef]
61. Lie, B.A.; Thorsby, E. Several Genes in the Extended Human MHC Contribute to Predisposition to Autoimmune Diseases. *Curr. Opin. Immunol.* **2005**, *17*, 526–531. [CrossRef]
62. Palmer, R.E.; Lee, S.B.; Wong, J.C.; Reynolds, P.A.; Zhang, H.; Truong, V.; Oliner, J.D.; Gerald, W.L.; Haber, D.A. Induction of BAIAP3 by the EWS-WT1 Chimeric Fusion Implicates Regulated Exocytosis in Tumorigenesis. *Cancer Cell* **2002**, *2*, 497–505. [CrossRef] [PubMed]
63. Franzè, E.; Stolfi, C.; Troncone, E.; Scarozza, P.; Monteleone, G. Role of Interleukin-34 in Cancer. *Cancers* **2020**, *12*, 252. [CrossRef] [PubMed]
64. Lu, J.-J.; Abudukeyoumu, A.; Zhang, X.; Liu, L.-B.; Li, M.-Q.; Xie, F. Heme Oxygenase 1: A Novel Oncogene in Multiple Gynecological Cancers. *Int. J. Biol. Sci.* **2021**, *17*, 2252–2261. [CrossRef] [PubMed]
65. Sun, H.; Li, L.; Yan, J.; Huang, T. Prioritization of Drug Targets for Thyroid Cancer: A Multi-Omics Mendelian Randomization Study. *Endocrine* **2024**. [CrossRef]
66. Li, Y.-Z.; Zhang, C.; Pei, J.-P.; Zhang, W.-C.; Zhang, C.-D.; Dai, D.-Q. The Functional Role of Pescadillo Ribosomal Biogenesis Factor 1 in Cancer. *J. Cancer* **2022**, *13*, 268–277. [CrossRef]
67. Li, J.; Zhuang, Q.; Lan, X.; Zeng, G.; Jiang, X.; Huang, Z. PES1 Differentially Regulates the Expression of ERα and ERβ in Ovarian Cancer. *IUBMB Life* **2013**, *65*, 1017–1025. [CrossRef]
68. Namasu, C.Y.; Katzerke, C.; Bräuer-Hartmann, D.; Wurm, A.A.; Gerloff, D.; Hartmann, J.-U.; Schwind, S.; Müller-Tidow, C.; Hilger, N.; Fricke, S.; et al. ABR, a Novel Inducer of Transcription Factor C/EBPα, Contributes to Myeloid Differentiation and Is a Favorable Prognostic Factor in Acute Myeloid Leukemia. *Oncotarget* **2017**, *8*, 103626–103639. [CrossRef]

Special Issue "Biomarkers and Early Detection Strategies of Ovarian Tumors"

Laura Aleksandra Szafron [1] , **Jolanta Kupryjanczyk** [2] **and Lukasz Michal Szafron** [1,*]

[1] Department of Experimental Oncology, Maria Sklodowska-Curie National Research Institute of Oncology, 02-781 Warsaw, Poland; laura.szafron@gmail.com
[2] Department of Cancer Pathomorphology, Maria Sklodowska-Curie National Research Institute of Oncology, 02-781 Warsaw, Poland; jolanta.kupryjanczyk@nio.gov.pl
[*] Correspondence: lukszafron@gmail.com

1. Introduction

Although progress has been made in developing new therapies and deepening the biological understanding of ovarian carcinoma (OvCa), it continues to be the most lethal gynecologic cancer in women. According to estimates from the American Cancer Society, approximately 20,890 new cases and 12,730 deaths from ovarian cancer are expected in the United States in 2025 [1]. Mortality rates are even higher in countries with limited cancer prevention, screening, and diagnostic programs. The poor prognosis of OvCa is largely due to the challenges of detecting the disease at an early, more treatable stage.

Ovarian carcinomas are classified into two major subtypes: high-grade (hgOvCa) and low-grade (lgOvCa). High-grade tumors are the predominant form and are marked by extensive genomic instability, chromosomal alterations, and frequent mutations in tumor suppressor genes such as *TP53*, *BRCA1*, and *BRCA2* [2]. In contrast, low-grade tumors are rare, typically diagnosed at a younger age, show relative resistance to chemotherapy, and are associated with longer survival. Unlike high-grade tumors, lgOvCa seldom harbor *TP53* or *BRCA1/2* mutations [3,4] and, particularly in the serous subtype, share molecular similarities with borderline ovarian tumors (BOTs) [5].

BOTs are uncommon tumors with low malignant potential, showing an intermediate characteristics between benign and invasive ovarian cancers. They generally arise in women of reproductive age, are diagnosed at early FIGO stages, and carry favorable survival rates. Preoperative imaging methods (ultrasound, MRI) aid in distinguishing BOTs from carcinomas, but definitive diagnosis requires histopathology. Surgical resection remains the primary treatment, with fertility-sparing approaches considered for younger patients desiring pregnancy. Chemotherapy, however, is not recommended [6,7]. Even after complete resection, about 20% of BOTs may recur—most as borderline tumors but, in some cases, as low-grade carcinomas [5,8–10].

While biomarkers in BOTs are poorly characterized, OvCa—particularly hgOvCa—has been extensively studied. Nonetheless, uncertainties persist regarding the clinical utility of some molecular markers. Thus, identifying reliable prognostic and predictive biomarkers remains critical for improving treatment outcomes and reducing OvCa-related mortality.

2. Ovarian Cancer Risk Factors

The most significant risk factors are inherited mutations in the *BRCA1* and *BRCA2* genes, which increase OvCa risk significantly, and have a strong influence on patient survival. Thus, such genetic alterations are considered a valuable stratification factor [11].

Consistently, mutations in other genes involved in homologous recombination repair, such as *RAD51C/D* and *BRIP1,* also elevate OvCa risk [12]. The higher OvCa risk is also observed in women, who have never been pregnant or have had fewer full-term pregnancies, likely due to uninterrupted (incessant) ovulation and hormonal exposure [13]. Early menarche and late menopause extend the number of ovulatory cycles, thus also raising OvCa risk [14]. Conversely, the use of combined oral contraceptives has been shown to reduce ovarian cancer risk, with longer use correlating with greater protection [15].

It is noteworthy that OvCa risk increases with aging and peaks between the ages of 50 and 80 years [16]. However, lifestyle factors, like inappropriate diet leading to obesity, may increase the risk of developing ovarian tumors. Obesity is associated with chronic inflammation and increased estrogen levels, which may promote tumor development. Moreover, some studies demonstrate that up to 40% of obese patients with ovarian cancer receive suboptimal doses of chemotherapy, which are not proportional to actual body weight, and such reduced dosage of chemotherapeutic agents may compromise progression-free survival (PFS) and overall survival (OS) [17].

Endometriosis and pelvic inflammatory disease are also linked to elevated ovarian cancer risk, however, some studies suggest that the cumulative incidence rate of ovarian cancer is significantly higher in patients with endometriosis than in those with pelvic inflammatory disease [18].

3. Prevention

Women with mutations in *BRCA1/2* are advised to undergo regular screening, including transvaginal ultrasound and CA-125 blood tests, although the effectiveness of screening alone is limited. Prophylactic removal of ovaries and fallopian tubes is currently the most effective preventive measure, significantly reducing the risk of ovarian cancer in *BRCA1/2*-mutation carriers [19].

Asymptomatic progression of OvCa underscores the urgent need for sensitive, minimally invasive diagnostic tools. One promising approach in recent years has been the use of circulating tumor DNA (ctDNA) as a biomarker for early cancer detection. ctDNA originates from fragments of DNA released by tumor cells into the bloodstream (and also to saliva, urine or cerebrospinal fluid). These fragments carry tumor-specific genetic mutations and epigenetic changes, providing a window into tumor biology through a simple blood draw—often termed a "liquid biopsy" [20]. Elevated ctDNA levels in OvCa patients correlate with poorer progression-free and overall survival [21]. Unlike traditional imaging techniques and CA-125 measurements, ctDNA enables real-time monitoring, detection of minimal residual disease, and earlier relapse identification. It was shown that after surgery the presence of ctDNA was a strong predictor of relapse (hazard ratio ~17.6), outperforming CA-125 [22]. Thus, while ctDNA-based screening for OvCa has neither been widely used in clinical practice nor approved by the American Food and Drug Administration (FDA) yet, it holds great promise for the diagnosis and recurrence monitoring of this neoplasm.

4. Diagnosis

The methods for ovarian cancer diagnosis include, e.g., the OVA1 test, which involves the assessment of five serum biomarkers—CA-125, tranthyretin, apolipoprotein A1, beta-2 microglobulin, and transferrin—into a single numerical score that reflects the malignant risk. OVA1 can detect malignancies (including early-stage ovarian cancers) that might be overlooked when evaluating CA-125 levels only [23]. Admittedly, the current guidelines from the Society of Gynecologic Oncology (SGO) do not recommend OVA1 as a standalone diagnostic or screening test for assessing adnexal masses preoperatively. Still, the SGO endorses OVA1 as an auxiliary tool in OvCa diagnosis [24].

5. Chemotherapy

Despite using the standard systemic chemotherapy for OvCa (typically a combination of platinum agents (like cisplatin or carboplatin) and taxanes (paclitaxel)), there has been growing interest in hyperthermic intraperitoneal chemotherapy (HIPEC). HIPEC involves perfusing the peritoneal cavity with heated chemotherapy immediately after cytoreductive surgery, aiming to eradicate microscopic residual disease. Hyperthermia enhances drug penetration and synergizes with platinum agents and taxanes, while limiting systemic toxicity. Additionally, hyperthermia has been shown to reduce the mechanisms of induced cellular resistance to cisplatin [25].

6. Targeted Therapy

Targeted therapies have become essential additions to standard platinum-taxane chemotherapy in the treatment of ovarian cancer. Among the most widely used are anti-angiogenic agents, Poly (ADP-Ribose) Polymerase (PARP) inhibitors or immune checkpoint inhibitors. Bevacizumab, a monoclonal antibody targeting VEGF-A, which inhibits angiogenesis, has demonstrated clinical usability in OvCa. The GOG-0218 and ICON7 clinical trials showed a significant PFS benefit when bevacizumab was added to standard chemotherapy [26].

Another monoclonal antibody, pembrolizumab, is an immune checkpoint inhibitor (it blocks the PD-1 receptor), which has been explored in platinum-resistant ovarian cancer. While the activity of pembrolizumab as a single-agent is modest, its combinations with bevacizumab and low-dose cyclophosphamide demonstrated clinical benefits in 25% of patients with recurrent OvCa [27].

PARP inhibitors (PARPi) exploit defects in DNA repair mechanisms, particularly in *BRCA1/2*-mutated and homologous recombination repair-deficient (HRD) tumors. Currently, four PARPi, olaparib, rucaparib, talazoparib and niraparib, are approved by regulatory agencies for the treatment of multiple tumor types including OvCa [28]. In patients with germline or somatic *BRCA1/2* mutations (which were deleterious or suspected to be deleterious), the olaparib monotherapy (SOLO1 trial) resulted in a three-year PFS benefit (HR, 0.30; 95% CI 0.23–0.41). On the other hand, the niraparib monotherapy in the PRIMA trial (which enrolled patients regardless of their *BRCA1/2* mutation status) demonstrated a median PFS benefit (HR, 0.40; 95% CI 0.27–0.62) [29].

7. Invitation for Paper Contribution

Given the considerations presented in this editorial, discovering novel molecular biomarkers that reflect qualitative or quantitative changes in the genomes, methylomes, transcriptomes, proteomes, or metabolomes of BOTs and OvCas is crucial in advancing the fight against these tumors. We hope that the findings shared in this Special Issue will lay the foundation for innovative, more effective, and less burdensome approaches to the detection, diagnosis, and treatment of ovarian neoplasms.

In order to make this Special Issue even more scientifically sound and interesting for the broader group of scientists, both clinicians and basic researchers, we would like to invite You to contribute a manuscript to this international endeavor (to date, six valuable research articles written by scientists from Japan, USA, Russia, Denmark, Switzerland, and Poland have been published). It is worth noting that both original and review articles are gladly welcome. If You wish to participate in this Special Issue by supporting it with Your knowledge and study results, we truly solicit Your involvement and warmly encourage You to submit Your manuscript by the deadline, i.e., 20 December 2025. We hope that this issue is likely to achieve another major goal, being its publication as a digital book available

online, and that the precious contribution of You and all the other scientists involved will help us meet book-publishing requirements.

Author Contributions: Conceptualization: L.A.S., J.K., and L.M.S.; Supervision: L.M.S.; Writing—Original Draft: L.A.S. and L.M.S.; Writing—Review and Editing: J.K. All authors have read and agreed to the published version of the manuscript.

Conflicts of Interest: The authors declare no conflicts of interest.

References

1. Ovarian Cancer Statistics | How Common Is Ovarian Cancer? Available online: https://www.cancer.org/cancer/types/ovarian-cancer/about/key-statistics.html (accessed on 13 August 2025).

2. Guo, T.; Dong, X.; Xie, S.; Zhang, L.; Zeng, P.; Zhang, L. Cellular Mechanism of Gene Mutations and Potential Therapeutic Targets in Ovarian Cancer. *Cancer Manag. Res.* **2021**, *13*, 3081–3100. [CrossRef]

3. Babaier, A.; Mal, H.; Alselwi, W.; Ghatage, P. Low-Grade Serous Carcinoma of the Ovary: The Current Status. *Diagnostics* **2022**, *12*, 458. [CrossRef]

4. Wong, K.-K.; Bateman, N.W.; Ng, C.W.; Tsang, Y.T.M.; Sun, C.S.; Celestino, J.; Nguyen, T.V.; Malpica, A.; Hillman, R.T.; Zhang, J.; et al. Integrated Multi-Omic Analysis of Low-Grade Ovarian Serous Carcinoma Collected from Short and Long-Term Survivors. *J. Transl. Med.* **2022**, *20*, 606. [CrossRef] [PubMed]

5. Hauptmann, S.; Friedrich, K.; Redline, R.; Avril, S. Ovarian Borderline Tumors in the 2014 WHO Classification: Evolving Concepts and Diagnostic Criteria. *Virchows Arch.* **2017**, *470*, 125–142. [CrossRef]

6. Bourdel, N.; Huchon, C.; Abdel Wahab, C.; Azaïs, H.; Bendifallah, S.; Bolze, P.-A.; Brun, J.-L.; Canlorbe, G.; Chauvet, P.; Chereau, E.; et al. Borderline Ovarian Tumors: French Guidelines from the CNGOF. Part 2. Surgical Management, Follow-up, Hormone Replacement Therapy, Fertility Management and Preservation. *J. Gynecol. Obstet. Hum. Reprod.* **2021**, *50*, 101966. [CrossRef] [PubMed]

7. Timor-Tritsch, I.E.; Foley, C.E.; Brandon, C.; Yoon, E.; Ciaffarrano, J.; Monteagudo, A.; Mittal, K.; Boyd, L. New Sonographic Marker of Borderline Ovarian Tumor: Microcystic Pattern of Papillae and Solid Components. *Ultrasound Obstet. Gynecol.* **2019**, *54*, 395–402. [CrossRef] [PubMed]

8. Niu, L.; Tian, H.; Xu, Y.; Cao, J.; Zhang, X.; Zhang, J.; Hou, J.; Lv, W.; Wang, J.; Xin, L.; et al. Recurrence Characteristics and Clinicopathological Results of Borderline Ovarian Tumors. *BMC Women's Health* **2021**, *21*, 134. [CrossRef]

9. Shih, K.; Zhou, Q.; Huh, J.; Morgan, J.; Iasonos, A.; Aghajanian, C.; Chi, D.; Barakat, R.; Abu-Rustum, N. Risk Factors for Recurrence of Ovarian Borderline Tumors. *Gynecol. Oncol.* **2011**, *120*, 480–484. [CrossRef]

10. Gershenson, D.M.; Silva, E.G.; Levy, L.; Burke, T.W.; Wolf, J.K.; Tornos, C. Ovarian Serous Borderline Tumors with Invasive Peritoneal Implants. *Cancer* **1998**, *82*, 1096–1103. [CrossRef]

11. Alsop, K.; Fereday, S.; Meldrum, C.; deFazio, A.; Emmanuel, C.; George, J.; Dobrovic, A.; Birrer, M.J.; Webb, P.M.; Stewart, C.; et al. BRCA Mutation Frequency and Patterns of Treatment Response in BRCA Mutation-Positive Women with Ovarian Cancer: A Report from the Australian Ovarian Cancer Study Group. *J. Clin. Oncol.* **2012**, *30*, 2654–2663. [CrossRef]

12. Suszynska, M.; Ratajska, M.; Kozlowski, P. BRIP1, RAD51C, and RAD51D Mutations Are Associated with High Susceptibility to Ovarian Cancer: Mutation Prevalence and Precise Risk Estimates Based on a Pooled Analysis of ~30,000 Cases. *J. Ovarian Res.* **2020**, *13*, 50. [CrossRef]

13. Husby, A.; Wohlfahrt, J.; Melbye, M. Pregnancy Duration and Ovarian Cancer Risk: A 50-Year Nationwide Cohort Study. *Int. J. Cancer* **2022**, *151*, 1717–1725. [CrossRef] [PubMed]

14. Pięta, B.; Chmaj-Wierzchowska, K.; Opala, T. Past Obstetric History and Risk of Ovarian Cancer. *Ann. Agric. Environ. Med.* **2012**, *19*, 385–388.

15. Arshadi, M.; Hesari, E.; Ahmadinezhad, M.; Yekta, E.M.; Ebrahimi, F.; Azizi, H.; Esfarjani, S.V.; Rostami, M.; Khodamoradi, F. The Association between Oral Contraceptive Pills and Ovarian Cancer Risk: A Systematic Review and Meta-Analysis. *Bull. Cancer* **2024**, *111*, 918–929. [CrossRef] [PubMed]

16. Zheng, G.; Yu, H.; Kanerva, A.; Försti, A.; Sundquist, K.; Hemminki, K. Familial Risks of Ovarian Cancer by Age at Diagnosis, Proband Type and Histology. *PLoS ONE* **2018**, *13*, e0205000. [CrossRef] [PubMed]

17. Benedetto, C.; Salvagno, F.; Canuto, E.M.; Gennarelli, G. Obesity and Female Malignancies. *Best Pract. Res. Clin. Obstet. Gynaecol.* **2015**, *29*, 528–540. [CrossRef]

18. Huang, J.-Y.; Yang, S.-F.; Wu, P.-J.; Wang, C.-H.; Tang, C.-H.; Wang, P.-H. Different Influences of Endometriosis and Pelvic Inflammatory Disease on the Occurrence of Ovarian Cancer. *Int. J. Environ. Res. Public Health* **2021**, *18*, 8754. [CrossRef]

19. Gadducci, A.; Sergiampietri, C.; Tana, R. Alternatives to Risk-Reducing Surgery for Ovarian Cancer. *Ann. Oncol.* **2013**, *24*, viii47–viii53. [CrossRef]

20. Golara, A.; Kozłowski, M.; Cymbaluk-Płoska, A. The Role of Circulating Tumor DNA in Ovarian Cancer. *Cancers* **2024**, *16*, 3117. [CrossRef]

21. Taliento, C.; Morciano, G.; Nero, C.; Froyman, W.; Vizzielli, G.; Pavone, M.; Salvioli, S.; Tormen, M.; Fiorica, F.; Scutiero, G.; et al. Circulating Tumor DNA as a Biomarker for Predicting Progression-Free Survival and Overall Survival in Patients with Epithelial Ovarian Cancer: A Systematic Review and Meta-Analysis. *Int. J. Gynecol. Cancer* **2024**, *34*, 906–918. [CrossRef]

22. Hou, J.Y.; Chapman, J.S.; Kalashnikova, E.; Pierson, W.; Smith-McCune, K.; Pineda, G.; Vattakalam, R.M.; Ross, A.; Mills, M.; Suarez, C.J.; et al. Circulating Tumor DNA Monitoring for Early Recurrence Detection in Epithelial Ovarian Cancer. *Gynecol. Oncol.* **2022**, *167*, 334–341. [CrossRef] [PubMed]

23. Dunton, C.J.; Hutchcraft, M.L.; Bullock, R.G.; Northrop, L.E.; Ueland, F.R. Salvaging Detection of Early-Stage Ovarian Malignancies When CA125 Is Not Informative. *Diagnostics* **2021**, *11*, 1440. [CrossRef]

24. SGO Position Statement: OVA-1. Society of Gynecologic Oncology. Available online: https://www.sgo.org/news/sgo-position-statement-ova-1/ (accessed on 10 August 2025).

25. Riggs, M.J.; Pandalai, P.K.; Kim, J.; Dietrich, C.S. Hyperthermic Intraperitoneal Chemotherapy in Ovarian Cancer. *Diagnostics* **2020**, *10*, 43. [CrossRef]

26. Babaier, A.; Ghatage, P. Among Patients with Advanced Ovarian Carcinoma, Who Benefits from Bevacizumab the Most? *Ann. Transl. Med.* **2023**, *11*, 367. [CrossRef]

27. Zsiros, E.; Lynam, S.; Attwood, K.M.; Wang, C.; Chilakapati, S.; Gomez, E.C.; Liu, S.; Akers, S.; Lele, S.; Frederick, P.J.; et al. Efficacy and Safety of Pembrolizumab in Combination With Bevacizumab and Oral Metronomic Cyclophosphamide in the Treatment of Recurrent Ovarian Cancer: A Phase 2 Nonrandomized Clinical Trial. *JAMA Oncol.* **2021**, *7*, 78–85. [CrossRef] [PubMed]

28. Herzog, T.J.; Vergote, I.; Gomella, L.G.; Milenkova, T.; French, T.; Tonikian, R.; Poehlein, C.; Hussain, M. Testing for Homologous Recombination Repair or Homologous Recombination Deficiency for Poly (ADP-Ribose) Polymerase Inhibitors: A Current Perspective. *Eur. J. Cancer* **2023**, *179*, 136–146. [CrossRef] [PubMed]

29. Kim, J.H.; Kim, S.I.; Park, E.Y.; Kim, E.T.; Kim, H.; Kim, S.; Park, S.-Y.; Lim, M.C. Comparison of Survival Outcomes between Olaparib and Niraparib Maintenance Therapy in BRCA-Mutated, Newly Diagnosed Advanced Ovarian Cancer. *Gynecol. Oncol.* **2024**, *181*, 33–39. [CrossRef]

Oświadczenie współautorów

Oświadczam, że mój wkład jako autora w publikacji pt."*An Analysis of Genetic Polymorphisms in 76 Genes Related to the Development of Ovarian Tumors of Different Aggressiveness*" jest zgodny z opisem znajdujacym sie w podrozdziale "Author Contributions" w ww. pracy.

Piotr Sobiczewski
Data, podpis

18.11. 2024

Jolanta Kupryjańczyk
Data podpis

4.11. 2024

Agnieszka Dansonka-Mieszkowska
Data, podpis

18.11. 2024

Łukasz Szafron
Data podpis

17.10.2024

Oświadczenie współautorów

Oświadczam, że mój wkład jako autora w publikacji pt.”*The diversity of methylation patterns in serous borderline ovarian tumors and serous ovarian carcinomas*” jest zgodny z opisem znajdujacym sie w podrozdziale “Author Contributions” w ww. pracy.

Roksana Iwanicka-Nowicka
Data, podpis

27. 11. 2024

Marta Koblowska
Data, podpis

26.11 2024

Jolanta Kupryjańczyk
Data podpis

4. 11. 2024

Piotr Sobiczewski
Data, podpis

18. 11. 2024

Agnieszka Dansonka-Mieszkowska
Data, podpis

18. 11. 2024

Łukasz Szafron
Data podpis

17.10.2024

Oświadczenie współautorów

Oświadczam, że mój wkład jako autora w publikacji pt.*"Special Issue "Biomarkers and Early Detection Strategies of Ovarian Tumors"* jest zgodny z opisem znajdujacym sie w podrozdziale "Author Contributions" w ww. pracy.

Jolanta Kupryjańczyk
Data podpis

6.10.25

Łukasz Szafron
Data podpis

02.10.2025

DECYZJA KOMISJI BIOETYCZNEJ

numer 49/2003

Na podstawie art. 29, ust.2 ustawy z dnia 5 grudnia 1996r. o zawodzie lekarza (Dz.U. z 1999r. nr 28 poz. 152 i nr 88 poz.554 oraz z 1998r. nr 106 poz. 668 i nr 162 poz. 1115) oraz rozporządzenia MZiOS z dnia 11 maja 1999r. w sprawie szczegółowych zasad powoływania i finansowania oraz trybu działania komisji bioetycznych (Dz.U. z 1999r. nr 47 poz.480) i zarządzenia Dyrektora Centrum Onkologii-Instytutu nr 65/99 z dnia 26.11.1999r. i nr 114/02 z dnia 19.11.2002r.

Komisja Bioetyczna przy Centrum Onkologii Instytucie w Warszawie na zebraniu w dniu 6 listopada 2003r. zapoznała się z projektem badania pt:
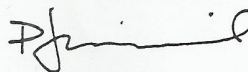
Analiza czynników prognostycznych i predykcyjnych w rakach jajnika.

przedstawionego przez: **doc. dr hab. med. Jolantę Kupryjańczyk, Kierownika Zakładu Patologii Molekularnej Centrum Onkologii Instytutu w Warszawie.**

Komisja Bioetyczna:

☒ wyraziła zgodę na rozpoczęcie badania (na podstawie materiału archiwalnego – bloczki parafinowe i archiwalne dane z historii chorób).

W ramach niniejszego zezwolenia badania mogą być prowadzone do odwołania.

podpis przewodniczącego Komisji

Warszawa, dnia 6 listopada 2003r.

OPINIA KOMISJI BIOETYCZNEJ

numer 39/2007

Na podstawie art. 29, ust.2 ustawy z dnia 5 grudnia 1996r. o zawodzie lekarza (Dz. U. z 1997r. nr 28 poz. 152 i nr 88 poz.554, z 1998r. nr 106 poz. 668, nr 162 poz. 1115), rozporządzenia MZiOS z dnia 11 maja 1999r.(Dz. U. z 1999r. nr 47 poz.480), z 2004r. (Dz.U. nr 92 poz. 882), MZ z dnia 3 stycznia 2007 (Dz. U.nr 6 poz. 46) oraz zarządzenia Dyrektora Centrum Onkologii-Instytutu nr 148/2005 z dnia 28.11.2005r. z późn. zmianami.

Komisja Bioetyczna przy Centrum Onkologii Instytucie w Warszawie na posiedzeniu w dniu 13 listopada 2007r. zapoznała się z dokumentami do badania pt:

Badanie molekularnej patogenezy nowotworów narządu rodnego i czynników ryzyka zachorowania na te nowotwory (badania mutacji i polimorfizmów genów).

przedstawionego przez: **Prof. dr hab. med. Jolantę Kupryjańczyk, Kierownika Zakładu Patologii Molekularnej Centrum Onkologii-Instytutu im. M. Skłodowskiej-Curie w Warszawie.**
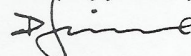
Do komisji wpłynęły następujące dokumenty:
☒ Wniosek do Komisji Bioetycznej;
☒ Informacja dla pacjenta i formularz zgody pacjenta na przeprowadzenie badania nosicielstwa genów predyspozycji do zachorowania na nowotwór;
☒ Oświadczenie lekarza;
☒ Oświadczenie pacjenta.

Po zapoznaniu się z całością dokumentacji oraz w wyniku przeprowadzonej dyskusji i głosowania Komisja Bioetyczna:
☒ podjęła uchwałę o pozytywnym zaopiniowaniu dokumentów po uzupełnieniu informacji i zgody pacjenta o informację o pobraniu materiału operacyjnego do badania oraz oświadczenie pacjenta, że wyraża zgodę na takie badanie i na badanie bloczków parafinowych.

przewodniczący Komisji Bioetycznej

dr n. med. Piotr Siedlecki

Warszawa, dnia 13 listopada 2007r.